

323

Copy  
RM E57D24

~~CONFIDENTIAL~~

NACA RM E57D24

14455  
JUL 31 1957

0143928

TECH LIBRARY KAFB, NM

NACA

# RESEARCH MEMORANDUM

SURVEY OF HYDROGEN COMBUSTION PROPERTIES

By Isadore L. Drell and Frank E. Belles

Lewis Flight Propulsion Laboratory  
Cleveland, Ohio

Classification cancelled (or changed to UNCLASSIFIED)

By Authority of NASA Tech Rep Announcement #123  
(OFFICER AUTHORIZED TO CHANGE)

By 7 Jan 58  
NAME AND

ELM  
GRADE OF OFFICER MAKING CHANGE)

29 Mar 61  
DATE

~~CONFIDENTIAL~~  
NATIONAL ADVISORY COMMITTEE  
FOR AERONAUTICS

WASHINGTON

July 26, 1957



0143928

## TABLE OF CONTENTS

	Page
SUMMARY . . . . .	1
INTRODUCTION . . . . .	1
SYMBOLS . . . . .	3
FLAME TEMPERATURE . . . . .	4
Effect of mixture composition . . . . .	6
Effect of initial mixture temperature . . . . .	7
Effect of pressure . . . . .	7
Recommended flame temperatures . . . . .	7
Burned-gas composition . . . . .	8
BURNING VELOCITY . . . . .	8
Laminar Burning Velocity . . . . .	8
Effect of mixture composition . . . . .	9
Effect of initial mixture temperature . . . . .	10
Effect of pressure . . . . .	10
Turbulent Burning Velocity . . . . .	12
QUENCHING DISTANCE . . . . .	12
Effect of mixture composition . . . . .	13
Effect of pressure . . . . .	13
Effect of temperature . . . . .	13
Effect of nature of quenching surface . . . . .	13
Flame traps . . . . .	14
FLAMMABILITY LIMITS . . . . .	14
Effect of direction of propagation . . . . .	15
Flammable range . . . . .	15
Recommended limits at atmospheric temperature and pressure . . . . .	16
Effect of mixture temperature . . . . .	16
Effect of inert diluents . . . . .	16
Effect of pressures below 1 atmosphere . . . . .	17
Effect of pressures above 1 atmosphere . . . . .	18
SPARK IGNITION ENERGY . . . . .	18
Effect of mixture composition . . . . .	19
Effect of pressure . . . . .	19
Effect of temperature . . . . .	20
FLAME STABILITY . . . . .	20
Flashback and Blowoff of Burner Flames . . . . .	20
Flashback . . . . .	21
Blowoff . . . . .	22
Blowoff of Confined Flames from Flameholders . . . . .	23

~~CONFIDENTIAL~~~~WADO ADJ 37 54 2-2~~

~~CONFIDENTIAL~~

DETONATION PROPERTIES . . . . .	25
EXPLOSION LIMITS, SPONTANEOUS IGNITION, AND THE CHEMISTRY OF	
HYDROGEN OXIDATION . . . . .	26
Explosion Limits . . . . .	26
Description of phenomenon . . . . .	26
Effects of variables on explosion limits . . . . .	27
Chemistry of Hydrogen Oxidation . . . . .	28
Spontaneous Ignition . . . . .	29
Relation between spontaneous ignition and explosion limits . . . . .	29
Theoretical considerations . . . . .	30
Sources of spontaneous-ignition data . . . . .	34
Effect of temperature . . . . .	34
Effect of fuel concentration . . . . .	35
Effect of pressure . . . . .	36
Safety Considerations . . . . .	36
RELATIONS AMONG COMBUSTION PROPERTIES . . . . .	37
Flame Reaction Rates . . . . .	37
Relations Useful for Estimating Data . . . . .	38
Flashback velocity gradient, burning velocity, and quenching distance . . . . .	38
Burning velocity and quenching distance . . . . .	39
Spark ignition energy and quenching distance . . . . .	40
Flashback velocity gradient and blowoff from flameholders . . . . .	40
SUMMARY OF RECOMMENDED VALUES OF COMBUSTION PROPERTIES . . . . .	42
REFERENCES . . . . .	42
TABLES . . . . .	50
FIGURES . . . . .	55

~~CONFIDENTIAL~~

NACA RM E57D24

~~CONFIDENTIAL~~

## NATIONAL ADVISORY COMMITTEE FOR AERONAUTICS

RESEARCH MEMORANDUM

## SURVEY OF HYDROGEN COMBUSTION PROPERTIES

By Isadore L. Drell and Frank E. Belles

## SUMMARY

A literature survey of the combustion properties of hydrogen-air mixtures was made to provide a single source of information useful in research and development work where hydrogen is burned. Data are presented on flame temperature, burning velocity, quenching distance, flammability composition limits, minimum spark ignition energy, flash-back and blowoff limits, detonation properties, explosion limits, spontaneous ignition, and the chemistry of hydrogen oxidation. The survey was not meant to be historically complete or exhaustive but to cover the basic material of importance for flight propulsion applications.

The validity of experimental methods is discussed, and the data are assessed wherever possible. Recommended values for the combustion properties of hydrogen-air mixtures are presented. The report also includes some original material. Relations among various combustion properties of hydrogen are discussed; calculated adiabatic flame temperatures for a range of pressure from 0.01 to 100 atmospheres and a range of initial temperature from 0° to 1400° K for all possible hydrogen-air mixtures are presented; and a theoretical treatment of the variation of spontaneous-ignition lag with temperature, pressure, and composition based on the reaction kinetics of hydrogen oxidation is given.

## INTRODUCTION

The use of hydrogen as a possible fuel for aircraft and missiles has been considered for a number of years (ref. 1). Among the many problems associated with the use of this material are those of efficient burning under a variety of conditions. In the research and development effort that will be necessary before these problems can be fully solved it would be useful to have a single source of information on the many aspects of hydrogen combustion. Therefore, as a part of the fundamental combustion work at the NACA Lewis laboratory, the literature was surveyed and the present knowledge on hydrogen-air flames was collected and digested.

~~CONFIDENTIAL~~~~WADD-AD-57-5422~~

A great deal of literature exists, because hydrogen has often been used as a fuel in combustion research from the earliest studies up to the present. One reason for this has been the ready availability of hydrogen in a fairly pure state. Furthermore, its high burning velocity, wide flammability range, high heating value per unit weight, and great flame stability are of much scientific interest. Of the common fuel-oxidant systems, the hydrogen-oxygen (or hydrogen-air) system is probably the simplest, the one about which much of the chemistry is known, and thus the one about which there is the greatest likelihood of learning more.

This survey is not meant to be historically complete or exhaustive, but to cover the important basic material. It is mainly concerned with hydrogen-air combustion properties, but some data are included for hydrogen-oxygen and hydrogen-oxygen-nitrogen systems.

The combustion data presented include observations on:

- (1) Flame temperature
- (2) Burning velocity
- (3) Quenching distance
- (4) Flammability limits
- (5) Spark ignition energy
- (6) Flame stability
- (7) Detonation properties
- (8) Explosion limits, spontaneous ignition, and the chemistry of hydrogen oxidation

Values of the combustion properties are given under stated conditions of temperature, pressure, and composition (and vessel size and other specifications of the apparatus where significant). The variation of each property with temperature, pressure, and composition is then discussed if information is available.

Experimental methods and data are interpreted and evaluated, and recommended values are given. Relations among various combustion properties of hydrogen are discussed. Other original material includes: calculated adiabatic flame temperatures over the entire hydrogen-air composition range, for pressures of 0.01 to 100 atmospheres and initial temperatures of 0° to 1400° K; and a theoretical treatment of the effects of temperature, pressure, and composition on spontaneous-ignition lag based on the reaction kinetics of hydrogen oxidation.

NACA RM E57D24

~~CONFIDENTIAL~~

3

## SYMBOLS

$c_p$	specific heat at constant pressure
$c_1, c_3$	proportionality constants
$c_2(T)$	temperature-dependent proportionality constant
$D$	width of flameholder
$d$	diameter of burner tube
$d_q$	quenching distance
$E$	activation energy, cal/mole
$F$	Fanning friction factor
$g$	boundary velocity gradient, (cm/sec)/cm
$I$	spark ignition energy, millijoules
$i$	rate of initiation (rate of formation of OH radicals per unit time and volume)
$K_1, K_2$	constants
$k_1, k_2, \dots$	rate constants for chemical reactions
$L$	length of recirculation zone behind flameholder
$[M]$	molar concentration of all molecules other than free radicals
$N_O$	fuel concentration in unburned mixture, molecules/cm <sup>3</sup>
$n_O$	mole fraction of fuel in unburned mixture
$P$	pressure, atm
$R$	gas constant, cal/(mole)(°K)
$Re$	Reynolds number
$T$	temperature, °K
$T_F$	equilibrium adiabatic flame temperature, °K
$T_O$	initial mixture temperature, °K
$t$	ignition time available behind flameholder, sec

~~CONFIDENTIAL~~

4

~~CONFIDENTIAL~~

NACA RM E57D24

$t_c$	characteristic ignition time of mixture, sec
$U$	average flow velocity
$U_L$	laminar burning velocity, cm/sec
$w$	reaction rate
$\bar{w}_F$	average reaction rate in flame
$x, y, z$	empirical exponents
$\tau$	ignition lag, sec
$\phi$	equivalence ratio, fuel-oxidant ratio divided by stoichiometric fuel-oxidant ratio (mixture compositions in this paper are given as mole percent by volume or as equivalence ratio; the relation between these units for hydrogen-air mixtures is shown in fig. 1)

## Subscripts:

bo	blowoff
f	flashback
max	maximum
a	condition a
b	condition b
L	laminar
T	turbulent
300	300° K initial mixture temperature

## FLAME TEMPERATURE

One of the most important of the factors that characterize and influence combustion behavior in any fuel-oxidant system is the flame temperature. Flame temperature as used here refers to flames burning at constant pressure and with no appreciable external heat losses or gains. Table I and figure 2 give measured and calculated flame temperatures for hydrogen-air mixtures reported since 1930; earlier data are not considered reliable. The data are for a pressure of 1 atmosphere and an initial mixture temperature of 25° C.

~~CONFIDENTIAL~~

The criterion of negligible heat loss makes any experimental measurement very difficult. The values of Passauer (ref. 2, pp. 314 to 316 and 319) are thought to be low because they were obtained with rather large thermocouples. For temperatures above 2223° K a thermocouple made of 0.48-millimeter wire was used. The hot junction was placed 1 millimeter above the cone tip of a flame on a 4-millimeter cylindrical burner, both with and without a split-flame tube (Smithells separator) that enclosed the primary zone and isolated it from surrounding air.

The sodium-D-line-reversal measurements of Morgan and Kane (ref. 3) were of an approximate nature; furthermore, they were made at a position 4 millimeters above the tip of a flame on a 4.8-millimeter-nozzle burner, which admittedly may not be the locus of maximum temperature. The earlier line-reversal measurements of Jones, Lewis, and Seaman (ref. 4) probably furnish the best experimental values. They obtained flame temperatures of 2293° K for the stoichiometric mixture (29.5 percent hydrogen) and 2318° K for the maximum-temperature mixture (31.6 percent hydrogen). Even these values may be somewhat low because of heat transfer to the Meker burner used and because of the inherent averaging effect of the line-reversal technique.

Calculated flame temperatures, accounting for dissociation, are obtained with the assumptions of an adiabatic system and of chemical equilibrium among all species present in the burned gas. The calculated values are in error if these assumptions are not justified or if the thermodynamic data used are inaccurate. Good agreement between calculated and measured flame temperatures has been obtained by a refined thermocouple method (ref. 5) for very lean propane-air flames. This tends to support the validity of the calculated temperatures. However, various sources of error exist in any method of measuring flame temperature, and it is not always clear just how corrections should be applied. In reference 5 the errors were minimized, and after the raw data were corrected as carefully as possible, a measured temperature of 1530° K was obtained, compared with a calculated value of 1560° K. Equally good agreement cannot be expected in every case, especially in richer mixtures with hotter flames. In short, it is not possible at present to confirm the general validity of calculated flame temperature by experiment. Therefore, the attitude of this report is that the calculated temperatures are valid, particularly for premixed laminar flames large enough so that quenching effects are not significant. Premixed flames on small burners where there is appreciable heat loss, diffusion flames, and turbulent flames will normally fail to reach the full theoretical temperature (ref. 6).

The theoretical hydrogen-air flame temperatures from the recent literature (refs. 3 and 6 to 10) vary considerably. In fact, the difference between high and low values for stoichiometric mixtures is 65° K (table I), which is almost as great as the range of experimental temperatures. This spread is probably due to differences in thermodynamic



data and air composition assumed by various workers. The theoretical values computed for this report are  $2387^{\circ}$  K for the stoichiometric mixture and  $2403^{\circ}$  K for the maximum-temperature mixture.

For hydrogen-oxygen flames under the same initial conditions the theoretical flame temperature for the stoichiometric mixture (66.7 percent hydrogen in oxygen) is about  $3080^{\circ}$  K (ref. 6, p. 280, and refs. 8, 11, and 12); the maximum is practically the same. Line-reversal measurements by Pothmann (quoted in ref. 13) agree fairly well with theoretical values. These measurements gave a maximum of  $3123^{\circ}$  K at 66 percent hydrogen; surprisingly, this is higher than the theoretical value. Lurie and Sherman (ref. 13) reported a lower temperature,  $2933^{\circ}$  K, by the same method. Their reported maximum-temperature mixture of 78 percent hydrogen in oxygen is widely different from the calculated result and from Pothmann's measurement.

Effect of mixture composition. - Figure 2 shows that the maximum flame temperature is obtained with a slightly rich mixture. Most of the curves presented, including the most recent one calculated for this report, show the maximum at around 31 percent hydrogen in air ( $\Phi = 1.07$ ). The curves drop off regularly on both sides of the maximum. Flame temperatures below  $1300^{\circ}$  K are obtained as the flammability limits are approached.

The two experimental curves of Passauer, obtained for open flames and for flames on a Smithells burner with the primary zone enclosed, show an interesting effect: The split-flame burner gave lower flame temperatures than the ordinary open burner on the rich side, above 32 percent hydrogen, while below that concentration the reverse was found. Thus, the two kinds of flames may not have comparable temperatures except near 32 percent hydrogen. The differences were thought to be due to diffusion or induced mixing of secondary air from the surrounding atmosphere into the open flame; these effects would tend to raise temperatures for rich mixtures and to lower them for lean mixtures.

According to Byrne (ref. 14) secondary oxygen does not penetrate to the inner cone of a rich flame; however, it does enter the outer mantle, where it reacts with excess fuel in certain rich Bunsen flames (such as methane- or propane-air flames) and raises the temperature. Heat transfer then raises the temperature of the mixture burning in the inner cone and increases the burning velocity. However, Byrne observed little effect of secondary oxygen on the size and shape (and consequently on the burning velocity) of a rich hydrogen-air flame. He concluded that in this case hydrogen molecules and atoms diffuse away from the flame faster than oxygen travels inward (whereas in most hydrocarbon flames the reverse is true); thus secondary burning occurs far from the inner cone and can have little effect upon it. This seeming discrepancy with the results of Passauer may be due to the fact that the burning velocity of

hydrogen is not as dependent on temperature as is the burning velocity of hydrocarbons. In other words, the temperature did presumably rise, but not enough to affect the burning velocity perceptibly. Consequently, the conclusion of Passauer (ref. 2) that rich hydrogen flames in the open air have higher flame temperatures than enclosed flames because of admixing of air may be valid.

Effect of initial mixture temperature. - Theoretical adiabatic equilibrium flame temperatures were calculated for various hydrogen-air mixtures over a range of initial temperatures from  $0^{\circ}$  to  $1400^{\circ}$  K. The results are shown in figure 3. Rich mixtures are shown by solid lines and lean to stoichiometric mixtures by dashed lines. Except for mixtures near stoichiometric, flame temperature increases almost linearly with initial temperature. In very rich or lean mixtures, where flame temperatures are low and there is little dissociation, flame temperature increases degree for degree with mixture temperature. As the composition approaches stoichiometric, however, dissociation becomes more important and flame temperature becomes less dependent on initial mixture temperature.

Passauer (ref. 2), using the older thermochemical data, calculated a curve for the stoichiometric mixture that is quite similar to the one in figure 3. He obtained about the same flame temperature for an initial temperature of  $300^{\circ}$  K as that from the present calculation, but his curve has greater slope.

Effect of pressure. - Dissociation of the burned gas is favored by reduced pressures, so flame temperature decreases as pressure is decreased. However, the size of the effect depends strongly on the general level of flame temperatures produced by a given mixture. Figure 4 shows calculated flame temperatures as a function of pressure for hydrogen-air mixtures at initial temperatures of  $298^{\circ}$ ,  $600^{\circ}$ , and  $1000^{\circ}$  K. Near-stoichiometric mixtures show a strong dependence of flame temperature on pressure, while lean and rich mixtures have little or no dependence. Mixtures that are quite lean or rich have flame temperatures too low to cause much dissociation, so pressure has little effect.

Edse (ref. 12, p. 39) presented a plot similar to figure 4 for a stoichiometric hydrogen-oxygen mixture. The calculations covered pressures from 1 to 100 atmospheres.

Recommended flame temperatures. - In view of the experimental difficulties in measuring flame temperatures, as well as the limited range of conditions over which measurements have been made, it is recommended that the calculated values of this report be used. These data are summarized in figure 5, where flame temperature is plotted against hydrogen concentration over the complete range of composition. There are atmospheric-pressure curves for initial temperatures of  $0^{\circ}$ ,  $298.16^{\circ}$ ,  $600^{\circ}$ ,  $1000^{\circ}$ , and

1400° K. In addition, curves for 0.01 and 100 atmospheres were computed for initial temperatures of 298.16°, 600°, and 1000° K. The calculations for extremely fuel-rich mixtures and for high initial temperatures are included for use in the consideration of novel engine cycles and of flight conditions where inlet temperatures are high.

Burned-gas composition. - The calculations of equilibrium adiabatic flame temperatures for this report also provided data on the composition of the burned gas. The data are listed in table II. Mole fractions at various pressures, initial temperatures, and mixture compositions are given for the following atoms and molecules: H, O, N, OH, NO, N<sub>2</sub>, O<sub>2</sub>, H<sub>2</sub>, and H<sub>2</sub>O. Figure 6 is a plot of these data for a pressure of 1 atmosphere and an initial temperature of 298.16° K as a function of equivalence ratio. This figure is presented mainly to show the typical orders of magnitude of the amounts of various constituents in the burned gas. The mole fractions range from about 10<sup>-6</sup> to values approaching 1. Figure 6 also illustrates how dissociation depends on flame temperature; the mole fractions of the main dissociation products, H, O, and OH, peak not far from the equivalence ratio for maximum flame temperature. The equivalence ratios for these four maximums do not coincide, however, because the dissociation equilibria depend on concentration as well as temperature.

## BURNING VELOCITY

### Laminar Burning Velocity

The laminar burning velocity is defined as the velocity at which unburned gas of given composition, pressure, and temperature flows into a flame in a direction normal to the flame surface. The normal direction is specified in order to make burning velocity independent of the actual shape of the flame. The aim in measuring laminar burning velocity is always to obtain a physical constant for the mixture that is free of any effects of geometry, external heat sources or sinks, and nature of the flow. The burning velocity should be distinguished from the spatial flame speed, which is simply the gross speed of a flame traveling through a mixture.

Table III gives burning velocities for the hydrogen-air stoichiometric mixture and the mixture of maximum burning velocity at atmospheric pressure and room temperature. Results of 18 investigations covering the years between 1889 and 1956 are reported (refs. 2, 3, 8, 10, and 15 to 27). About six spatial flame speeds, starting with the work of Mallard and Le Chatelier done in 1881 (ref. 28), have been omitted.

The values in table III have a large spread for a quantity that is defined so as to be a physical constant. The burning velocities range

from 153 to 232 centimeters per second for the stoichiometric mixture and from 200 to 320 centimeters per second for the mixture of maximum burning velocity. Furthermore, the reported hydrogen concentrations for the maximum burning velocity vary from 40 to 46 percent. Of course, not all the work was done under strictly comparable conditions, since the ambient pressure and temperature and the degree of saturation with water vapor differed. However, the effects of these variables are thought to be less important than the effects of the experimental method.

An experimental measurement of burning velocity on a Bunsen or nozzle burner in essence requires recording an optical image of some surface in the flame zone and then measuring the area of the surface or its inclination to the flow. All the workers cited in table III used some form of this general method, except Manton and Milliken (ref. 26), who used a spherical constant-volume bomb. Both steps in the burner method are subject to error. At present it is believed that schlieren observation is best, since it gives a flame surface with a temperature close to that of the unburned gas (ref. 29). The best method of measuring the area of the surface is not so clearly defined.

In the bomb method used by Manton and Milliken (ref. 26) the radius of a spherically expanding flame was recorded as a function of time by schlieren photography. Simultaneously, the pressure in the bomb was recorded. From various well-founded thermodynamic assumptions, burning velocities may be calculated from both types of data, and the agreement provides an internal check of the assumptions. In the bomb method there are no heat losses such as occur near the base of a burner flame, and flame curvature effects are minimized by making measurements on flames of large radius.

It is believed that the data of references 3, 10, 23, 24, 26, and 27 and the unpublished data listed in table III represent the best values of burning velocity for hydrogen-air mixtures. These are recent data, and they were obtained by satisfactory experimental techniques. It is not possible at present to choose any single investigation as the best. Therefore, the recommended burning velocities for hydrogen-air mixtures at 1 atmosphere and about 300° K initial temperatures are averages of the values from these seven sources. The recommended maximum burning velocity is 310 centimeters per second at about 43 percent hydrogen ( $\Phi = 1.8$ ). The stoichiometric burning velocities show a larger spread than do maximum burning velocities from the same sources and range from 193 to 232 centimeters per second, with an average of 215 centimeters per second. Inasmuch as burning velocity changes very rapidly with hydrogen concentration near stoichiometric, the wide range of values is to be expected.

Effect of mixture composition. - Figure 7 shows typical plots of burning velocity against hydrogen concentration taken from four recent

investigations (refs. 10, 26, and 27 and unpublished data). As already stated, the maximum occurs near 43 percent hydrogen; the curves fall off smoothly on either side. It should be noted that maximum burning velocity occurs in a mixture richer than either the stoichiometric mixture or the maximum-flame-temperature mixture. Discrepancies among results of various workers become quite large on a percentage basis, especially for mixtures rich of the maximum-burning-velocity mixture. It does not seem possible to account for these differences at present.

Burning-velocity measurements cannot be extended too far to the lean side of stoichiometric. Because of preferential diffusion effects, the tip of a burner flame may open up in mixtures leaner than 17 percent hydrogen (ref. 30), and a stream of mixture may escape the flame zone without being burned.

Effect of initial mixture temperature. - Figure 8 is a logarithmic plot of burning velocity against initial temperature for several mixtures. The solid lines with symbols are unpublished NACA data. The dashed line represents the maximum burning velocities of Passauer (ref. 2), which are considered less reliable than the more recent data. It appears from figure 8 that the mixture of maximum burning velocity is least sensitive to changes in initial temperature. The following equation expresses the relation between initial temperature and maximum burning velocity over the range of temperatures given:

$$U_{L,max} = 0.09908 T_0^{1.413} \quad (1)$$

The exponent on  $T_0$  is considerably less for hydrogen-air mixtures than for hydrocarbon-air mixtures. For example, expressing some of the data of reference 31 in the form of equation (1) gives temperature dependencies of  $U_{L,max}$  of about  $T_0^{1.64}$  and  $T_0^{1.85}$  for *n*-heptane and isooctane, respectively.

Effect of pressure. - Measurements of burning velocity at pressures other than atmospheric are difficult; this is especially true for reduced pressures. The experimental difficulties are reflected in large discrepancies in the data of the few workers who have studied hydrogen-air mixtures. Reference 17 reports nearly constant burning velocity at total pressures from 1 to 4 atmospheres. Reference 32 gives values of 164 centimeters per second at 0.393 atmosphere and 140 centimeters per second at 1 atmosphere for a mixture with  $\phi = 4.78$ . Reference 26 reports that the burning velocity of a mixture with  $\phi = 3.58$  increased when the pressure was raised from 0.25 to 1.0 atmosphere, and reference 27 gives data showing the same trend between  $\phi = 1.10$  and  $\phi = 1.90$ .

The data of reference 26 are probably most nearly right, because the spherical-bomb technique is not subject to some of the important

sources of error that affect results obtained by other methods. Moreover, a previously unsuspected effect was discovered that may explain some of the discrepancies in pressure dependence reported in the literature. It is generally agreed that burning velocity is proportional to the pressure raised to some power. The disagreements concern the value and sign of the exponent. Manton and Milliken (ref. 26) studied many fuel-oxygen-inert-gas mixtures with atmospheric burning velocities from 8 to 1000 centimeters per second and determined  $x$  for each mixture from the empirical relation

$$U_{L,a}/U_{L,b} = (P_a/P_b)^x \quad (2)$$

When these values of  $x$  were plotted against the reference burning velocity  $U_{L,a}$  (the value at atmospheric pressure), data for all mixtures defined a single curve. The curve, which is reproduced from reference 26 in figure 9, shows that the pressure dependence of burning velocity is variable and depends on the reference burning velocity. Thus, slow-burning mixtures ( $U_L < 50$  cm/sec) have a negative pressure exponent, and hence  $U_L$  increases as pressure decreases; whereas for fast-burning mixtures ( $U_L > 100$  cm/sec) the reverse is true. In the intermediate range ( $50$  cm/sec  $< U_L < 100$  cm/sec) there is no effect of pressure. Figure 7 shows that both zero and positive pressure exponents may be expected for hydrogen-air mixtures, depending on the fuel concentration; negative exponents should appear for very rich or very lean mixtures only. In any case, the exponent should be small.

The work of reference 27 agrees qualitatively with that of reference 26 but shows pressure dependence to be much larger. Figure 10 shows burning velocities from references 26 and 27 plotted logarithmically against pressure for four rich equivalence ratios. The data from reference 27 were obtained by a Bunsen burner total-area method, and care was taken to avoid quenching effects from too-small burner tubes. The straight lines obtained support the assumption of reference 26 that the data follow a relation like equation (2); however, the slope  $x$  varies randomly between 0.208 and 0.256 for equivalence ratios from 1.10 to 1.90, the average value being 0.23 (ref. 27), whereas figure 9 would predict a slope of less than 0.1.

The cause of the discrepancy between references 26 and 27 is not known. Reference 27 tries to resolve the question with the aid of certain theoretical relations among combustion properties, but the result is inconclusive. One relation favors the small pressure dependence of reference 26, while the other favors the larger dependence of reference 27. In any event, recent work agrees that burning velocity of hydrogen-air flames increases with increasing pressure. Pending further evidence, it is suggested that a pressure exponent of 0.16 may be used to estimate

the pressure effect for mixtures near the maximum burning velocity without causing too great an error. The suggested value is the average of those reported in references 26 and 27.

### Turbulent Burning Velocity

A flame in turbulent flow differs considerably in appearance from a laminar flame. Both the naked eye and time-exposed photographs show the luminous zone as a brush-like region, thin near the burner port, thicker toward the top of the flame, and of more or less indefinite extent. It is not yet known whether the flame brush represents a thickened reaction zone or a laminar flame that has been wrinkled, distorted, and caused to fluctuate by the turbulence. As a result, there is no flame surface on which burning-velocity measurements should obviously be based, and it is necessary to choose some arbitrary surface.

The only turbulent burning velocities that have been measured for hydrogen-air flames are given in reference 33. A mean flame surface was chosen in images of visible flames and its area was measured. All measurements were made on a 1.02-centimeter-diameter burner at a Reynolds number of 3500, over a range of pressures from 0.30 to 0.75 atmosphere, and at an equivalence ratio of 1.8. The data are shown in figure 11; the laminar-burning-velocity curve (ref. 27) is included for comparison. As is generally observed, the turbulent burning velocities are higher than the laminar under the same conditions of temperature, pressure, and composition. The turbulent burning velocities appear to depend on pressure a little more than do the laminar, and as a result the extrapolated turbulent line crosses the experimental laminar line. It is very difficult to understand why this should be true; one suspects that turbulent burning velocities based on a mean flame surface may have little meaning at low pressures. Much work needs to be done on the nature of turbulent flames before turbulent burning velocity can have real meaning. At present it is only possible to make the following qualitative statement: For the most part, turbulent flames consume mixture more rapidly than laminar flames; that is, the maximum flow velocity at which the mixture can be completely burned is larger for turbulent flames than for laminar flames.

### QUENCHING DISTANCE

Flames are quenched by excessive loss of heat or active particles or both to adjacent walls. Experiments have shown that flames in a mixture of given temperature, pressure, and composition, cannot pass through openings smaller than some minimum size. This size is the quenching distance. Its actual magnitude depends on the geometry; for instance, the minimum diameter for a cylinder is greater than the minimum separation distance of parallel plates. The geometrical relations among

quenching distances for ducts of various shapes have been worked out theoretically and agree quite well with experiment (refs. 34 and 35).

Effect of mixture composition. - In figure 12 quenching distances (minimum separation of parallel plates) from reference 36 (pp. 408 to 412) are plotted against fuel concentration. The data were obtained in connection with measurements of ignition energy. The curves show minimum quenching distances at or near stoichiometric composition. The minimum quenching distance at 1 atmosphere and ambient temperature is 0.063 centimeter. From data given by Friedman (ref. 8) one may interpolate a value of 0.057 centimeter for a stoichiometric hydrogen-air mixture. This number, obtained in an entirely different way (by the flashback technique), agrees fairly well with the value given by reference 36.

For a stoichiometric hydrogen-oxygen mixture, Friedman's data indicate a quenching distance of 0.019 centimeter (ref. 8). It is not known how close this would be to the minimum of the curve.

Effect of pressure. - Figure 13 is a logarithmic plot of quenching distance for parallel plates against pressure. There are data for three equivalence ratios from reference 37. Four points from work by Lewis and von Elbe (ref. 36) for an equivalence ratio of 1.0 are also included. It is believed that the data of reference 37 are more nearly correct because of the method used (described in ref. 38).

The straight lines in figure 13 show that

$$d_q \propto p^{-x} \quad (3)$$

The pressure exponent  $x$  varies with hydrogen concentration. The data of reference 37 give the following pressure dependencies: for  $\phi = 0.5$ ,  $x = 1.051$ ; for  $\phi = 1.0$ ,  $x = 1.138$ ; and for  $\phi = 2.0$ ,  $x = 1.097$ .

Effect of temperature. - No data are available on the temperature dependence of quenching distance for hydrogen-air mixtures. However, it may be assumed that the quenching distance decreases as the temperature of the mixture (and of the surface) is raised; in other words, the flames will be able to pass through smaller openings. This statement is based both on theory (ref. 39) and on the behavior observed for propane-air flames (ref. 40).

Effect of nature of quenching surface. - No appreciable effect of the nature of the surface on quenching distance has ever been found. In an attempt to observe a change for hydrogen flames, Friedman (ref. 8) lined his apparatus with platinum, which is an efficient catalyst for hydrogen atom recombination. No effect was found for the hydrogen-oxygen-nitrogen mixture used.



~~CONFIDENTIAL~~

Flame traps. - In the quenching-distance experiments just discussed, there was no large pressure gradient driving the flame and hot gas, and the flame had to propagate on its own through the constricted space. In practical operations the situation is often quite different. For example, a flame traveling through a long duct filled with combustible mixture may build up a large pressure, and the flame may be driven through a gap narrower than the quenching distance. Flame traps are commonly used to protect such systems. For hydrocarbon-air mixtures fine-mesh screens are often used; hydrogen flames are more difficult to quench, however, and other methods are necessary.

The value of sintered metals as flame traps was studied in the work of reference 41. These traps were able to stop flames in stoichiometric hydrogen-oxygen mixtures, and thus would be even more effective with hydrogen-air flames. Also important is the fact that the sintered-metal traps cause surprisingly small pressure drops.

The results of reference 41 are reported in terms of the limiting safe pressures below which the trap will always stop the flame. A sintered bronze disk 0.235 inch thick, with a statistical particle size of 0.01575 inch and a porosity of 29.6 percent, gave a limiting safe pressure of more than 1 atmosphere for stoichiometric hydrogen-oxygen flames. Little correlation was found between flame-trap effectiveness and porosity, but there was a gain in effectiveness as the disks were made thicker. Sintered bronze was more effective than sintered stainless steel.

The work of reference 41 was of a preliminary nature, and it is not clear how specific the results may have been to the particular apparatus used. It appears at present that the only sure way to design a flame trap for a given hydrogen-air system is by means of tests on a full-scale model. A word of caution: these sintered disks are flame stoppers, and they may not be effective against detonations. (Detonation waves and the transition of flames to detonations are discussed in a later section.)

#### FLAMMABILITY LIMITS

The rich and lean flammability limits are the fuel concentrations that bound the flammable range at a given temperature and pressure. Mixtures containing more fuel than the rich limit or less than the lean limit will not sustain a flame. No extensive survey of flammability limits was made for the present work, since this had already been done by Coward and Jones (ref. 42).

~~CONFIDENTIAL~~

Flammability limits should be physicochemical constants of a fuel-oxidant combination and should be free of apparatus effects. However, wall-quenching may have an effect on flammability limits. It was therefore desired to delay consideration of the subject until flame quenching had been discussed.

In the usual method of measuring flammability limits (ref. 42) mixtures are ignited at one end of a tube, which is wide enough to preclude quenching, by an ignition source strong enough to ensure that it is not the limiting factor. The tube is quite long (about 4 ft) so that the observer can be sure the flame does indeed propagate on its own and is not driven by excess ignition energy. If the flame travels the full length of the tube, the mixture is considered flammable. Various mixtures are tested until the flammability limits are defined.

Effect of direction of propagation. - The flammability limits for most fuels vary, depending on whether they are measured for upward- or downward-propagating flames, because convection assists flames traveling upward. For instance, the lean and rich limits of methane are: upward, 5.3 and 13.9 percent by volume in air; downward, 5.8 and 13.6 percent by volume in air (ref. 42). For hydrogen the behavior is different. The rich limit of hydrogen is the same for both directions of flame travel, 74 percent by volume in air (ref. 42). The lean limit is affected, but not in the usual way. It is 9.0 percent for downward propagation (ref. 42), whereas for upward propagation there are two lean limits. One of them is called the limit of coherent flames; it is 9.0 percent (ref. 43) and is the leanest mixture that burns completely. Leaner mixtures down to the noncoherent limit of 4.0 percent are still flammable (ref. 43), but the flame is made up of separated globules that slowly ascend the tube. Although these globules do not consume all the fuel, they have to be reckoned with for safety. The noncoherent flames occur because of the high diffusivity of hydrogen; it appears that the flamelets actually consume a mixture richer in hydrogen than the original mixture (refs. 36 and 42).

Flammable range. - The flammable range, that is, the difference between the rich- and lean-limit concentrations, is exceptionally wide for hydrogen. Coherent flames can propagate in lean hydrogen-air mixtures down to 9.0 mole percent fuel, as already stated. This is an equivalence ratio of about 0.24, as compared with a lean flammability limit of about  $\phi = 0.5$  for most hydrocarbon fuels. The very high rich limit, 74 percent or  $\phi = 6.8$ , is also outstandingly different from those for most ordinary fuels. From figure 2, it may be seen that the lean- and rich-limit flame temperatures are about 1000° and 1200° K, respectively, values much lower than those for hydrocarbons (ref. 43). Egerton suggests that these effects peculiar to hydrogen are due to the high concentration of active particles and their high mobility (ref. 43).

Recommended limits at atmospheric temperature and pressure. - As shown by the data collected in reference 42, the various workers who have used the accepted method agree with one another quite well. It is therefore unnecessary to make any further assessment of the data. The following table gives recommended flammability limits for hydrogen in air at atmospheric pressure and about 300° K:

	Flammability limits, volume percent hydrogen in air	
	Lean	Rich
Upward propagation		
Coherent flame	a <sub>9.0</sub>	b <sub>74</sub>
Noncoherent flame	a <sub>4.0</sub>	
Downward propagation	b <sub>9.0</sub>	b <sub>74</sub>

<sup>a</sup>Ref. 43.

<sup>b</sup>Ref. 42.

For hydrogen burning in pure oxygen the lean limits are about the same and behave in the same way as those for hydrogen in air. The rich limit for upward propagation is 93.9 percent (ref. 42).

Effect of mixture temperature. - The flammable range is widened by heating the unburned mixtures. That is, the lean limit occurs at lower concentrations and the rich limit at higher concentrations as the mixture temperature is increased. The data of White (ref. 44), which are considered most reliable by Coward and Jones, are plotted in figure 14. These are limits for downward propagation, so the lean limits refer to coherent flames. There is a linear change in the limits with mixture temperature, and the rich limit is somewhat more strongly affected than the lean. From figure 14 and the flame temperatures of figure 5, it can be seen that the rich limit for all mixture temperatures occurs for mixtures having a nearly constant flame temperature of about 1300° K. The lean-limit flame temperature is lower but more variable; for  $T_0 = 300^\circ \text{K}$ , it is 1060° K; and for  $T_0 = 600^\circ \text{K}$ , it is 1140° K.

Effect of inert diluents. - By addition of enough inert gas to a flammable hydrogen-air mixture, the mixture can be diluted to nonflammability. Figure 15 shows the limits as a function of the amount of carbon dioxide or of added nitrogen in air (ref. 42). The rich limit is sharply decreased as inert gas is added, whereas the lean limit is scarcely changed. From the coordinates of the "nose" of the curve one may calculate that no mixture of hydrogen, air, and nitrogen can propagate flame at atmospheric temperature and pressure if it contains less

than 4.9 percent oxygen; similarly, no mixture of hydrogen, air, and carbon dioxide can propagate flame if it contains less than 7.5 percent oxygen. It thus takes more nitrogen than carbon dioxide to prevent flame propagation, presumably because of the greater heat capacity of the latter. Water vapor behaves about like carbon dioxide, even though it is a product of combustion; the oxygen limit in this case is about 7.5 percent at 86° C (ref. 42).

Other diluents are much more effective than nitrogen or carbon dioxide in reducing flammability. "Air" containing 14.8 percent methylbromide or 39 percent dichlorodifluoromethane cannot form flammable mixtures with hydrogen (ref. 45). Such compounds may interfere chemically with combustion reactions and should not be considered merely inert diluents. Reference 42 warns that the result obtained with methylbromide may not apply in practice, because some mixtures of methylbromide and air are themselves flammable with a sufficiently strong ignition source.

Effect of pressures below 1 atmosphere. - Coward and Jones (ref. 42) summarized the literature on effects of reduced pressure on flammability limits. They observed that the flammable range narrowed as the pressure was reduced, gradually at first, and more rapidly below 200 or 300 millimeters of mercury. A minimum pressure was reached, below which no mixture propagated flame. It is now known that such results are due to wall-quenching. As shown in the section on quenching distance, the walls exert a larger effect at low pressures. It has been found that a plot of "flammability limit" against pressure is merely a curve showing the concentrations and pressures for which the quenching distance is equal to the diameter of the flame tube (ref. 46).

In other words, it appears that the flammability limits are unchanged at reduced pressures and that flame can propagate down to extremely low pressures if the flame tube is large enough. For example, Garner and Pugh (ref. 47) found a limit of 4 millimeters of mercury for hydrogen-oxygen flames in a 10-centimeter tube. Presumably this trend would continue to still lower pressures with larger tubes.

The pressure-concentration boundary for flame propagation imposed by quenching in a particular tube is often useful for practical applications. Although such data have not been measured for hydrogen-air flames, they may be estimated from quenching distances. Figure 16 shows estimated curves for downward flame propagation in cylindrical tubes from 0.02 to 20 inches in diameter. The curves were constructed from the quenching distances of reference 37 (measured with parallel plates) multiplied by a geometrical factor of 1.53 (ref. 35) to convert them to quenching distances for cylindrical tubes. Flames are expected to propagate at pressures as low as 2 to 3 millimeters of mercury in a 20-inch-diameter tube (fig. 16). Some of the curves are extended to rich and

lean mixtures to illustrate the probable behavior as the rich and lean flammability limits are approached. An estimated curve is also included for upward propagation of noncoherent flames in lean mixtures in a 2-inch-diameter tube. Although figure 16 represents the best estimates that can be made, it is emphasized that the curves for the larger tube diameters were obtained from long extrapolations of the data of reference 37.

Effect of pressures above 1 atmosphere. - The effects of high pressure on flammability limits are not well established. The data surveyed in reference 42 indicate that the flammable range is narrowed by the first increases in pressure, perhaps up to 5 atmospheres; thereafter, the range is gradually widened. In any event, the effects appear to be small. At pressures as high as 100 atmospheres, the limits are not much different from the atmospheric values.

#### SPARK IGNITION ENERGY

The modern method of measuring spark ignition energy was designed mainly by Lewis and von Elbe and is discussed fully in reference 36. A measured amount of electrical energy in the form of a short-duration capacitance spark is introduced very rapidly into a mixture of given pressure, temperature, and composition and with a given electrode separation. The smallest energy that will ignite the mixture is found, and the process is repeated for other electrode spacings to find the gap for which the energy is least. The data are more reproducible if the electrodes are flanged at the tips with a dielectric material. Then the spacing for minimum ignition energy is equal to the quenching distance. Lewis and von Elbe were the first to recognize the importance of the quenching effect in such measurements.

The ignition-energy data to be discussed were all obtained by the general method just described. However, they represent ideal conditions that are not met outside the laboratory, so one should not expect the small energies found under these conditions to be sufficient for practical ignition systems. For instance, the gap of a spark plug is fixed, so it may be less than the quenching distance under some conditions (although ignition is still sometimes possible if enough energy is expended to heat the electrodes and to increase the volume of the discharge). Furthermore, the laboratory measurements are made in quiescent mixtures, whereas in practical cases the gas is usually moving and may be turbulent. Finally, the spark duration may affect the energy needed for ignition. No work is known to have been done on the effects of flow velocity, turbulence level, and spark duration on ignition energies of hydrogen-air mixtures. Studies with propane-air mixtures show that ignition energy increases with velocity and turbulence intensity (ref. 48), and the same trends would no doubt appear with hydrogen-air mixtures.

As to the effect of spark duration, for hydrocarbon fuels sparks lasting 100 to 1000 microseconds give lower ignition energies than slower or faster sparks (refs. 48 and 49).

The remaining variables, temperature, pressure, and composition, have been studied and are discussed in the next paragraphs. It is again pointed out that the small energies cited may not suffice for practical cases, but the trends should apply.

Effect of mixture composition. - Figure 17 is a plot of ignition energy in millijoules against fuel concentration for mixtures at atmospheric temperature and several pressures (ref. 36). The 1-atmosphere curve indicates a minimum energy of 0.019 millijoule at about the stoichiometric mixture and rises steeply toward the lean and rich flammability limits. By way of contrast, the ignition energy of a 70-percent mixture of hydrogen in oxygen is 0.007 millijoule (ref. 36), and this is apparently not the minimum of the ignition-energy - concentration curve.

Effect of pressure. - As the pressure is lowered, the ignition energy increases rapidly, as shown by figure 17. Although there are too few points to define the curves closely, it appears that the minimum occurs near stoichiometric regardless of the pressure. The minimum ignition energies change by more than an order of magnitude over the pressure range studied.

Figure 18 is a logarithmic cross plot of data from figure 17 for three equivalence ratios. Although curves might have been faired through the data more closely, a linear relation was assumed so as to show the average effect of pressure. This effect is, approximately,

$$I \propto P^{-x} \quad (4)$$

Data from reference 9 for stoichiometric mixtures are also included; the points are higher than those from reference 36 and also show a greater pressure dependence. There is too much scatter in both sets of data to define the slopes of the lines very well, but in general the exponent  $x$  in equation (4) has a value of about 2.

Minimum ignition pressures are sometimes reported for various fuels. These pressures are obtained with fixed electrode spacings and occur either because of quenching effects or because of the limited spark energy available. In other words, it has not yet been shown that there is an absolute low-pressure limit below which ignition can never occur. However, minimum ignition pressures are of practical value. For example, it is possible to ignite the most favorable hydrogen-air mixture down to 0.015 atmosphere by use of a gap 0.28 centimeter wide and 8.64 joules of energy (ref. 50). This is one of the cases mentioned earlier, in which

the quenching effect may be overpowered by sufficient energy, because the gap is less than the quenching distance at pressures less than about 0.2 atmosphere (fig. 13).

Effect of temperature. - Reference 51 contains the only work found on the effect of mixture temperature on spark ignition energy. The authors state that the following relation holds, except perhaps at temperatures less than 243° K:

$$\log I \propto 1/T_0 \quad (5)$$

The position of the minimum in curves of ignition energy against fuel concentration shifted to leaner mixtures as the temperature was increased. The following table gives the data of reference 51 for stoichiometric hydrogen-air mixtures at a pressure of 1 atmosphere:

Mixture temperature, °K	Spark ignition energy, millijoules
273	0.0315
298	.028
373	.018

#### FLAME STABILITY

Flames are stable because of interactions among the flame, the flow, and nearby solid surfaces. If a condition of a stable flame seated on a burner port or flameholder is changed (e.g., flow velocity), the flame may not remain seated. With burner flames, flashback or blowoff may occur; with flames on flameholders in ducts, flashback is not usually encountered, only blowoff. The mechanisms of stabilization for the two kinds of flames are different, so the data are discussed separately.

#### Flashback and Blowoff of Burner Flames

The flashback and blowoff of burner flames are governed by the gradient of flow velocity near the burner wall, as pointed out by Lewis and von Elbe (ref. 36). Burner stability data are, therefore, usually correlated by plotting the critical boundary velocity gradient calculated for the conditions at flashback  $g_f$  or at blowoff  $g_{bo}$  against

fuel concentration. The gradients are given by the following expression (ref. 52):

$$g_{f,bo} = \frac{FRe}{2d} \quad (6)$$

Reference 52 contains friction factors to be used for various regimes of laminar and turbulent flow. For laminar flow in long cylindrical tubes,  $F = 16/Re$ ; hence,

$$(g_{f,bo})_L = 8U/d \quad (7)$$

Flashback. - Figure 19 shows the only data found for flashback of laminar hydrogen-air burner flames at atmospheric temperature and pressure (ref. 53). Critical boundary velocity gradients are plotted against fuel concentration. The solid curve represents flashback completely into the burner tube. The dashed curves refer to cases in which the flames tilted and partly entered the tube before finally flashing back. In these cases the burner wall was presumably well heated, and thus quenching was reduced and the flames were more prone to flash back; consequently, for a given mixture and burner diameter a higher flow velocity was required to prevent flashback, and  $g_{f,L}$  was accordingly greater.

The effects of reduced pressure on flashback of laminar hydrogen-air flames have recently been studied (ref. 27). In that work tilted flames were considered to have flashed back, even though they only partially entered the burner. Since tilted flames existed over a pressure range of only a few millimeters of mercury, little error was incurred. Figure 20 shows curves of  $g_{f,L}$  against fuel concentration for two reduced pressures; the atmospheric curve from figure 19 is repeated for comparison. The maximum occurs near 38 percent hydrogen regardless of the pressure. The pressure dependence of  $g_{f,L}$  for equivalence ratios from 0.95 to 2.25 can be expressed as follows (ref. 27):

$$g_{f,L} \propto P^{1.35} \quad (8)$$

All the data discussed were obtained with a water-cooled burner. If the burner is not cooled, the results are not reproducible and depend on the burner size and the thickness and material of the burner wall. Such effects were studied by Bollinger and Edse for hydrogen-oxygen mixtures (ref. 54).

Reference 33 extends the study of flashback at reduced pressures to turbulent flow. The critical boundary velocity gradients for flashback  $g_{f,T}$  were calculated by means of equation (6) by use of the appropriate



friction factor. In figure 21 data from reference 33 for three pressures are plotted against mole percent of hydrogen in air. Comparison with figure 20 shows that the values of  $g_{f,T}$  are much larger than those of  $g_{f,L}$  but that the peaks of the curves occur at about the same concentration. Reference 33 reports the following pressure dependence of  $g_{f,T}$ :

$$g_{f,T} \propto p^{1.31} \quad (9)$$

Within experimental error the exponent is the same as that for laminar flames (eq. (8)). Therefore, the following relation holds, regardless of pressure, burner diameter, and composition:

$$\frac{g_{f,T}}{g_{f,L}} = 2.8 \quad (10)$$

It is hard to explain why  $g_{f,T}$  should be almost three times as large as  $g_{f,L}$ . Turbulent burning velocities are not enough greater than laminar burning velocities to account for equation (10). Reference 33 tentatively concludes that the explanation lies in the penetration of the flame into the laminar sublayer at the burner wall and that the flame approaches the wall more closely in turbulent than in laminar flow.

Blowoff. - In figure 22 the known data for blowoff of hydrogen-air burner flames at atmospheric pressure are shown as  $g_{bo}$  plotted against fuel concentration. The work was done by von Elbe and Mentser (ref. 53), who correlated their data in terms of  $g_{bo}$  as calculated by equation (7), the simple equation for laminar flow. However, the points they took in the turbulent flow regime fell off the curve. It was later shown by Wohl, Kapp, and Gazley (ref. 55) that all the data would fall nicely on a single curve if  $g_{bo}$  were calculated by the correct expression, equation (6). It is the latter curve that is reproduced in figure 22. For laminar flow equation (7) was used, while for turbulent flow the gradient was calculated from equation (6) in the following form:

$$g_{bo,T} = \frac{0.023 \text{ Re}^{0.8} U}{d} \quad (11)$$

The data cover only a limited range of hydrogen concentrations, those lean of stoichiometric. However, on the basis of work with other fuels the blowoff curve for open burner flames is expected to level off with increasing equivalence ratio; at some rich equivalence ratio blowoff

would stop and would be replaced by flame lifting (ref. 55). This would occur because of dilution of rich mixtures by ambient air. If ambient air is excluded, as in a Smithells burner, the blowoff curve peaks at a concentration near that for maximum burning velocity, just as does the flashback curve (see figs. 19 to 21).

Further burner blowoff data, obtained at reduced pressures in both laminar and turbulent flow, are reported in reference 33. These data do not fit into a simple correlation with boundary velocity gradient, such as the one shown in figure 22. Blowoff of hydrogen-air flames from burners is not fully understood, and the theoretical model (ref. 36) which leads to the concept of a critical boundary velocity gradient may have to be modified (ref. 33).

#### Blowoff of Confined Flames from Flameholders

Flames held on bluff bodies in ducts owe their stability to the recirculation zone behind the flameholder. This zone may be thought of as a pilot which keeps the main flame established as long as it is able to ignite the mixture flowing past. Blowoff occurs if the main stream flows so fast that sustained ignition cannot be achieved. The flow velocity at which this condition arises depends on the size and shape of the flameholder as well as on the temperature, pressure, and composition of the incoming mixture.

Most flameholder blowoff data are correlated on a single curve by plotting fuel concentration against a parameter of the form

$$U_{bo}/D^x P^y T_o^z = f(\phi) \quad (12)$$

where  $x$ ,  $y$ , and  $z$  are empirical exponents, all positive in sign (ref. 52).

DeZubay reports the following correlation parameter for blowoff of hydrogen flames from disk-type flameholders in reference 56:

$$U_{bo}/D^{0.74} P^{0.61} = f(\phi) \quad (13)$$

(The data are not given in ref. 56, however.) The work on which this parameter is based was done at reduced pressures. The effects of mixture temperature were not studied. DeZubay pointed out that the maximum value obtained for the parameter was 11 times as great as the corresponding maximum value for propane-air flames, an effect that reflects the much greater stability of hydrogen flames.

The work of reference 57 dealt with the effects of the diameter of water-cooled cylindrical-rod flameholders. It was found that there are the following two separate regimes of flameholder stability:

(1) Laminar-flame regime. The composition of the mixture burning in the recirculation zone behind the flameholder is affected by molecular diffusion. Since hydrogen diffuses more readily than oxygen, in contrast to almost all ordinary fuels, small flameholders actually stabilize hydrogen flames to higher flow velocities than do larger flameholders at a given lean equivalence ratio.

(2) Turbulent-flame regime. At a Reynolds number near  $10^4$  the recirculation-zone shear region becomes turbulent. The stability behavior of lean hydrogen flames reverses, and larger flameholders become more effective. Zukoski (ref. 57) concludes from an examination of the literature that for mixtures near stoichiometric the blowoff velocity for any fuel varies approximately as the square root of the flameholder diameter in the turbulent-flame regime. His data are not complete enough to support this conclusion for the specific case of hydrogen-air flames; however, DeZubay's statement that  $U_{bo} \propto D^{0.74}$  for hydrogen flames supported on disks (ref. 58) is in general agreement with Zukoski's conclusion.

These points are perhaps clarified by figure 23, which shows data adapted from reference 57. It appeared that the blowoff velocities and rod diameters corresponding to low Reynolds numbers could be correlated roughly by the parameter  $U_{bo}/D^{-0.384}$ . (Note the negative diameter exponent, which agrees with the discussion just given of the laminar-flame regime.) This parameter was accordingly plotted against equivalence ratio. Solid data points correspond to flow velocities and rod diameters such that  $Re > 10^4$ , and open data points to those such that  $Re < 10^4$ . It is clear from figure 23 that two blowoff curves are obtained. One is defined by points for which  $Re > 10^4$ , and the other by points for which  $Re < 10^4$ .

The fact that flames were stabilized at very lean equivalence ratios (fig. 23) provides added proof that the recirculation zone is enriched by diffusion. The mixtures were homogeneous and would not ordinarily be expected to support combustion below the flammability limit for coherent flames, that is, below  $\Phi \approx 0.24$ .

Figure 23 also makes it clear that much work remains to be done on the flameholder stability of hydrogen-air flames; the data are confined to lean mixtures and small flameholders. The difficulty is that the flames are extremely stable, and large air-handling facilities are needed to provide flows high enough to cause blowoff.

## DETONATION PROPERTIES

Under certain conditions an ordinary flame traveling through a vessel filled with combustible mixture can transform into a detonation. The detonation wave then advances at several times the speed of sound into the unburned mixture.

Whereas in ordinary flames there is a small pressure drop from the unburned to the burned gas, in a detonation there is a very considerable pressure rise. The calculated ratio of pressure behind the wave, in the burned gas, to that ahead of the wave is 18 for a stoichiometric hydrogen-oxygen mixture and about 15 for a stoichiometric hydrogen-air mixture (ref. 36, p. 607). Moreover, there is a strong convective flow of burned gas following the wave. When such a pressure wave meets an obstacle, the momentum of the burned gas is added to the pressure effect, and very large forces may be exerted.

The reasons for the transformation from ordinary burning to detonation are not fully understood. In the usual laboratory experiments the strength of the ignition source and the diameter and surface roughness of the tube affect the runup distance, that is, the distance from the igniter at which detonation occurs. These variables are, therefore, carefully controlled. The flame, ignited with a minimal ignition source, must travel a considerable distance in a smooth tube before detonation occurs. For a stoichiometric hydrogen-oxygen mixture, for example, the flame must travel 70 centimeters in a 25-millimeter tube at an initial pressure of 1 atmosphere (ref. 36, p. 588). The runup distance decreases with increasing pressure.

In practical cases, however, these distances probably do not apply. Excess ignition energy may tend to drive the flame, and rough walls may cause the gas flowing ahead of it to become turbulent. Both factors would tend to shorten the distance for runup to detonation. Thus, one should not count on a definite runup distance; it is safer to assume that the possibility of detonation always exists if the mixture is within the limits of detonability. However, the onset of detonation could be delayed by making the tube walls of an acoustically attenuating material, such as porous sintered bronze (ref. 59). The runup distance could be increased by as much as a factor of 2. Another safety device is a sudden enlargement in a duct. Reference 60 shows that detonation waves traveling through stoichiometric hydrogen-oxygen mixtures in a 7-millimeter tube were transformed to slow-moving flames on passing an abrupt transition to a larger tube. However, if the larger tube were long enough, a new transition to detonation would subsequently occur.

Figure 24 shows detonation velocities in hydrogen-air and hydrogen-oxygen mixtures plotted against fuel concentration (ref. 36, pp. 585 and 586). The limits of detonability are also shown. For hydrogen-air

mixtures these are 18.3 and 59.0 percent, and for hydrogen-oxygen mixtures, 15 and 90 percent. Since these concentrations are within the flammability limits, not all flammable mixtures are detonable. It is interesting to note that the detonation velocity does not have a pronounced peak at some favored equivalence ratio, as burning velocity does.

It is also noteworthy that detonation velocity depends much less on temperature and pressure than does burning velocity. This can be seen from the data in table IV (ref. 36, p. 583). A temperature increase from 283° to 373° K at constant pressure actually causes a slight drop in detonation velocity, perhaps because the density decreases. At constant temperature the velocity apparently increases slowly with pressure. The same conclusion is reached in reference 61, which extends the study of hydrogen-oxygen mixtures to a pressure of 10 atmospheres. The changes, although consistent in direction, are not far outside the expected error of the measurement.

## EXPLOSION LIMITS, SPONTANEOUS IGNITION, AND THE

### CHEMISTRY OF HYDROGEN OXIDATION

#### Explosion Limits

Description of phenomenon. - When heated to a high enough temperature, a mixture of hydrogen and oxidant may spontaneously ignite after the lapse of some time called the ignition lag. But with certain combinations of pressure and vessel size, the mixture may fail to ignite at a temperature that would cause ignition under other conditions; this is the phenomenon of explosion limits. It is not in the province of this report to give a thorough review of explosion limits; this has been done elsewhere, for example, in reference 36. In the present report the phenomenon is described, some data are shown, and some of the important conclusions as to the chemistry of hydrogen oxidation are presented.

Explosion limits are measured in closed vessels at relatively low temperatures (usually 600° C or less). The ignition lags are reasonably long at such temperatures; in fact, as is pointed out later ignition lags are effectively infinite.

Figure 25 is a collection of curves of explosion limits as a function of temperature and pressure (ref. 36). Consider the solid curve, which is for a stoichiometric hydrogen-oxygen mixture in a spherical vessel 7.4 centimeters in diameter and lightly coated with potassium chloride. Along a vertical line of constant temperature there is at first no explosion. Then at some low pressure the first explosion limit is reached, and the mixture remains explosive with increasing pressure until the second limit is reached. Above the pressure of the second

limit (which increases with increasing temperature) the mixture is non-explosive and only undergoes slow reaction up to the pressure of the third limit. At all higher pressures the mixture remains explosive.

This curve represents limits in the following sense. If data were taken at a series of temperatures and constant pressure, as along the 1000-millimeter-of-mercury isobar of figure 25, the ignition lags would increase more and more rapidly as the temperature was decreased toward  $542^{\circ}\text{C}$ . These lags refer to the time from the instant at which mixture is introduced into the hot vessel until the explosion occurs. Near the temperature of the limit the lags would go up very rapidly from a finite value at a temperature just over  $542^{\circ}\text{C}$  to effectively an infinite value at a temperature just under  $542^{\circ}\text{C}$ . Inasmuch as the system is closed, what really happens is that below a critical temperature reactants are used up and diluted with product (water), and these effects overpower those due to acceleration of the reaction by self-heating and chain-branching.

Effects of variables on explosion limits. - Explosion limits depend on the size of the vessel and the nature of the walls. This is indicated by the dashed curves in figure 25. The larger the vessel, the lower the pressure of the third limit. The junction of the first and second limits is displaced to higher temperatures as the vessel is made smaller. Along the second-limit curve, vessel size has little effect if the diameter is large (7.4 to 10 cm for the data shown), but the pressure is decreased considerably for small vessels.

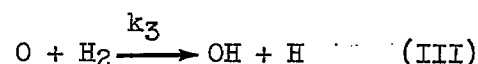
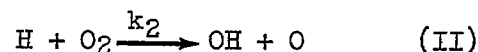
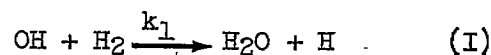
The effects of surface coating with various salts are very pronounced, especially near the junction of the first and second limits. For example, this junction occurs for a 7.4-centimeter flask at about  $340^{\circ}\text{C}$  if the walls are coated with potassium tetraborate and at  $400^{\circ}\text{C}$  if they are lightly coated with potassium chloride.

If nitrogen is added to the stoichiometric hydrogen-oxygen mixture so as to make the mixture stoichiometric hydrogen in air, the second limit in a 7.4-centimeter vessel (with sodium chloride coating) at  $530^{\circ}\text{C}$  is raised from 85 to 117 millimeters of mercury. The mole fraction of nitrogen in such a mixture is 0.558. Other inert gases in the same amount have quite different effects. In argon "air" under the same conditions the limit is raised to about 160 millimeters of mercury. In carbon dioxide "air" the effect is reversed, and the second limit is lowered to 56 millimeters of mercury. The specific effects of these inert gases are clearer if the partial pressures of hydrogen and oxygen in the mixtures are compared, rather than the total pressures. On this basis, argon has no specific effect, because the partial pressures of hydrogen and oxygen total 85 millimeters of mercury. Nitrogen and carbon dioxide both reduce the partial pressure at the second limit, nitrogen, from 85 to 65 millimeters of mercury, and carbon dioxide, from 85 to 31 millimeters of mercury.

In view of the very complicated behavior of explosion limits and their sensitivity to surface effects, it is difficult to answer questions on safety. For example, the question of whether it is safe to heat a static mixture to a given temperature should be accompanied by a statement of the pressure, vessel diameter, and surface nature. Even then, it is unlikely that any experimental data will be found to answer practical questions dealing with metal containers and with the precise mixture under consideration. The data in figure 25 do no more than set very approximate bounds.

### Chemistry of Hydrogen Oxidation

The complex behavior of explosion limits has been used to establish the details of the oxidation of hydrogen. The full story is not given here, but may be found in references 36 and 62. The basic fact is that the oxidation reaction proceeds by a chain mechanism, with the hydrogen and oxygen atoms (H and O) and the hydroxyl free radical (OH) as chain carriers:



The OH radicals that start the sequence are assumed to arise by a reaction between  $\text{O}_2$  and  $\text{H}_2$ , the details of which are not specified (ref. 36). The radicals lead directly to the final product, water, and in so doing produce a hydrogen atom. This starts chain branching (reactions (II) and (III)) in which two chain carriers are produced for each one used up. If left unchecked, chain branching will lead to an explosion through an exponential growth in chain-carrier concentration, and hence, in reaction rate. Actually, reaction (II) is strongly endothermic and occurs very rarely until a sufficiently high temperature is reached. It is for this reason that hydrogen-oxygen mixtures are stable at room temperature.

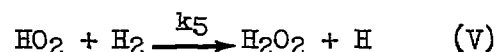
Chain breaking imposes another check on the exponential increase in chain carriers. H, O, and OH may be destroyed if they meet a wall. This is the reason for the existence of the first explosion limit. It occurs at pressures so low that on the average a chain carrier strikes the wall before it has a fruitful collision in the gas phase. However, if the wall reflects rather than destroys the chain carrier, the limit is shifted; this explains the dependence on surface nature.

Chain carriers are also destroyed in the gas phase. The mechanism is probably as follows:



where M is any molecule other than a chain carrier.  $\text{HO}_2$ , while reactive, still can survive long enough to reach the wall, where it may be destroyed. The frequency of these three-body reactions increases with increasing pressure, until at some critical pressure they overcome the chain branching and thereby produce the second explosion limit. Since the second limit is caused by gas-phase events, it is relatively insensitive to vessel factors; but there are some effects when the wall is reflective toward  $\text{HO}_2$  and returns it to the reaction zone.

The mixture again becomes explosive at the third limit, where the pressure is so high that  $\text{HO}_2$  cannot get to the wall before reacting. It is likely that the reaction of  $\text{HO}_2$  in the gas phase is:



(ref. 36). This reaction restores the chain carrier lost in reaction (IV), and chain breaking can no longer overcome chain branching.

This brief discussion explains qualitatively the existence of explosion limits, but is not complete enough to explain all the details of the observed effects, particularly of surface effects. The arguments may be summarized by stating that explosion limits arise because of competition in the gas and at the wall between reactions that inactivate the chain carriers H, O, and OH and those that perpetuate the carriers and increase their number.

### Spontaneous Ignition

Relation between spontaneous ignition and explosion limits. - In the discussion of explosion limits, it is pointed out that the limit could be obtained from the variation of ignition lag with temperature at constant pressure. This would be a spontaneous-ignition experiment. In other words, spontaneous-ignition temperatures lie in the region to the right of an explosion-limit curve such as shown in figure 25.

In general, modern work on spontaneous-ignition temperatures (to which this review is limited) has dealt with conditions that give short ignition lags. Therefore, it has been necessary to use flow systems rather than the static closed systems used in the study of explosion limits, in which the time needed to admit mixture to the hot vessel



becomes long compared to the ignition lag. For every spontaneous-ignition apparatus there should be a particular explosion-limit curve for a given hydrogen mixture, fixed by the size, shape, and material of construction. The curves are seldom determined in practice, so spontaneous-ignition data are taken at conditions removed an unknown distance from the limit curve. Thus, the contributions of the various gas-phase and surface reactions to the spontaneous-ignition process are hard to estimate, even though the chemistry is no doubt the same as it is at the explosion limits.

In summary, explosion limits are determined by the balance between chain breaking and branching and are independent of time. Spontaneous ignition, on the other hand, is a rate process that may be affected to a greater or lesser degree by chain breaking or chain branching, depending on the apparatus, the pressure, and the temperature.

Theoretical considerations. - The complexity of the chemistry of spontaneous ignition has led to attempts to simplify the concepts. The general procedure is to consider the process as a whole and to ignore the individual steps of the reaction mechanism; this type of approach has recently been reviewed in reference 63. For the hydrogen-oxygen reaction one might hope that the reaction rate could be expressed in the following Arrhenius form:

$$w = [H_2]^x [O_2]^y \exp\left(-\frac{E}{RT}\right) \quad (14)$$

(Chemical symbols in brackets denote molar concentrations.) The reasonable assumption is then made that the ignition lag is inversely proportional to the reaction rate:

$$\tau \propto 1/w \quad (15)$$

From equations (14) and (15) the following relation may be obtained:

$$\ln \tau = E/RT - x \ln [H_2] - y \ln [O_2] + \text{Constant} \quad (16)$$

If the concentrations are converted to molecules per unit volume by means of the gas law, the expected pressure dependence may be found:

$$\ln \tau = E/RT - (x + y) \ln P + (x + y) \ln T + \text{Constant} \quad (17)$$

Equation (17) holds for a given mixture.

Equations (16) and (17) are really little more than guides for handling spontaneous-ignition data; they show how to plot the results with a reasonable expectation of getting straight lines. Furthermore, if

a plot of  $\ln \tau$  against  $1/T$  is linear, its slope has the value  $E/R$ ; hence, the slope yields an over-all activation energy, but this value cannot be related to the real chemistry of the process without further consideration.

The procedure just described is about all one can do on theoretical grounds with most fuels, because the combustion chemistry is poorly understood. But hydrogen is one of the few fuels for which the chemistry is known, so the theory of spontaneous ignition can be elaborated. This is done in the following paragraphs, which give new interpretations of the effects of temperature, pressure, and concentration on spontaneous-ignition lags of hydrogen.

The set of reactions (I) to (IV) represents only a part of the total mechanism operative at the explosion limits. The surface chemistry is left out altogether. But for a homogeneous reaction under conditions where the walls are unimportant, that is, at reasonably high pressures, these equations may be sufficient to describe the reaction.

The over-all reaction rate  $w$  is the rate of formation of water:

$$w = d[H_2O]/dt \quad (18)$$

From reaction (I),

$$d[H_2O]/dt = k_1[H_2][OH] \quad (19)$$

After a short induction period, the rate of water formation attains a steady state, and OH concentration becomes (ref. 36, p. 10):

$$[OH] = \frac{1}{k_1[H_2] \left( 1 - \frac{2k_2}{k_4[M]} \right)} \quad (20)$$

Combining equations (19) and (20) gives

$$d[H_2O]/dt = \frac{1}{1 - \frac{2k_2}{k_4[M]}} \quad (21)$$

It is next assumed, as before, that the ignition lag is inversely proportional to the over-all rate (eq. (18)). The following relation is obtained:

$$\tau = c_1 \left( \frac{1 - \frac{2k_2}{k_4[M]}}{1} \right) \quad (22)$$

The nature of the initiation reactions, which are lumped together in the term  $i$ , is fairly well understood (ref. 36, p. 42). If they are introduced explicitly into the simple scheme of reactions (I) to (IV), the calculations become very complicated. For the present purpose it is sufficient to use the pressure dependence of the rate of initiation, and this known from explosion-limit work to be at least as great as second order (ref. 36, p. 37). Therefore, it is assumed that

$$\left. \begin{array}{l} i \propto P^2 \\ \text{or} \\ i = c_2(T)P^2 \end{array} \right\} \quad (23)$$

where  $c_2(T)$  is a proportionality constant dependent on temperature. The concentration  $[M]$ , which refers to any of the molecules of the mixture, is directly proportional to the pressure and inversely proportional to the temperature:

$$[M] = c_3 \frac{P}{T} \quad (24)$$

When equations (23) and (24) are combined with equation (22), the following expression is obtained:

$$\tau = \frac{c_1}{c_2(T)P^2} \left( 1 - \frac{2k_2}{k_4 c_3} \frac{T}{P} \right) \quad (25)$$

In this equation the terms  $c_2(T)$ ,  $k_2$ , and  $k_4$  are all functions of temperature. If the temperature is held constant, the variation of ignition lag with pressure may be investigated. Equation (25) in that case takes the form:

$$\tau = K_1/P^2 - K_2/P^3 \quad (26)$$

Differentiation of equation (26) with respect to pressure shows that the curve of  $\tau$  against  $P$  has either a maximum or a minimum at the place where

$$P = \frac{3K_2}{2K_1} \quad (27)$$

Differentiation a second time shows that at this value of  $P$  the second derivative is negative. Therefore, the curve of  $\tau$  against  $P$  at

constant temperature should have a maximum. Of course the pressure at which the maximum occurs could not be calculated unless the values of the constants were known.

Some remarks may also be made about the variation of ignition lag with temperature at constant pressure. Equation (17), derived from the simplified concepts discussed first, predicts a linear plot of  $\ln \tau$  against  $1/T$  with a slope  $E/R$ . (Data are usually taken over too small a temperature range to show any effect of the other temperature-dependent term in equation (17).) Later in this report it is shown that spontaneous-ignition data do conform to this simple relation. Examination of equation (25) shows that, in order that the linear relation hold, the second term inside the parentheses should be relatively independent of temperature. Then,

$$\tau \propto \frac{1}{c_2(T)} \quad (28)$$

Since the factor  $c_2(T)$  expresses a chemical rate, it may be expected to vary as  $\exp(-E/RT)$ . The observed relation then follows. The advantage of this treatment is that it focuses attention on the reaction whose activation energy is actually obtained from the plot of  $\ln \tau$  against  $1/T$ , that is, on the chain-initiation reaction, not on the propagation or chain-breaking reaction. Physically, it is logical that this should be so in a spontaneous-ignition process.

Finally, the expected dependence of ignition lag on hydrogen concentration may be discussed. The approximate relation, equation (28), is used. Inasmuch as  $c_2(T)$  is related to the chemical rate expression for the chain-initiation process,  $c_2(T)$  depends not only on temperature but also on concentration. Once again, the dependence cannot be stated explicitly because the complete chemical mechanism has not been used. However, explosion-limit studies show that the rate of initiation increases strongly with increasing hydrogen concentration and depends hardly at all on oxygen concentration (ref. 36, p. 40). In fact, oxygen seems to be simply an inert diluent so far as chain initiation is concerned. Therefore, ignition lag should decrease sharply with increasing hydrogen concentration.

The main conclusions of the extended treatment of spontaneous ignition of hydrogen based on real reaction kinetics may be summarized as follows:

- (1) The curve of ignition lag against pressure at constant temperature should show a maximum.

(2) The observed linear dependence of  $\ln \tau$  on  $1/T$  shows that the chain-initiation process is dominant in spontaneous-ignition experiments. Activation energies derived from such plots apply to the initiation process.

(3) Ignition lags should decrease sharply with increasing hydrogen concentration and should show little, if any, dependence on oxygen concentration.

Sources of spontaneous-ignition data. - The subject of the spontaneous ignition of hydrogen is a very old one, but much of the earlier work is only qualitative. The following paragraphs consider the more recent work contained in references 64 to 67. Despite the extensive work on spontaneous ignition, even the data from recent sources are strongly dependent on apparatus. Therefore, data for a particular application are best chosen from work done in a manner that resembles the practical situation in question. For this reason the general features of the experiments reported in references 64 to 67 are described here.

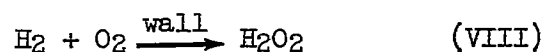
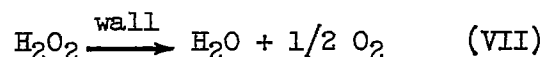
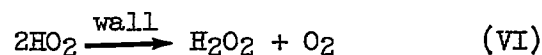
References 64 and 65 report studies at lower temperature and long ignition lags (0.1 to 10 sec). The delays were therefore measured directly and refer to the time from the instant of mixing of hot streams of hydrogen and oxidant to the instant at which flame appeared. References 66 and 67 cover spontaneous-ignition temperatures high enough to give ignition delays in the millisecond range. In these cases stable flame fronts were formed in the ducts, and the lags were calculated from the known average flow velocity and the distance from a zero-reaction point to the flame. The high spontaneous-ignition temperatures are probably not the only cause of the short lags reported in references 66 and 67; the presence of the flame may also have had an effect.

Other sources of discrepancy are the degree of mixing and the method of heating. In the work of reference 66 the hydrogen was injected into an airstream heated (and vitiated) by preburning upstream. In the work of reference 64 the fuel and air were heated separately, and no special effort was made to produce rapid mixing. In reference 65 the gases were heated separately and rapidly mixed. And in the work of reference 67 a premixed stream was heated to a static temperature below the spontaneous-ignition temperature and then passed into a diffuser, where the increase in static temperature and pressure caused ignition. The zero-reaction point in this case was arbitrarily chosen as the diffuser exit.

Effect of temperature. - It has already been pointed out that simple theory anticipates a linear relation between the logarithm of the ignition lag and the reciprocal of the spontaneous-ignition temperature. Figure 26 (taken from ref. 63) shows that this relation does hold for data of two investigators, and it is assumed to hold for the data of

reference 65 as well. This linear relation also reemphasizes the large discrepancies among the various methods, differences of as much as two orders of magnitude.

According to equation (16) or (17), over-all activation energies may be computed from the slopes of these lines. Values are listed on figure 26; they range from 34 to 86 kilocalories per mole. The extended theory points out that the activation energies are over-all values for the chain-initiation process. The wide spread probably means that unrecognized experimental variables affected the results. For example, two points are included in figure 26 from work of Lewis and von Elbe on explosion limits (ref. 68). At pressures near atmospheric such data lie in the same range as those from some of the experiments in flowing systems. However, the presence of a surface effect in this work (salt or sodium tungstate coating) shows that such effects may very well be present in the other data. Chain initiation is indirectly tied in with surface effects through the following reactions (ref. 36, pp. 42 to 43):



Therefore, wall effects may affect the observed activation energy if they act to inhibit one or more of the above reactions. This is a subject that has not been dealt with in spontaneous-ignition work.

Effect of fuel concentration. - It was concluded from the theoretical considerations that ignition lag should decrease with increasing hydrogen concentration but should be quite independent of oxygen concentration. Mullins found no variation with over-all fuel-air ratio for carbon monoxide or methane and implicitly assumed that this result holds for very lean mixtures of any fuel (ref. 66). But in the two experiments in which hydrogen concentration was actually known and was varied, a strong dependence was found. Data of references 65 and 67 are shown in figure 27. Both experiments showed that the lag decreases with increasing hydrogen concentration over the range covered. However, both the form of the dependence and the orders of magnitude of the lags are entirely different in the two cases, even though the spontaneous-ignition temperatures are nearly the same.

There have been no studies in which the oxygen concentration of homogeneous mixtures was systematically varied; however, the data of reference 65 (fig. 27) represent changes in oxygen content from about 13 to 20 percent because of the wide range of hydrogen concentrations

4362

CN-5 back

covered. The data would be expected to deviate from a straight line if there were a very strong effect of oxygen concentration. Other evidence comes from Dixon's experiments (ref. 64), in which hydrogen was injected into both air and oxygen and the differences in the spontaneous-ignition temperature were only 3° to 6° C for a 0.5-second ignition lag. Both sets of data therefore confirm the prediction that ignition lag should be independent of oxygen concentration.

Effect of pressure. - Both Dixon (ref. 64) and Mullins (ref. 66) studied the effect of pressure on spontaneous ignition. Mullins' data are plotted in figure 28; the curves of ignition lag against pressure at constant spontaneous-ignition temperature contain maximums. This agrees with the prediction of the extended theory of spontaneous ignition. As pressure is decreased below 1 atmosphere, ignition lags increase until a pressure near 0.5 atmosphere is reached; further decreases in pressure cause the lags to decrease. Dixon noted similar behavior for constant 0.5-second ignition lag, that is, as pressure was decreased from about 1.5 atmospheres, the curve of spontaneous-ignition temperature against pressure went through a maximum near 1 atmosphere (ref. 64). Thus, there is a difference of about 0.5 atmosphere in the pressure at which these two authors found the promoting effect of reduced pressure to begin. Furthermore, the spontaneous-ignition temperatures at which Dixon found 0.5-second lags were in the range where Mullins found lags of a few milliseconds, so again there was the kind of discrepancy noted in figure 27.

#### Safety Considerations

In view of the many factors that affect ignition lags and spontaneous-ignition temperatures and the wide discrepancies in the results obtained, it is not possible to state absolutely safe limits of temperature and soaking time for hydrogen mixtures. However, it seems significant that the really large differences are found when one compares experiments with and without a stabilized flame. In both figures 26 and 27 the lags found by Mullins and by Fouré with a flame present throughout the test (refs. 66 and 67, respectively) are in the millisecond range; those of all other workers were obtained from systems in which a flame was not initially present and are about two orders of magnitude greater. Considering all the data, it is likely that, in the absence of a flame, hydrogen-air mixtures at 1 atmosphere, either flowing or static, may be held at temperatures up to 550° C for at least 1 second.

In recent work at the Bureau of Mines, minimum spontaneous-ignition temperatures were measured for hydrogen-air mixtures diluted with water vapor (ref. 69). The minimum spontaneous-ignition temperature is the lowest temperature at which a mixture will ignite in a closed apparatus, even if allowed to soak for a very long time, and is therefore the same

as an explosion-limit temperature. Reference 69 reports minimum spontaneous-ignition temperatures from 515° C (no water vapor) to 580° C (30 percent water vapor) at a pressure of 7.8 atmospheres. Other tests showed that pressure has little effect in the interval from 1 to 10 atmospheres. On the basis of these and other data, reference 69 recommends that any temperature above 500° C be considered a potential spontaneous-ignition hazard for long soaking times at pressures near atmospheric. At low pressures, with certain surfaces, ignition can occur at temperatures as low as 340° C (fig. 25).

### RELATIONS AMONG COMBUSTION PROPERTIES

The combustion properties of hydrogen have been discussed more or less individually, and the data are valuable in themselves. However, there are also interrelations among several of the properties which should be pointed out. The importance of these relations is twofold. First, they may be used to estimate voids in the data on one property from available data on another. Second, there are relations between burning velocity and quenching distance from which chemical rates in flames may be estimated. The rates are significant in establishing the volumetric requirements for combustion.

#### Flame Reaction Rates

Combustion properties in general depend both on chemical rates and on transport processes. Certain combustion properties can, however, be combined to give quantities that depend only on one or the other. This can be done only for flames of a given chemical family, such as hydrogen-oxygen-nitrogen flames. In reference 70, a thermal quenching equation

$$\text{Quenching distance} \propto \left( \frac{\text{Transport property}}{\text{Reaction rate}} \right)^{1/2} \quad (29)$$

is combined with a thermal burning-velocity equation

$$\text{Burning velocity} \propto [(\text{Reaction rate})(\text{Transport property})]^{1/2} \quad (30)$$

to give

$$\frac{\text{Burning velocity}}{\text{Quenching distance}} \propto \text{Reaction rate} \quad (31)$$

From this approach, it was calculated (ref. 70) that the average reaction rate in a stoichiometric hydrogen-air flame is 169 (moles)(liter<sup>-1</sup>)(sec<sup>-1</sup>).



The average rates for hydrocarbon fuels are very much lower. The values reported in reference 70 for propane-air and isooctane-air mixtures are 1.04 and 0.24 (mole)(liter<sup>-1</sup>)(sec<sup>-1</sup>), respectively.

The very high reaction rate is the basic reason for the outstanding vigor of hydrogen flames compared to flames of hydrocarbon fuels. Flame temperatures are not much different, so flame temperature is not the driving force of the hydrogen reaction. Hydrogen is oxidized by a free-radical chain mechanism, and the same is probably true for hydrocarbons at or near flame temperatures. It is quite possible that the activation energies of the individual steps of the reaction mechanism are comparable in both cases. However, absolute rate theory shows that reactions of atoms and other small free radicals with the polyatomic hydrocarbon molecules will be as much as 10<sup>-4</sup> slower than the corresponding reactions with the simple diatomic hydrogen molecule, even if activation energies are similar for the two cases. One might speculate, therefore, that hydrogen burns so vigorously because it is a very simple molecule.

#### Relations Useful for Estimating Data

Flashback velocity gradient, burning velocity, and quenching distance. - Wohl has stated that the boundary velocity gradient for flashback is directly proportional to the reaction rate (ref. 55). Reference 71 extends this concept and shows that the reaction rate in question is not complicated by the effects of transport processes and that the following relation holds for flames of a given chemical family

$$g_F^{0.857} \propto \frac{\bar{w}_F}{N_O} \quad (32)$$

It had previously been shown (ref. 70) that burning velocity, quenching distance, and reaction rate are related as follows, as implied by equation (31):

$$\frac{U_L}{d_q} \propto \frac{\bar{w}_F}{N_O} \quad (33)$$

When equations (32) and (33) are combined, the following is obtained:

$$g_F \propto \left( \frac{U_L}{d_q} \right)^{1.168} \quad (34)$$

Figure 29 is a logarithmic plot based on equation (34) for data on hydrogen-air mixtures at 25° C and various pressures. Two sets of recent

atmospheric-pressure burning-velocity data (refs. 10 and 26) were used to show the spread that may be expected (in spite of which the correlation is definite). The line as drawn has a slope of 1.03 rather than 1.168 as predicted by equation (34).

Figure 29 may be used to estimate data on one of the properties involved if the other two properties are known. Aside from this practical purpose, the plot is valuable because it shows that the theoretical ideas leading to equation (34) are probably correct; the same basic chemistry is involved in flashback, flame propagation, and flame quenching. The consistency shown when the results of various workers are plotted in the form of figure 29 indicates that the data are basically correct, even though there is some spread from the usual experimental errors. Results that depart widely from the correlation should be suspected; such a departure might result, for example, if burning velocity were measured at low pressure without proper care to prevent quenching effects.

Burning velocity and quenching distance. - Reference 70 points out that the product of burning velocity and quenching distance should be proportional to a transport property, namely the apparent thermal conductivity (see eqs. (29) and (30)), for chemically similar systems such as various hydrocarbon-oxygen-nitrogen mixtures. From the definition of apparent thermal conductivity given in reference 70 it was predicted that the following relation should hold for such systems:

$$U_L d_q \propto \frac{T_o T_F}{P} \quad (35)$$

It was found that equation (35) holds very well for hydrocarbon-oxygen-nitrogen flames. But attempts to apply the relation to hydrogen-air flames fail, because no account is taken of the very large effects of hydrogen concentration on the transport process. It was found empirically that the following modified relation fits the data fairly well:

$$U_L d_q \propto \left[ \left( \frac{T_o T_F}{P} \right) \left( \frac{n_o}{1 - n_o} \right) \right]^x \quad (36)$$

No attempt is made here to justify equation (36) on theoretical grounds. Figure 30 is a logarithmic plot made according to equation (36) for various hydrogen-air mixtures at reduced and atmospheric pressures. Except for three points at an equivalence ratio of 0.5 and pressures from 0.2 to 0.5 atmosphere, there is little scatter. The chief use of figure 30 is in finding the effect of initial mixture temperature on quenching distance. This effect can be found by use of available data that show the effect of temperature on burning velocity.

Spark ignition energy and quenching distance. - Lewis and von Elbe first pointed out that spark ignition energy and quenching distance yield a correlation line when plotted logarithmically (ref. 36, p. 415). Figure 31 shows such a plot for hydrogen-air mixtures at reduced and atmospheric pressures. The line shown is a segment of a general correlation that fits data on many fuel-oxidant combinations over a range of four orders of magnitude in ignition energy. The theoretical basis for the correlation is not well understood.

Flashback velocity gradient and blowoff from flameholders. - Studies by Zukoski and Marble (refs. 72 and 73) strongly indicate that the mechanism of flameholding on bluff bodies depends on ignition time, provided that the shear region between the free stream and the flameholder wake is fully turbulent. The length of the wake is essentially independent of stream velocity; for cylindrical-rod flameholders, the data of reference 73 indicate that the following relation holds for a wide range of flow velocities:

$$\left( \frac{L}{D^{1/2}} \right) = \text{Constant} = 5.5 \quad (37)$$

where  $L$  and  $D$  are in inches. The ignition time available to the gases flowing along the shear region is

$$t = L/U \quad (38)$$

where  $U$  is in inches per second. If  $t$  is equal to or less than a characteristic value for the given mixture, blowoff will occur because the gas cannot ignite and form a propagating flame; then, equation (38) becomes:

$$t_c = L/U_{bo} \quad (39)$$

Combining equations (37) and (39) yields, for cylindrical-rod flameholders,

$$U_{bo} = 5.5 \frac{\sqrt{D}}{t_c} \quad (40)$$

Ignition along the flameholder wake is known to occur at a temperature close to flame temperature (ref. 73). It is, therefore, reasonable to suppose that the process is one of spontaneous ignition at high temperature. It is assumed in the earlier discussion of spontaneous ignition that the ignition time is inversely proportional to the reaction rate, and in view of the high temperature at which ignition occurs, the rate in question may be taken as the average rate of reaction in a flame. It has already been pointed out that flashback velocity gradient depends

on average flame reaction rate in the manner shown by equation (32). Thus, it follows that

$$t_c \propto \left( \frac{1}{N_{O\&f}} \right)^{0.857} \quad (41)$$

Data on the blowoff of hydrogen-air flames from cylindrical-rod flame-holders at atmospheric pressure have been obtained only for lean mixtures and at low and intermediate Reynolds numbers (ref. 57). However, a complete flashback curve is available. With the aid of the relations just developed, it is therefore possible to estimate a complete blowoff curve. It should be noted that the curve will apply only when Reynolds number is high enough to give a fully turbulent shear layer between the wake and the free stream ( $Re > 10^4$ ).

The proportionality constant in equation (41) is unknown, so the following procedure is used:

(1) From equation (40), a characteristic time  $(t_c)_a$  is computed for a given mixture for which the blowoff velocity from a rod of a particular diameter has been measured.

(2) From equation (41), the following relation may then be expected to hold for other mixtures:

$$t_c = \frac{(t_c N_{O\&f})_a^{0.857}}{N_{O\&f}^{0.857}} \quad (42)$$

Equation (40) and (42) are combined to give the following result:

$$\frac{U_{bo}}{\sqrt{D}} = \frac{5.5 N_{O\&f}^{0.857}}{(t_c N_{O\&f})_a^{0.857}} = f(\phi) \quad (43)$$

For hydrogen-air flames at 1 atmosphere the normalization point for computing  $(t_c)_a$  was chosen at  $\phi = 0.5$ ,  $D = 0.254$  inch,  $U_{bo} \approx 900$  feet per second (ref. 57). The flashback data are from reference 53 (see fig. 19). The estimated blowoff curve is shown in figure 32. For comparison, the same procedure was followed for methane-air flames, using flashback data from reference 74 and blowoff data from reference 72.

Figure 32 shows that the maximum predicted value of  $U_{bo}/\sqrt{D}$  for hydrogen-air flames is more than an order of magnitude greater than that for methane-air flames. This is similar to the result of DeZubay, who found that the maximum value of the correlating parameter for blowoff of hydrogen-air flames at reduced pressure was 11 times greater than that

for propane-air flames (ref. 56). Stability is expected to remain high even in very rich mixtures. The few data points available agree with the calculated curves as well as could be expected, in view of the many approximations involved. Moreover, some of the points actually apply to conditions where the shear layer may not be fully turbulent, and these points of course would not be expected to lie on the curve.

According to equations (32) and (33), the blowoff curve could have been calculated equally well by use of  $U_L/\bar{a}_q$  in place of  $g_f^{0.857}$ . The choice of  $g_f$  was arbitrary.

The effects of pressure on blowoff could be estimated, if in addition to present knowledge the variation of wake length with pressure were known. Work is needed to establish the effects of pressure on the flameholder wake.

A final comment about the calculated blowoff curve: the effects of compressibility are not really known. From the work of reference 73, equation (37) appears to hold up to free-stream Mach numbers of about 0.7. However, the peak value of  $U_{bo}/\sqrt{D}$  in figure 32 implies that the blowoff velocity would be sonic (1640 ft/sec) for a flameholder only about 0.01 inch in diameter. It is not clear how the present analysis might be modified under such conditions.

#### SUMMARY OF RECOMMENDED VALUES OF COMBUSTION PROPERTIES

Table V is presented as a summary of recommended values of the various combustion properties of hydrogen-air mixtures. The values listed are for standard conditions, a pressure of 1 atmosphere and an initial temperature of about 25° C. Wherever possible, data are given for both the stoichiometric mixture and the mixture showing the maximum (or minimum) value. The form of the pressure and temperature dependence is stated, if known. Inasmuch as some of the numbers are averages, or involve the judgement of the authors, references are omitted from table V.

Lewis Flight Propulsion Laboratory  
National Advisory Committee for Aeronautics  
Cleveland, Ohio, April 26, 1957

#### REFERENCES

1. Olson, Walter T., and Gibbons, Louis C.: Status of Combustion Research on High-Energy Fuels for Ram Jets. NACA RM E51D23, 1951.

2. Passauer, H. Eisenstein: Verbrennungsgeschwindigkeit und Verbrennungstemperatur bei Vorwärmung von Gas und Luft. Das Gas- und Wasserfach, Jahrg. 73, Heft 17, Apr. 26, 1930, pp. 313-319; 343-348; 369-372; and 392-397.
3. Morgan, Gerry H., and Kane, Walter R.: Some Effects of Inert Diluents on Flame Speeds and Temperatures. Fourth Symposium (International) on Combustion, The Williams & Wilkins Co. (Baltimore), 1953, pp. 313-320.
4. Jones, G. W., Lewis Bernard, and Seaman, Henry: The Flame Temperatures of Mixtures of Methane-Oxygen, Methane-Hydrogen, and Methane-Acetylene with Air. Jour. Am. Chem. Soc., vol. 53, no. 11, Nov. 1931, pp. 3992-4001.
5. Friedman, Raymond: Measurement of the Temperature Profile in a Laminar Flame. Fourth Symposium (International) on Combustion, The Williams & Wilkins Co. (Baltimore), 1953, pp. 259-263.
6. Gaydon, A. G., and Wolfhard, H. G.: Flames - Their Structure, Radiation, and Temperature. Chapman & Hall (London), 1953.
7. Lewis, Bernard, and von Elbe, Guenther: Remarks on the Experimental Determination and Theoretical Calculation of Flame Temperatures and Explosion Pressures. Phil. Magazine, ser. 7, vol. 20, July 1935, pp. 44-65.
8. Friedman, Raymond: The Quenching of Laminar Oxyhydrogen Flames by Solid Surfaces. Third Symposium on Combustion and Flame and Explosion Phenomena, The Williams & Wilkins Co. (Baltimore), 1949, pp. 110-120.
9. Fenn, John B.: Lean Inflammability Limit and Minimum Spark Ignition Energy. Ind. and Eng. Chem., vol. 43, no. 12, Dec. 1951, pp. 2865-2868.
10. Burwasser, Herman, and Pease, Robert N.: Burning Velocities of Hydrogen-Air Flames. Jour. Am. Chem. Soc., vol. 77, no. 22, Nov. 20, 1955, pp. 5806-5808.
11. Bartholomé, E.: Die Flammengeschwindigkeit in stationär brennenden Flammen. Die Naturwissenschaften, Jahrg. 23, Heft 6, 1949, pp. 171-175; 206-213.
12. Edse, Rudolf: Studies on Burner Flames of Hydrogen-Oxygen Mixtures at High Pressures. Tech. Rep. 52-59, Flight Res. Lab., Wright Air Dev. Center, Wright-Patterson Air Force Base, Apr. 1952. (RDO No. R-467-1.)

13. Lurie, H. H., and Sherman, G. W.: Flame Temperatures of Combustible Gas-Oxygen Mixtures. Ind. and Eng. Chem., vol. 25, no. 4, Apr. 1933, pp. 404-409.
14. Byrne, John F.: The Influence of Atmospheric Oxygen on Bunsen Flames. Fourth Symposium (International) on Combustion, The Williams & Wilkins Co. (Baltimore), 1953, pp. 345-348.
15. Michelson, W.: Ueber die normale Entzündungsgeschwindigkeit explosiver Gasgemische. Ann. der Phys. und Chem., Bd. 37, 1889, pp. 1-24.
16. Ubbelohde, L., und Hofsass, M.: Über die Entzündungsgeschwindigkeit im Innenkegel der Bunsenflamme. Jour. Gasbel., Jahrg. 56, Nr. 51, Dec. 20, 1913, pp. 1225-1232; 1253-1262.
17. Ubbelohde, L., und Koelliker, E.: Zur Kenntnis des Innenkegels der Bunsenflamme. Jour. Gasbel., Jahrg. 59, 1916, pp. 49-57; 65-69; 82-86; 98-104.
18. Bunte, K., und Steding, A.: Über den Einfluss der Wärmeeinstrahlung auf die Entzündungsgeschwindigkeit der Gase. Gas u. Wasserfach, Bd. 71, 1928, pp. 673-677; 701-705; 731-734.
19. Bunte, K., und Litterscheidt, Walter: Die Entzündungsgeschwindigkeit von Gasgemischen. Gas u. Wasserfach, Bd. 73, 1930, pp. 837-842; 871-878; 890-896.
20. Corsiglia, John: New Method for Determining Ignition Velocity of Air and Gas Mixtures. Am. Gas Assoc. Monthly, vol. XIII, no. 10, Oct. 1931, pp. 437-442.
21. Jahn, Georg: Der Zündvorgang in Gasgemischen. Verlag R. Olenbourg, Munchen and Berlin, 1934.
22. Smith, Francis A., and Pickering, S. F.: Measurements of Flame Velocity by a Modified Burner Method. Jour. Res. Nat. Bur. Standards, vol. 17, no. 1, July 1936, pp. 7-43.
23. Bartholomé, E.: Zur Methoden der Messung von Flammengeschwindigkeiten. Z. Elektrochem., Bd. 53, Nr. 4, Aug. 1949, pp. 191-196.
24. Calcote, Hartwell F., Barnett, Charles M., and Irby, Moreland R.: The Burning Velocity of Various Compounds by the Bunsen Burner Method. Paper presented at meeting Am. Chem. Soc., Sept. 18-23, 1949.

25. Fenn, John B., and Calcote, Hartwell F.: Activation Energies in High Temperature Combustion. Fourth Symposium (International) on Combustion, The Williams & Wilkins Co. (Baltimore), 1953, pp. 231-239.
26. Manton, John, and Milliken, B. B.: Study of Pressure Dependence of Burning Velocity by the Spherical Vessel Method. Proc. Gas Dynamics Symposium (Aerothermochem.), Northwestern Univ., 1956, pp. 151-157.
27. Fine, Burton: Stability Limits and Burning Velocities of Laminar Hydrogen-Air Flames at Reduced Pressures. NACA TN 3833, 1956.
28. Bone, W. A., and Townend, Donald T. A.: Flame and Combustion in Gases. Longmans, Green & Co., Ltd. (London), 1927, p. 505.
29. Linnett, J. W.: Methods of Measuring Burning Velocity. Fourth Symposium (International) on Combustion, The Williams & Wilkins Co. (Baltimore), 1953, pp. 20-35.
30. Garside, J. E., and Jackson, B.: The Formation and Some Properties of Polyhedral Burner Flames. Fourth Symposium (International) on Combustion, The Williams & Wilkins Co. (Baltimore), 1953, pp. 545-552.
31. Heimel, Sheldon, and Weast, Robert C.: Effect of Initial Mixture Temperature on the Burning Velocity of Benzene-air, n-Heptane-Air, and Isooctane-Air Mixtures. Paper presented at Sixth Symposium (International) on Combustion, New Haven (Conn.), Aug. 19-24, 1956. (To be published.)
32. Dixon-Lewis, G.: Temperature Distribution in Flame Reaction Zones. Fourth Symposium (International) on Combustion, The Williams & Wilkins Co. (Baltimore), 1953, pp. 263-267.
33. Fine, Burton: Further Experiments on the Stability of Laminar and Turbulent Hydrogen-Air Flames at Reduced Pressures. NACA TN 3977, 1957.
34. Simon, Dorothy M., Belles, Frank E., and Spakowski, Adolph E.: Investigation and Interpretation of the Flammability Region for Some Lean Hydrocarbon-Air Mixtures. Fourth Symposium (International) on Combustion, The Williams & Wilkins Co. (Baltimore), 1953, pp. 126-138.
35. Berlad, A. L., and Potter, A. E.: Prediction of the Quenching Effect of Various Surface Geometries. Fifth Symposium (International) on Combustion, The Reinhold Pub. Corp., 1955, pp. 728-735.



36. Lewis, Bernard, and von Elbe, Guenther: Combustion, Flames and Explosions of Gases. Academic Press, Inc., 1951.
37. Potter, A. E., Jr., and Berlad, A. L.: Effect of Fuel Type on Flame Quenching. Paper presented at Sixth Symposium (International) on Combustion, New Haven (Conn.), Aug. 19-24, 1956. (To be published.)
38. Berlad, Abraham L.: Flame Quenching by a Variable-Width Rectangular-Slot Burner as a Function of Pressure for Various Propane-Oxygen-Nitrogen Mixtures. NACA RM E53K30, 1954. (See also Jour. Phys. Chem., vol. 58, no. 11, Nov. 1954, pp. 1023-1026.)
39. Belles, Frank E., and Berlad, A. L.: Chain Breaking and Branching in the Active-Particle Diffusion Concept of Quenching. NACA TN 3409, 1955.
40. Friedman, Raymond, and Johnston, W. C.: The Wall-Quenching of Laminar Flames as a Function of Pressure, Temperature, and Air-Fuel Ratio. Jour. Appl. Phys., vol. 21, no. 8, Aug. 1950, pp. 791-795.
41. Egerton, A. C., Everett, A. J., and Moore, N. P. W.: Sintered Metals as Flame Traps. Fourth Symposium (International) on Combustion, The Williams & Wilkins Co. (Baltimore), 1953, pp. 689-695.
42. Coward, H. F., and Jones, G. W.: Limits of Flammability of Gases and Vapors. Bull. 503, Bur. Mines, 1952.
43. Egerton, Alfred C.: Limits of Inflammability. Fourth Symposium (International) on Combustion, The Williams & Wilkins Co. (Baltimore), 1953, pp. 4-13.
44. White, Albert Greville: Limits for the Propagation of Flame in Inflammable Gas-Air Mixtures. III - The Effect of Temperature on the Limits. Jour. Chem. Soc. Trans. (London), vol. CXXVII, pt. I, 1925, pp. 672-684.
45. Burgoyne, J. H., and Williams-Leir, G.: The Influence of Incombustible Vapours on the Limits of Inflammability of Gases and Vapours in Air. Proc. Roy. Soc. (London), ser. A, vol. 193, July 21, 1948, pp. 525-539.
46. Belles, Frank E., Simon, Dorothy M., and Weast, Robert C.: Pressure Limits of Flame Propagation of Propane-Air Mixtures - Influence of Wall Quenching. Ind. and Eng. Chem., vol. 46, no. 5, May 1954, pp. 1010-1013.

47. Garner, W. E., and Pugh, A.: The Propagation of Flame in Hydrogen-Oxygen Mixtures. Trans. Faraday Soc., vol. 35, Jan. 1939, pp. 283-295.
48. Swett, Clyde C., Jr.: Spark Ignition of Flowing Gases. NACA Rep. 1287, 1956.
49. Jones, G. W., et al.: Research on the Flammability Characteristics of Aircraft Fuels. Tech. Rep. 52-35, Feb. 19, 1950-Feb. 19, 1952, Wright Air Dev. Center, Wright-Patterson Air Force Base, June 1952. (Contract AF 33(038) 50-1293E.)
50. Lakin, W. P., Thwaites, H. L., Skarstrom, C. W., and Baum, A. W.: Fourth Annual Report on Fundamental Studies of Combustion. Rep. No. RL-5M-48(69), Esso Labs., Res. Div. (Standard Oil Dev. Co.), Nov. 30, 1948. (Contract N6-ori-109.)
51. King, I. R., and Calcote, H. F.: Effect of Initial Temperature on Minimum Spark-Ignition Energy. Jour. Chem. Phys., vol. 23, no. 12, Dec. 1955, pp. 2444-2445.
52. Belles, Frank E.: Flame Propagation in Premixed Gases. Paper presented at Am. Chem. Soc. Meeting, Dallas (Texas), Apr. 8-13, 1956. (To be published in Advances in Chem. Ser.)
53. von Elbe, Guenther, and Mentser, Morris: Further Studies of the Structure and Stability of Burner Flames. Jour. Chem. Phys., vol. 13, no. 2, Feb. 1945, pp. 89-100.
54. Bollinger, Loren E., and Edse, Rudolph: Effect of Burner-Tip Temperature on Flashback of Hydrogen-Oxygen Flames. WADC Tech. Rep. 53-325, Wright Air Development Center, Wright-Patterson Air Force Base, Oct. 1953.
55. Wohl, Kurt, Kapp, Numer M., and Gazley, Carl: The Stability of Open Flames. Third Symposium on Combustion and Flame and Explosion Phenomena, The Williams & Wilkins Co. (Baltimore), 1949, pp. 3-21.
56. Friedman, J., Bennet, W. J., and Zwick, E. B.: The Engineering Application of Combustion Research to Ramjet Engines. Fourth Symposium (International) on Combustion, The Williams & Wilkins Co. (Baltimore), 1953, pp. 756-764; discussion by E. A. DeZubay, p. 764.
57. Zukoski, Edward Edom: Flame Stabilization on Bluff Bodies at Low and Intermediate Reynolds Numbers. Rep. No. 20-75, Jet Prop. Lab., C.I.T., June 30, 1954. (Contract DA-04-495-ORD-18.)

58. Longwell, J. P.: Flame Stabilization by Bluff Bodies and Turbulent Flames in Ducts. Fourth Symposium (International) on Combustion, The Williams & Wilkins Co. (Baltimore), 1953, pp. 90-97; discussion by E. A. DeZubay, p. 97.
59. Evans, Marjorie W., Given, Frank I., and Richeson, William E., Jr.: Effects of Attenuating Materials on Detonation Induction Distances. Jour. Appl. Phys., vol. 26, no. 9, Sept. 1955, pp. 1111-1113.
60. Laffitte, M. P.: Sur la propagation de l'onde explosive. Comptes Rendus, Dec. 15, 1924, pp. 1394-1396.
61. Hoelzer, C. A., and Stobaugh, W. K.: Influence of Initial Pressure on Detonation Parameters in Combustible Gases. GAE 54-11, Air Force Inst. Tech., Mar. 1954.
62. Hinshelwood, C. N., and Williamson, A. T.: The Reaction Between Hydrogen and Oxygen. Clarendon Press (Oxford), 1934.
63. Brokaw, R. S.: Thermal Ignition, with Particular Reference to High Temperatures. Selected Combustion Problems. Vol. II. Butterworths Sci. Pub. (London), 1956, pp. 115-138.
64. Coward, H. F.: Ignition Temperatures of Gases. "Concentric Tube" Experiments of (the late) Harold Bailey Dixon. Jour. Chem. Soc. (London), pt. II, July-Dec. 1934, pp. 1382-1406.
65. Anagnostou, E., Brokaw, R. S., and Butler, J. N.: Effect of Concentration on Ignition Delays for Various Fuel-Oxygen-Nitrogen Mixtures at Elevated Temperatures. NACA TN 3887, 1956.
66. Mullins, B. P.: Studies of the Spontaneous Ignition of Fuel Injected into a Hot Air Stream. IV - Ignition Delay Measurements on Some Gaseous Fuels at Atmospheric and Reduced Static Pressures. Fuel, vol. XXXII, no. 3, July 1953, pp. 343-362.
67. Fouré, C.: Stationary Flames in Cylindrical Flow of Homogeneous Air-Hydrogen Mixtures. Fifth Symposium (International) on Combustion, Reinhold Pub. Corp., 1955, pp. 736-741.
68. von Elbe, G., and Lewis, B.: Mechanism of the Thermal Reaction between Hydrogen and Oxygen. Jour. Chem. Phys., vol. 10, no. 6, June 1942, pp. 366-393.
69. Zabetakis, Michael G.: Research on the Combustion and Explosion Hazards of Hydrogen-Water Vapor-Air Mixtures. AECU-3327, Tech. Information Service Extension, U.S. Atomic Energy Comm., Sept. 4, 1956.

70. Potter, A. E., Jr., and Berlad, A. L.: A Relation Between Burning Velocity and Quenching Distance. NACA TN 3882, 1956.
71. Berlad, A. L., and Potter, A. E., Jr.: Relation of Boundary Velocity Gradient for Flash-back to Burning Velocity and Quenching Distance. Combustion and Flame, vol. 1, no. 1, Mar. 1957, pp. 127-128.
72. Zukoski, Edward E., and Marble, Frank E.: The Role of Wake Transition in the Process of Flame Stabilization on Bluff Bodies. Combustion Researches and Reviews, Butterworths Sci. Pub., 1955, pp. 167-180.
73. Zukoski, Edward E., and Marble, Frank E.: Experiments Concerning the Mechanism of Flame Blowoff from Bluff Bodies. Proc. Gas Dynamics Symposium (Aerothermochem.), Northwestern Univ., 1956, pp. 205-210.
74. Harris, Margaret E., Grumer, Joseph, von Elbe, Guenther, and Lewis, Bernard: Burning Velocities, Quenching, and Stability Data on Nonturbulent Flames of Methane and Propane with Oxygen and Nitrogen. Third Symposium on Combustion and Flame and Explosion Phenomena, The Williams & Wilkins Co. (Baltimore), 1949, pp. 80-89.
75. Huff, Vearl N., Gordon, Sanford, and Morrell, Virginia E.: General Method and Thermodynamic Tables for Computation of Equilibrium Composition and Temperature of Chemical Reactions. NACA Rep. 1037, 1951. (Supersedes NACA TN's 2113 and 2161.)
76. Glatt, Leonard, Adams, Joan H., and Johnston, Herrick L.: Thermodynamic Properties of the  $H_2O$  Molecule from Spectroscopic Data. Tech. Rep. 316-8, Cryogenic Lab., Dept. Chem., Ohio State Univ., June 1, 1953. (Navy Contract N6onr-225, Task Order XII, ONR Proj. NR-085-005.)

TABLE I. - HYDROGEN-AIR FLAME TEMPERATURES

[Pressure, 1 atm; initial temperature, 25° C.]

Source and Date	Reference	Stoichiometric mixture temperature, °K	Maximum temperature, °K	Hydrogen in maximum-temperature mixture, volume percent
Experimental				
Passauer, 1930 (split flame)	2	2263	2283	31
Jones, Lewis, and Seaman, 1931	4	2293	2318	31.6
Morgan and Kane, 1953	3 (fig. 7)	2220	----	----
Theoretical				
Lewis and von Elbe, 1935	7	----	2320	31.6
Friedman, 1949	8	2375	----	----
Fenn, 1951	9	2345	----	----
Morgan and Kane, 1953	3 (fig. 7)	2380	----	----
Gaydon and Wolfhard, 1953	6	2373	----	----
Burwasser and Pease, 1955	10	2315	----	----
This report		2387	2403	30.9

TABLE II. - COMPUTED EQUILIBRIUM ADIABATIC FLAME TEMPERATURES, THERMODYNAMIC PROPERTIES, AND BURNED-GAS COMPOSITIONS FOR HYDROGEN-AIR MIXTURES<sup>a</sup>

Initial temperature, $T_0$ , °K	Pressure, $P$ , atm	Equivalence ratio, $\phi$	Flame temperature, $T_f$ , °K	Molecular weight, gm/mole	Specific heat, $c_p$ , cal/(gm)(°K)	Ratio of specific heats	Burned-gas composition, volume fraction								
							H <sub>2</sub>	H <sub>2</sub> O	N <sub>2</sub>	OH	O <sub>2</sub>	NO	H	O	N
0	1.00	0.50	1383.1	26.483	0.5347	1.288	0.000000	0.190201	0.714432	0.000026	0.094880	0.000482	0.000000	0.000000	0.000000
		1.00	2220.2	24.410	.5375	1.200	.008503	.335483	.648369	.002891	.002763	.001443	.000573	.000175	.000000
		2.00	1822.5	18.732	.4992	1.271	.257692	.257782	.484294	.000013	.000000	.000001	.000219	.000000	.000000
		10.00	683.9	7.475	.9680	1.378	.757665	.084185	.158150	.000000	.000000	.000000	.000000	.000000	.000000
298.16	0.01	0.10	630.3	28.342	0.2610	1.367	0.000000	0.041176	0.773532	0.000000	0.185291	0.000000	0.000000	0.000000	0.000000
		.50	1639.8	26.485	.5561	1.267	.000065	.189753	.713721	.000695	.094127	.001556	.000007	.000079	.000000
		1.00	2193.4	25.893	1.1218	1.130	.050211	.287739	.633952	.011089	.011769	.002774	.009408	.003057	.000000
		2.00	2013.2	16.642	.7075	1.204	.252586	.255679	.481949	.000786	.000010	.000046	.008918	.000268	.000000
		10.00	971.7	7.475	1.0038	1.360	.757665	.084185	.158150	.000000	.000000	.000000	.000000	.000000	.000000
	1.00	0.10	630.3	28.342	0.2610	1.367	0.000000	0.041176	0.773532	0.000000	0.185291	0.000000	0.000000	0.000000	0.000000
		.50	1643.5	26.492	.5474	1.276	.000007	.190084	.713844	.000224	.094287	.001575	.000000	.000008	.000000
		1.00	2267.2	24.272	.6497	1.177	.018518	.324028	.644061	.006178	.005006	.002729	.001859	.003618	.000000
		2.00	2063.3	18.721	.5314	1.255	.257090	.257518	.484013	.000120	.000000	.000008	.001251	.000001	.000000
		10.00	971.7	7.475	1.0039	1.360	.757665	.084185	.158150	.000000	.000000	.000000	.000000	.000000	.000000
	100	0.10	630.3	28.342	0.2610	1.367	0.000000	0.041176	0.773533	0.000000	0.185292	0.000000	0.000000	0.000000	0.000000
		.50	1643.5	26.492	.5474	1.276	.000001	.190175	.713874	.000071	.094298	.001580	.000000	.000001	.000000
		1.00	2486.2	24.461	.4778	1.218	.005277	.339886	.649619	.001997	.001314	.001683	.006171	.000053	.000000
		2.00	2070.5	18.733	.5072	1.265	.257748	.257793	.484315	.000015	.000000	.000001	.000131	.000000	.000000
		10.00	971.7	7.475	1.0039	1.360	.757665	.084185	.158150	.000000	.000000	.000000	.000000	.000000	.000000
600	0.01	0.10	916.4	28.342	0.2779	1.337	0.000000	0.041176	0.773526	0.000000	0.185286	0.000012	0.000000	0.000000	0.000000
		.50	1871.2	26.451	.4187	1.231	.000030	.187662	.711787	.000581	.092399	.003501	.000159	.000781	.000000
		1.00	2275.7	23.574	1.4339	1.113	.039989	.277393	.624995	.015803	.015497	.003766	.018820	.006737	.000000
		2.00	2165.9	18.487	1.0079	1.164	.244933	.251144	.477866	.002681	.000080	.000000	.002866	.000224	.000000
		10.00	1258.8	7.475	1.0486	1.340	.757660	.084185	.158150	.000000	.000000	.000000	.000000	.000000	.000000
	1.00	0.10	916.4	28.342	0.2779	1.337	0.000000	0.041176	0.773526	0.000000	0.185285	0.000012	0.000000	0.000000	0.000000
		.50	1888.8	26.463	.3700	1.257	.000074	.189828	.712697	.001085	.092940	.003710	.000006	.000081	.000000
		1.00	2529.4	24.075	.7930	1.160	.024431	.308757	.635019	.010782	.007685	.004547	.004454	.001574	.000000
		2.00	2291.2	18.664	.6026	1.230	.255199	.256405	.483017	.000681	.000005	.000055	.004859	.000010	.000000
		10.00	1258.8	7.475	1.0481	1.340	.757664	.084185	.158150	.000000	.000000	.000000	.000000	.000000	.000000
	100	0.10	916.4	28.342	0.2779	1.337	0.000000	0.041176	0.773526	0.000000	0.185285	0.000012	0.000000	0.000000	0.000000
		.50	1892.9	26.490	.3611	1.263	.000008	.190013	.712728	.000551	.093129	.003761	.000000	.000009	.000000
		1.00	2689.6	24.384	.5278	1.204	.009791	.335005	.646851	.004184	.002336	.003117	.000639	.001178	.000000
		2.00	2319.4	18.728	.5235	1.256	.257520	.257658	.484195	.000078	.000000	.000007	.000541	.000000	.000000
		10.00	1258.8	7.475	1.0481	1.340	.757665	.084185	.158150	.000000	.000000	.000000	.000000	.000000	.000000
1000	0.01	0.10	1297.1	28.342	0.2967	1.310	0.000000	0.041168	0.773333	0.000015	0.185090	0.000392	0.000000	0.000001	0.000000
		.50	2360.3	25.094	1.8881	1.111	.051719	.249278	.611572	.022011	.019949	.008039	.029770	.010860	.000001
		1.00	2306.8	18.177	1.5852	1.133	.232489	.240180	.469637	.007084	.000505	.000631	.048219	.001257	.000000
		10.00	1627.5	7.473	1.1496	1.305	.757113	.084156	.158100	.000002	.000000	.000000	.000629	.000000	.000000
	1.00	0.10	1297.2	28.342	0.2965	1.310	0.000000	0.041173	0.773335	0.000005	0.185094	0.000392	0.000000	0.000000	0.000000
		.50	2204.8	26.436	.4272	1.225	.000737	.186575	.708992	.004832	.089500	.008301	.000157	.000906	.000000
		1.00	2688.0	23.730	1.0207	1.145	.037487	.284133	.627822	.018113	.011487	.006767	.010481	.003828	.000001
		2.00	2550.5	18.552	.7980	1.192	.249685	.251637	.479477	.003068	.000060	.000344	.015676	.000153	.000000
		10.00	1631.2	7.475	1.1082	1.318	.757607	.084182	.158146	.000000	.000000	.000000	.000065	.000000	.000000
	100	0.10	1297.2	28.342	0.2964	1.310	0.000000	0.041175	0.773336	0.000002	0.185095	0.000393	0.000000	0.000000	0.000000
		.50	2340.9	24.220	.8142	1.187	.018460	.319026	.641119	.008922	.004193	.005869	.002777	.000633	.000001
		1.00	2648.6	18.707	.5817	1.242	.256594	.256961	.483807	.000515	.000001	.000063	.002355	.000004	.000000
		10.00	1631.5	7.475	1.1038	1.317	.757658	.084185	.158150	.000000	.000000	.000000	.000007	.000000	.000000
1400	1.00	0.10	1680.2	28.341	0.3149	1.287	0.000000	0.041082	0.772167	0.000161	0.183907	0.002654	0.000000	0.000017	0.000000
		.50	2480.8	26.283	.5517	1.188	.003367	.176316	.702080	.012715	.084201	.013875	.001336	.004110	.000000
		1.00	2820.8	23.307	1.2763	1.136	.060357	.256652	.615111	.026116	.018065	.009313	.019883	.007698	.000003
		2.00	2750.1	16.311	1.1223	1.183	.241908	.241281	.472862	.008130	.000331	.001096	.033558	.000863	.000002
1400	1.00	10.00	1996.4	7.470	1.2180	1.286	.758458	.084113	.158040	.000013	.000000	.000000	.001377	.000000	.000000

<sup>a</sup>The method and thermochemical data for these computations were taken from ref. 75, with the following exceptions: Data for water were taken from ref. 76, and the equilibrium constants for the dissociation of N<sub>2</sub> were revised to conform with the recently accepted value of its dissociation energy, 9.756 electron volts. For simplicity, air was assumed to consist of oxygen and nitrogen only, in the molar ratio 1:3.7572, or 21.02 percent oxygen. The enthalpy change of this fictitious "air" between 300° and 2400° K is the same as that of standard air, which contains 20.95 percent oxygen plus nitrogen, argon, and other gases.

TABLE III. - HYDROGEN-AIR BURNING VELOCITIES

[Atmospheric pressure; room temperature.]

Source and date	Reference	Apparatus	Flame surface	Measurement	Stoichiometric burning velocity, cm/sec	Maximum burning velocity, cm/sec	Hydrogen in maximum-burning-velocity mixture, volume percent
Michelson, 1889	15	Cylindrical burner	Visible	Total area	230	277	40
Ubbelohde and Hofsass, 1913	16	Cylindrical burner	Visible	Cone height	153	200	45
Ubbelohde and Koelliker, 1916	17	Cylindrical burner	Visible	Cone height	155	200	46
Bunte and Steding, 1928	18	Cylindrical burner, cooled	Visible	Cone height	190	258	40
Bunte and Litterscheidt, 1930	19	Cylindrical burner	Visible	Cone height	185	266	42
Passauer, 1930	2	Cylindrical burner, cooled, enclosed	Visible	Cone height	187	210	44
Corsiglia, 1931	20	Cylindrical burner, cooled	Visible	Approximate area	200	285	42
Jahn, 1934	21	Cylindrical burner, cooled	Visible	Cone height	187	287	43
Smith and Pipkering, 1936	22	Cylindrical burner	Visible	Angle	170	252	42
Friedman, 1949	8	Cylindrical burner, cooled	-----	Cone height (corrected)	177	---	---
Bartholome, 1949	23	Nozzle burner	Visible	Angle	---	320	42
Calcote, Barnett, and Irby, 1949	24	Cylindrical burner	Shadowgraph	Frustum area	213	317	42
Fenn and Calcote, 1953	25	Cylindrical burner	-----	-----	170	---	---
Morgan and Kane, 1953	3	Nozzle burner, cooled	Schlieren	Area	215	---	---
Burwasser and Pease, 1953	10	Cylindrical burner, cooled, enclosed	Shadowgraph	Angle	230	320	42
Manton and Milliken, 1956	26	Spherical bomb	Schlieren	Flame diameter and pressure	232	300	41
Fine, 1956	27	Cylindrical burner, cooled	Schlieren	Total area	193	304	43
Heimel, 1956	Unpublished data	Cylindrical burner, cooled	Schlieren	Total area	208	297	43

TABLE IV. - DETONATION VELOCITIES  
OF STOICHIOMETRIC HYDROGEN-  
OXYGEN MIXTURES

[Data from ref. 36, p. 583.]

Tempera- ture, °K	Pressure, atm	Detonation velocity, m/sec
283	0.263	2627
	.395	2705
	.658	2775
	1.000	2821
	1.448	2856
	1.975	2872
373	0.513	2697
	.658	2738
	1.000	2790
	1.316	2828
	1.908	2842



TABLE V. - RECOMMENDED STANDARD VALUES OF HYDROGEN-AIR COMBUSTION PROPERTIES

Property	Value at equivalence ratio of 1.00 (stoichiometric)	Maximum or minimum value	Equivalence ratio for maximum or minimum of property	Pressure dependence	Temperature dependence	Remarks
Flame temperature	2387° K	2403° K	1.06	See fig. 4	$T_F \approx T_{F,300} + 0.5(T_o - 300)$ (near maximum) $T_F \approx T_{F,300} + (T_o - 300)$ (rich and lean mixtures)	
Laminar burning velocity	215 cm/sec	310 cm/sec	1.80	$U_L \propto P^{0.16}$	$U_{L,max} = 0.08908 T_o^{1.413}$	
Turbulent burning velocity						Meaning of turbulent burning velocity measurements is not clear at present
Quenching distance	0.057 cm		1.00	$d_q \propto P^{-1.051} (\phi=0.5)$ $d_q \propto P^{-1.138} (\phi=1.0)$ $d_q \propto P^{-1.097} (\phi=2.0)$	Unknown	
Spark ignition energy	0.019 millijoules		1.00	$I \propto P^{-2}$	$\log I \propto \frac{1}{T_o}$	
Detonation velocity	1850 m/sec	2150 m/sec	2.75	Small	Small	Limits of detonability: 18.3 to 59.0 percent by volume
Explosion limits and spontaneous ignition temperature						Consider mixtures at temperatures over 500° C as potential explosion hazards; at low pressures, explosions may occur at temperatures as low as 340° C
Flammability limits				None for reduced pressures; slight for high pressures	See fig. 14	Upward propagation: Lean limit, 4.0 percent hydrogen Rich limit, 74 percent hydrogen Downward propagation: Lean limit, 9.0 percent hydrogen Rich limit, 74 percent hydrogen

54

NACA RM E57D24

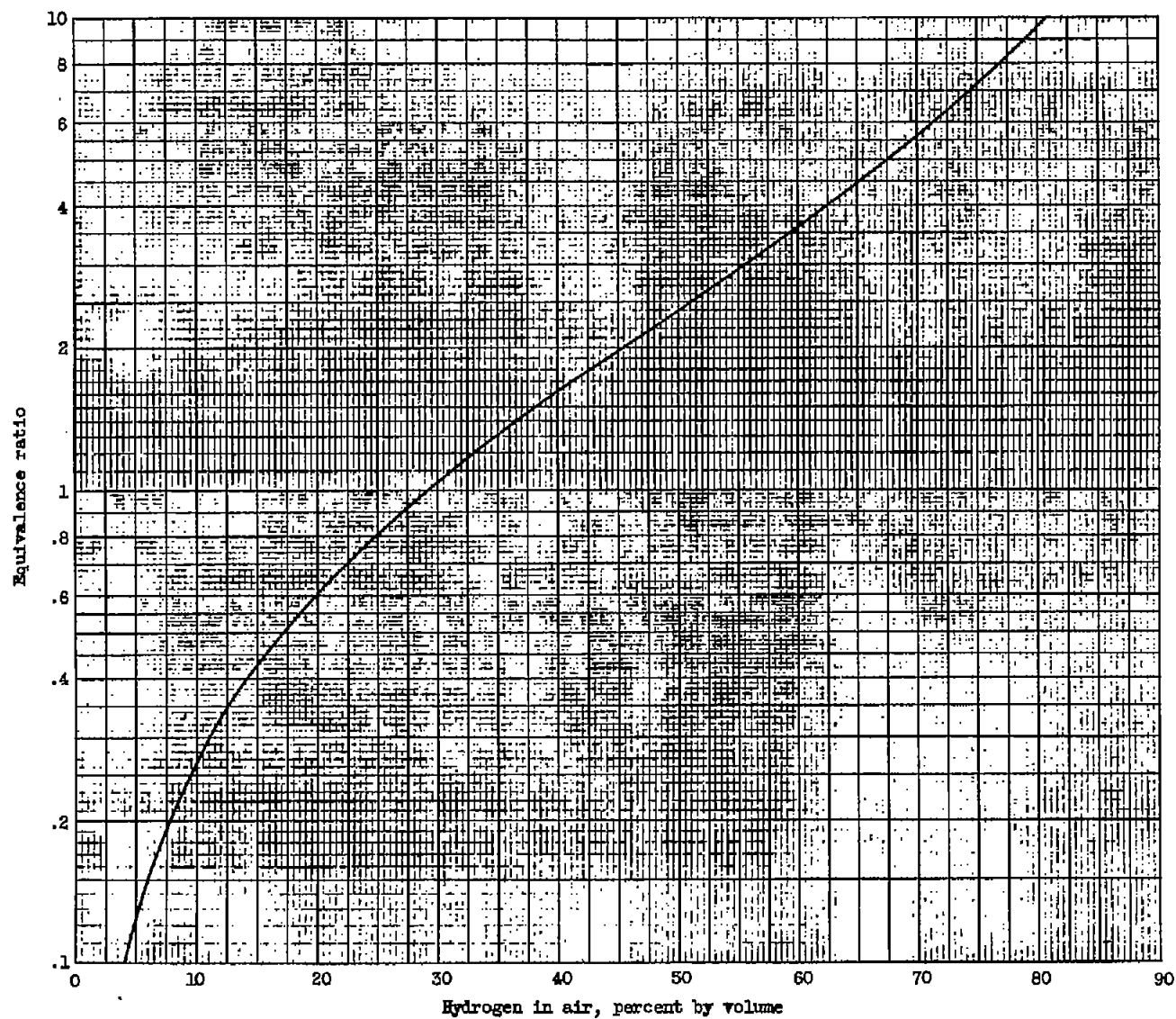


Figure 1. - Relation between equivalence ratio and volume percent hydrogen for hydrogen-air mixtures.

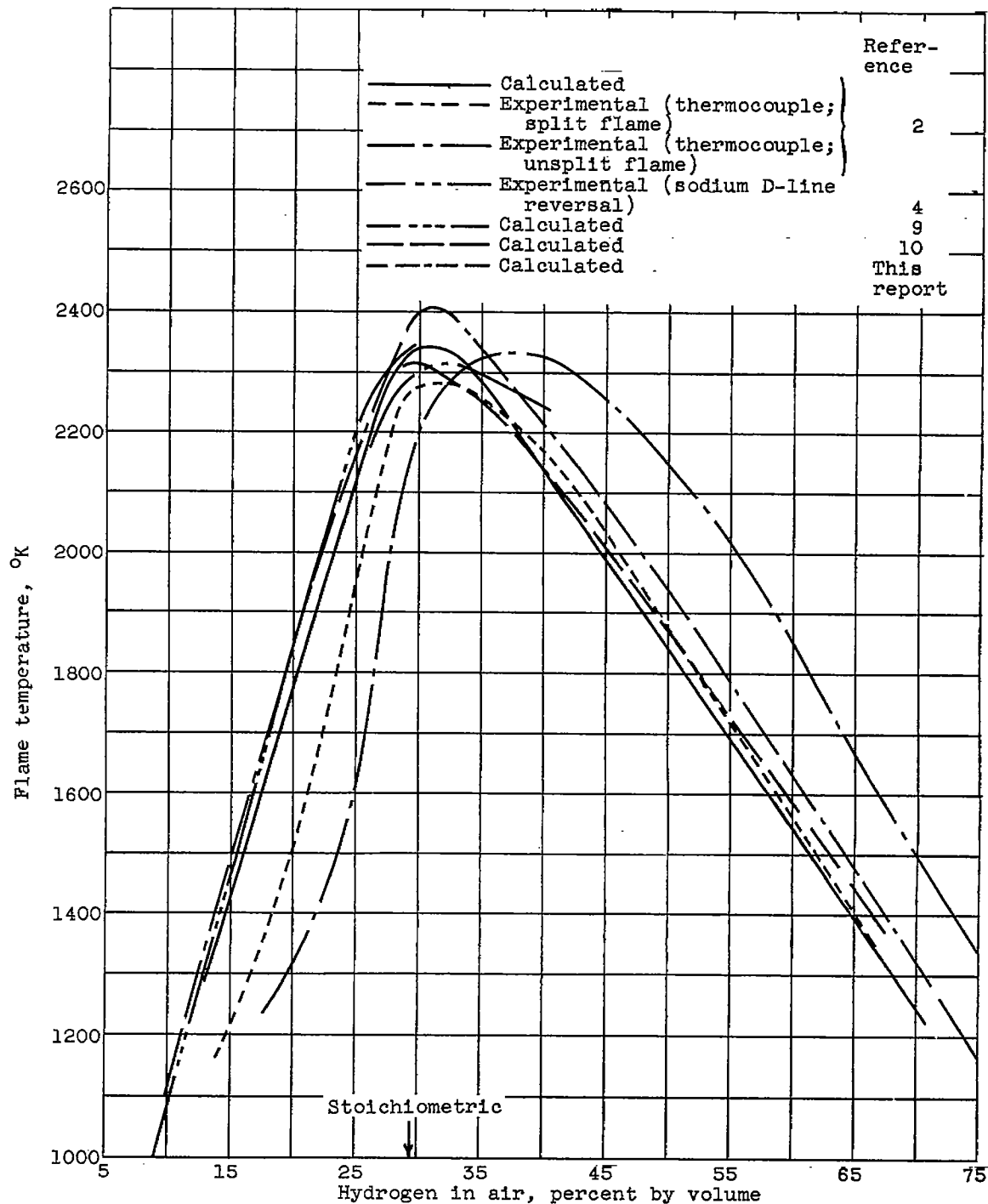
~~CONFIDENTIAL~~

Figure 2. - Calculated and measured flame temperatures for hydrogen-air mixtures. Pressure, 1 atmosphere; initial temperature, 25° C.

~~CONFIDENTIAL~~

4362

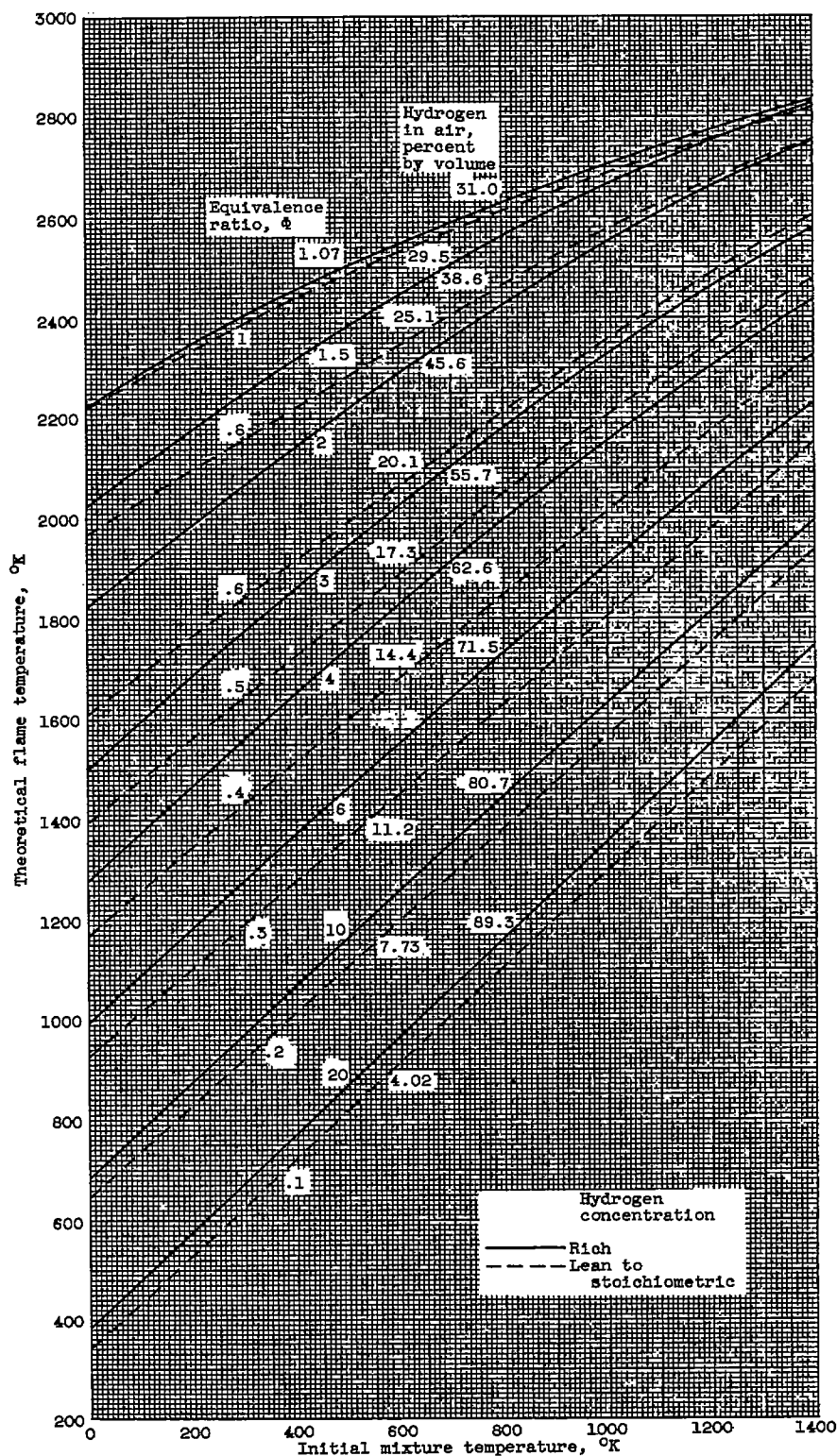
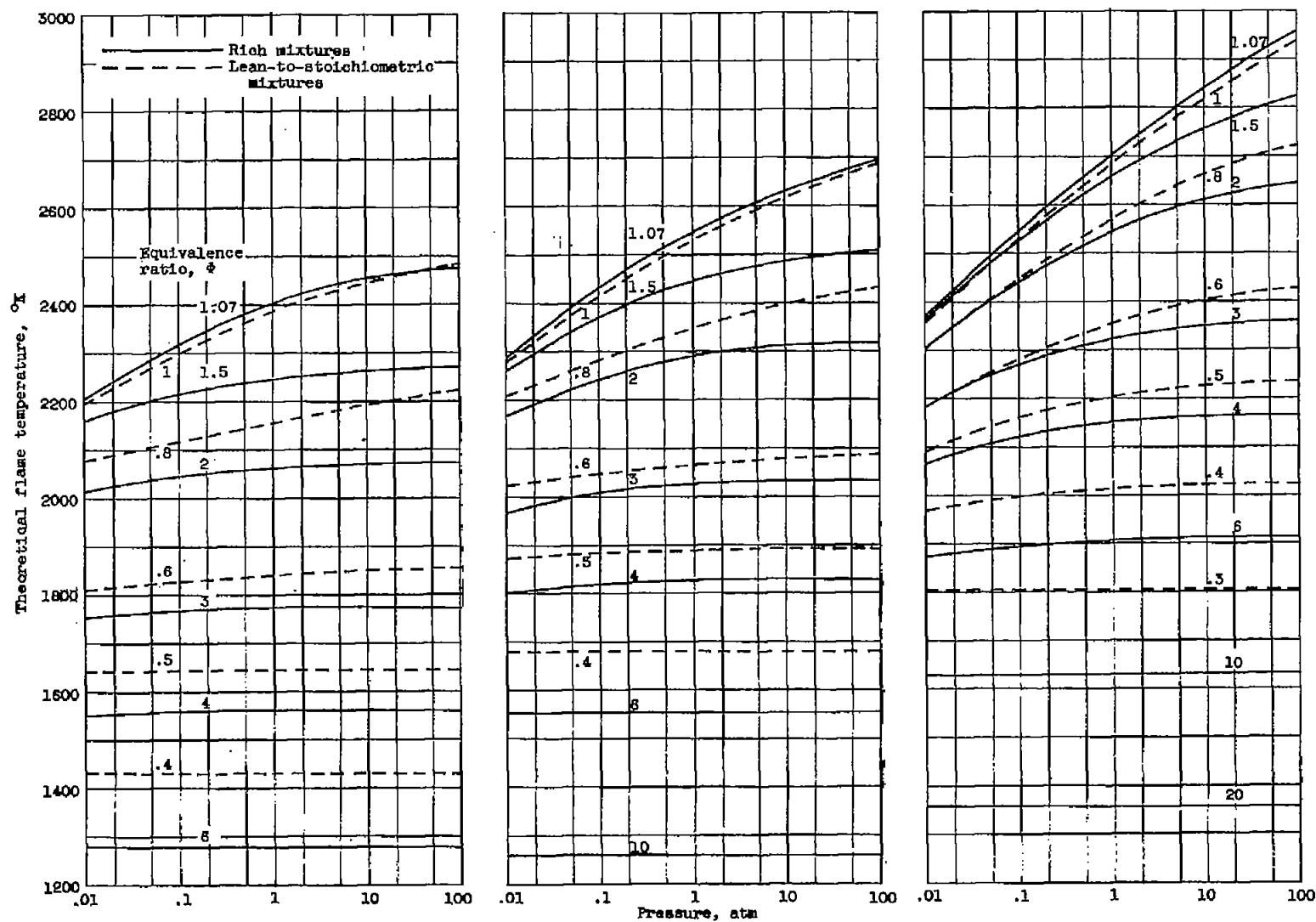


Figure 3. - Effect of initial mixture temperature on calculated flame temperature of hydrogen-air mixtures. Pressure, 1 atmosphere.



(a) Initial mixture temperature, 298.16° K. (b) Initial mixture temperature, 800° K. (c) Initial mixture temperature, 1000° K.

Figure 4. - Effect of pressure on calculated flame temperatures of hydrogen-air mixtures.

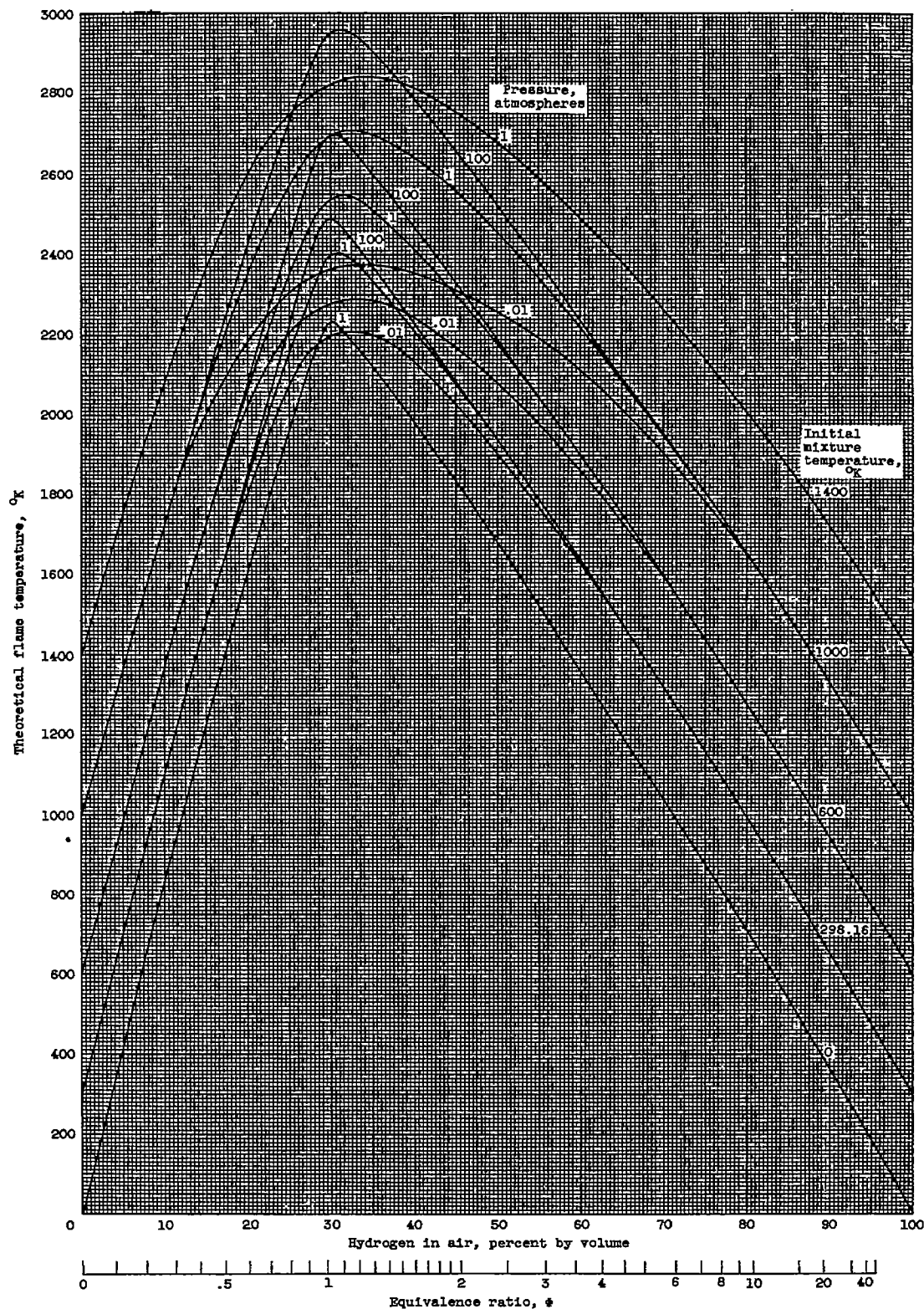


Figure 5. - Summary of effects of initial temperature, pressure, and composition on calculated flame temperatures of hydrogen-air mixtures.

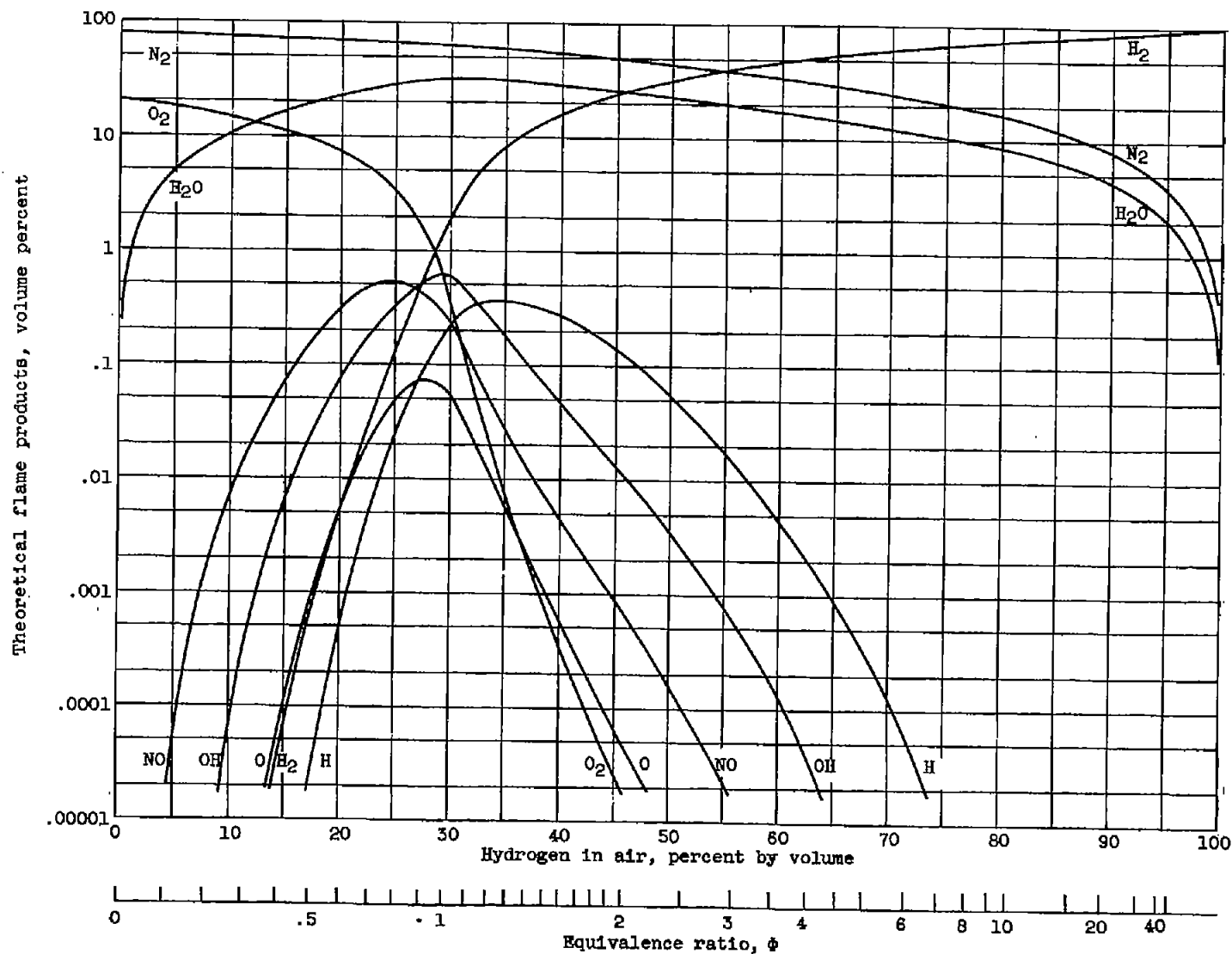


Figure 6. - Theoretical adiabatic flame composition for hydrogen-air mixtures. Pressure, 1 atmosphere; initial mixture temperature, 298.16° K.

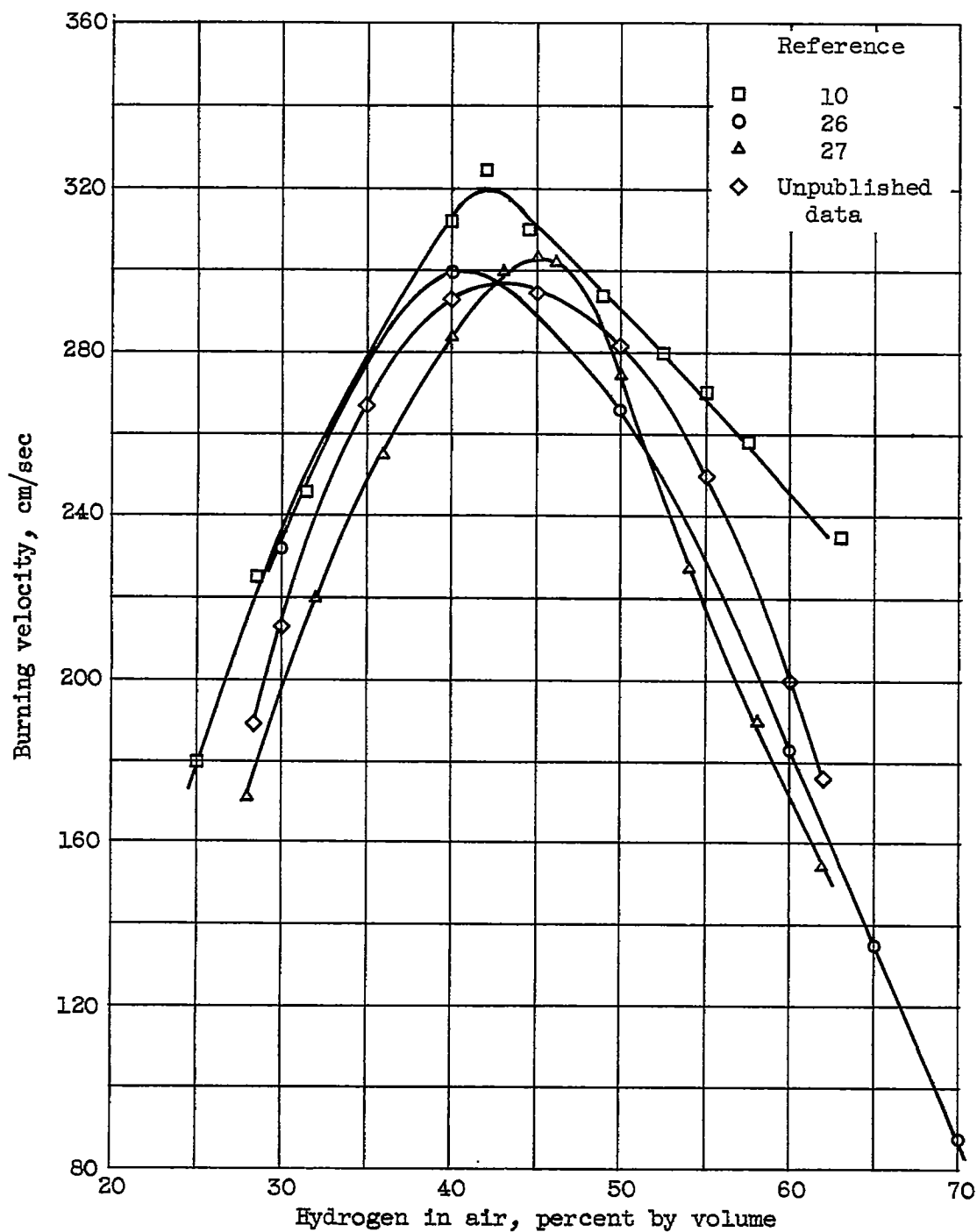


Figure 7. - Effect of hydrogen concentration on burning velocities of hydrogen-air mixtures. Pressure, 1 atmosphere; initial temperature, 300° K.



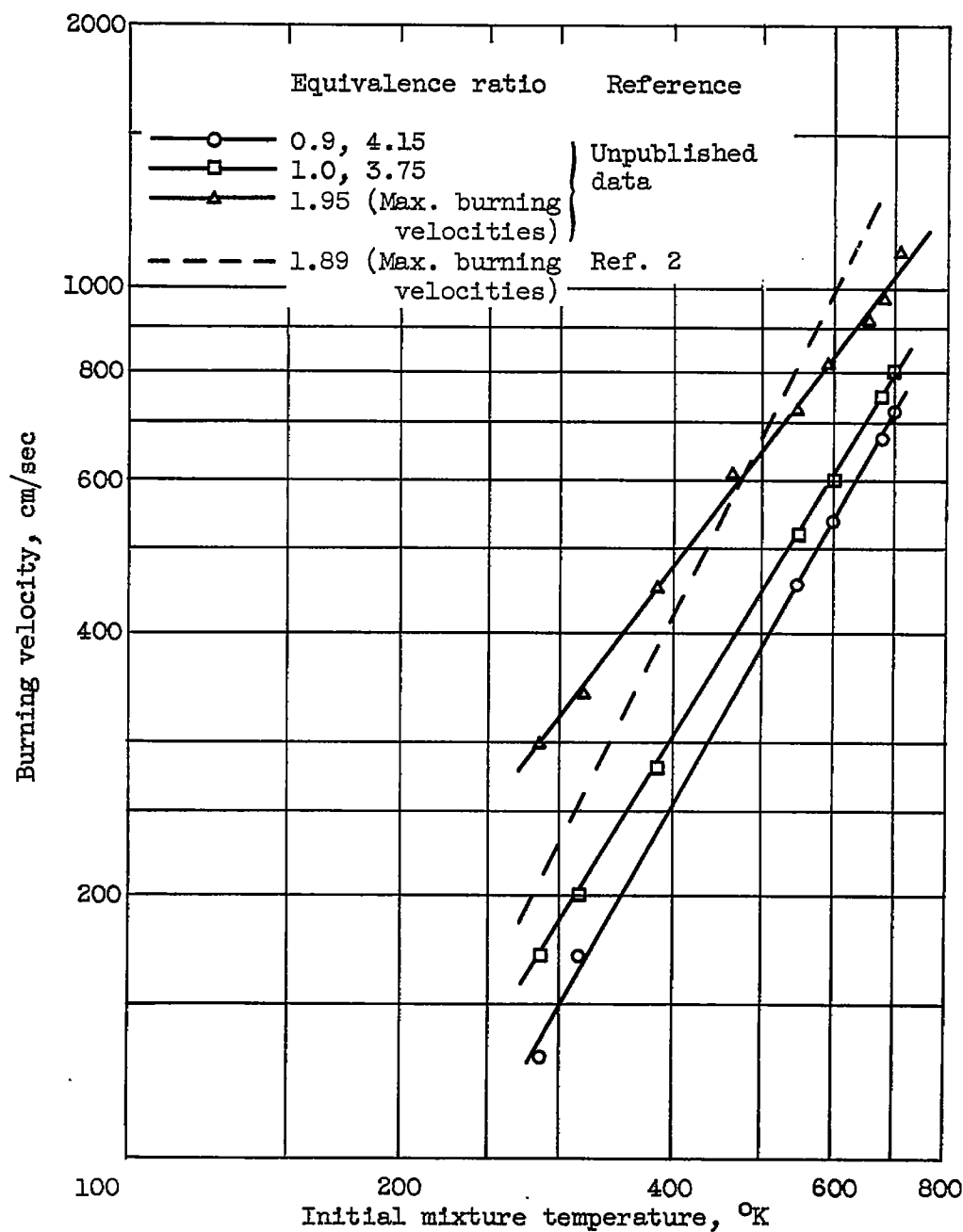


Figure 8. - Effect of initial temperature on burning velocities of hydrogen-air mixtures. Pressure, 1 atmosphere.

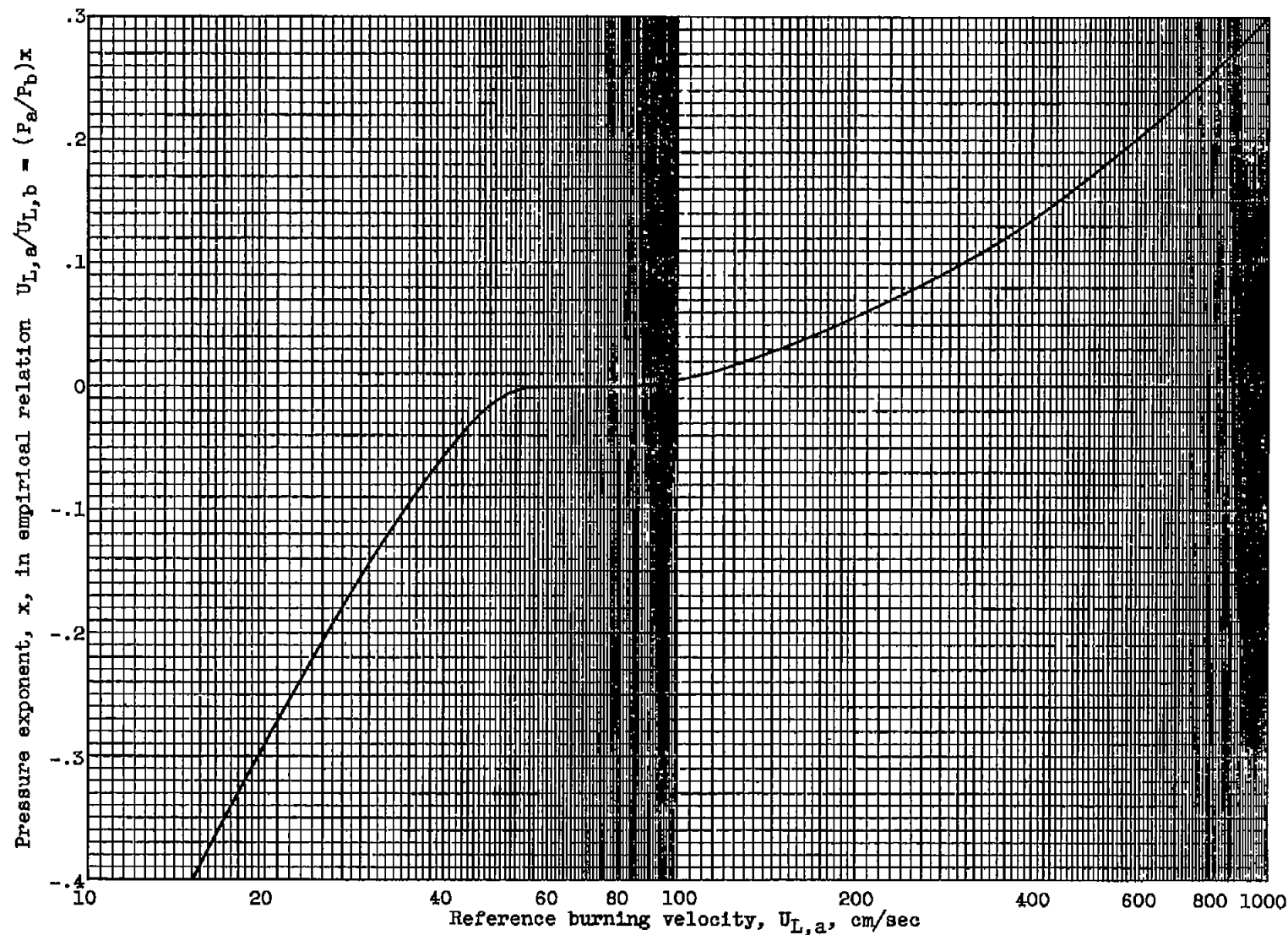


Figure 9. - Variation of pressure dependence of burning velocity with reference burning velocity (ref. 26).

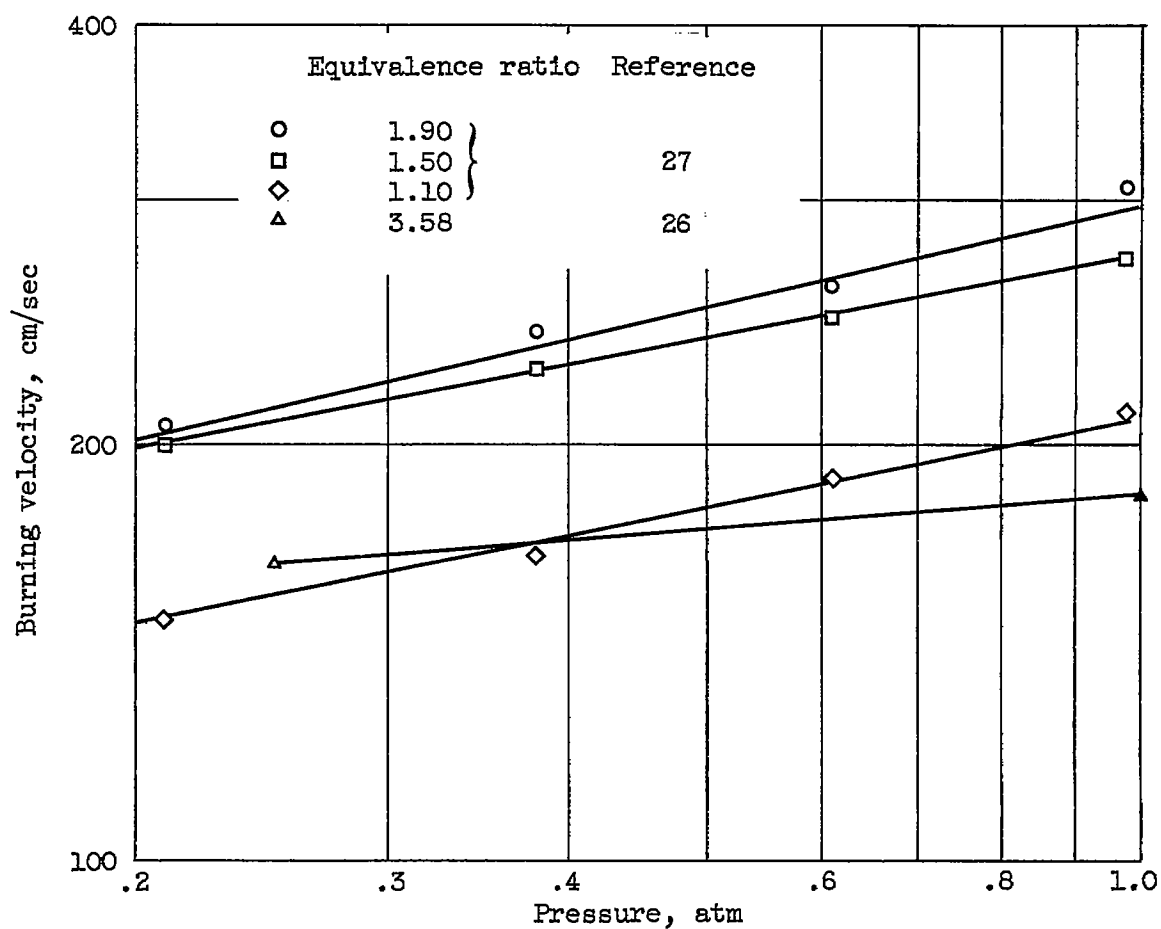


Figure 10. - Effect of pressure on burning velocity of hydrogen-air flames.

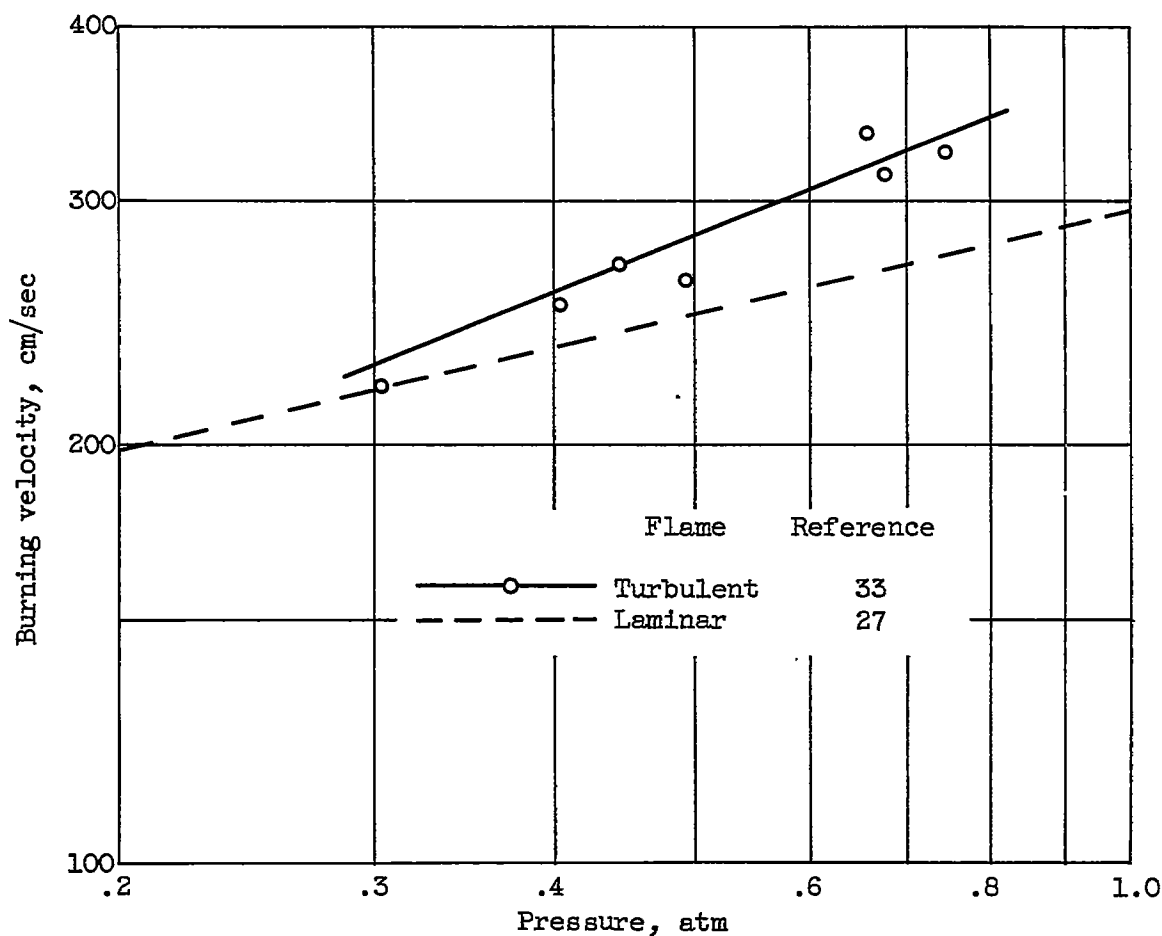


Figure 11. - Comparison of turbulent and laminar burning velocities for hydrogen-air mixtures as function of pressure. Equivalence ratio, 1.80.

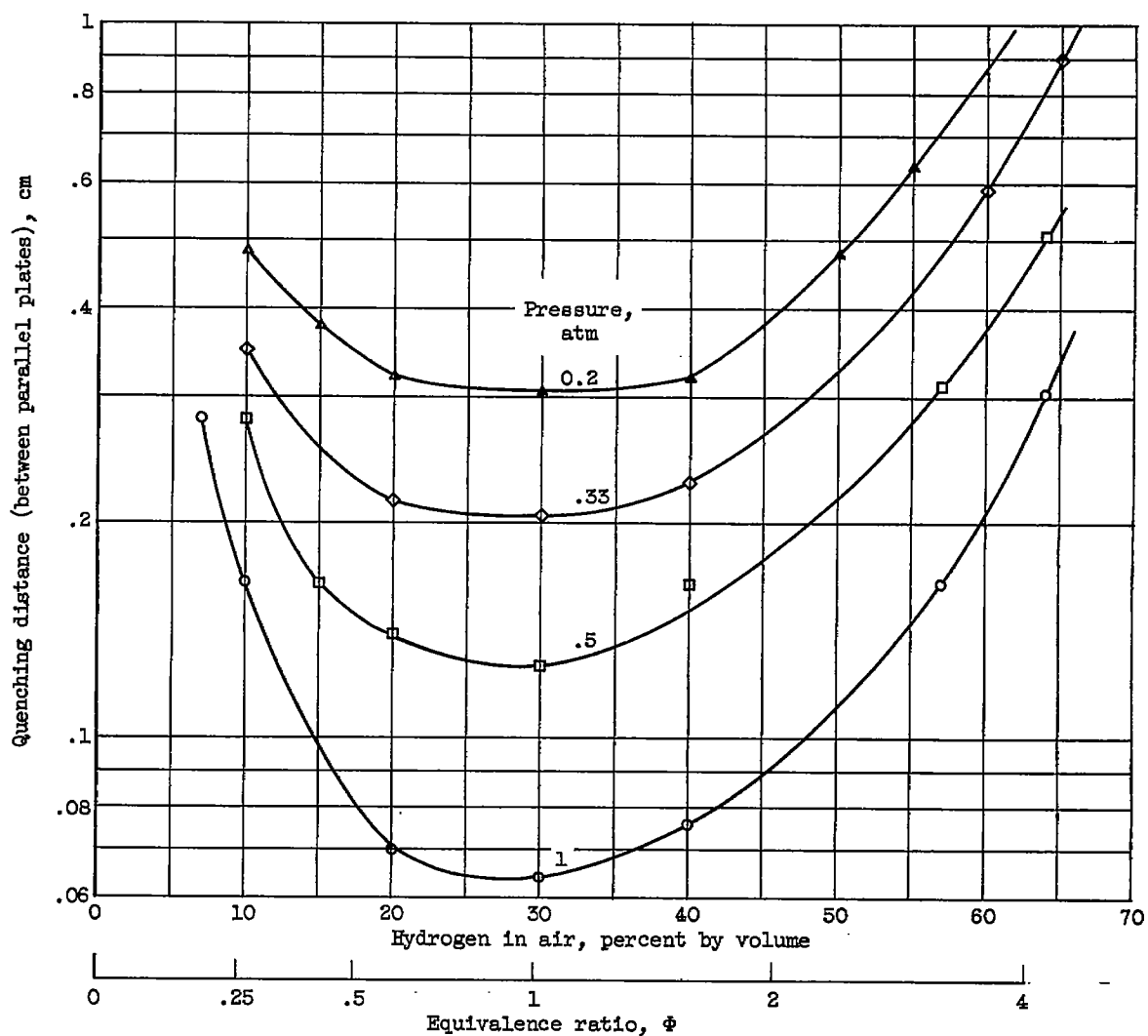


Figure 12. - Effect of hydrogen concentration on quenching distance of hydrogen-air mixtures (data from ref. 36).

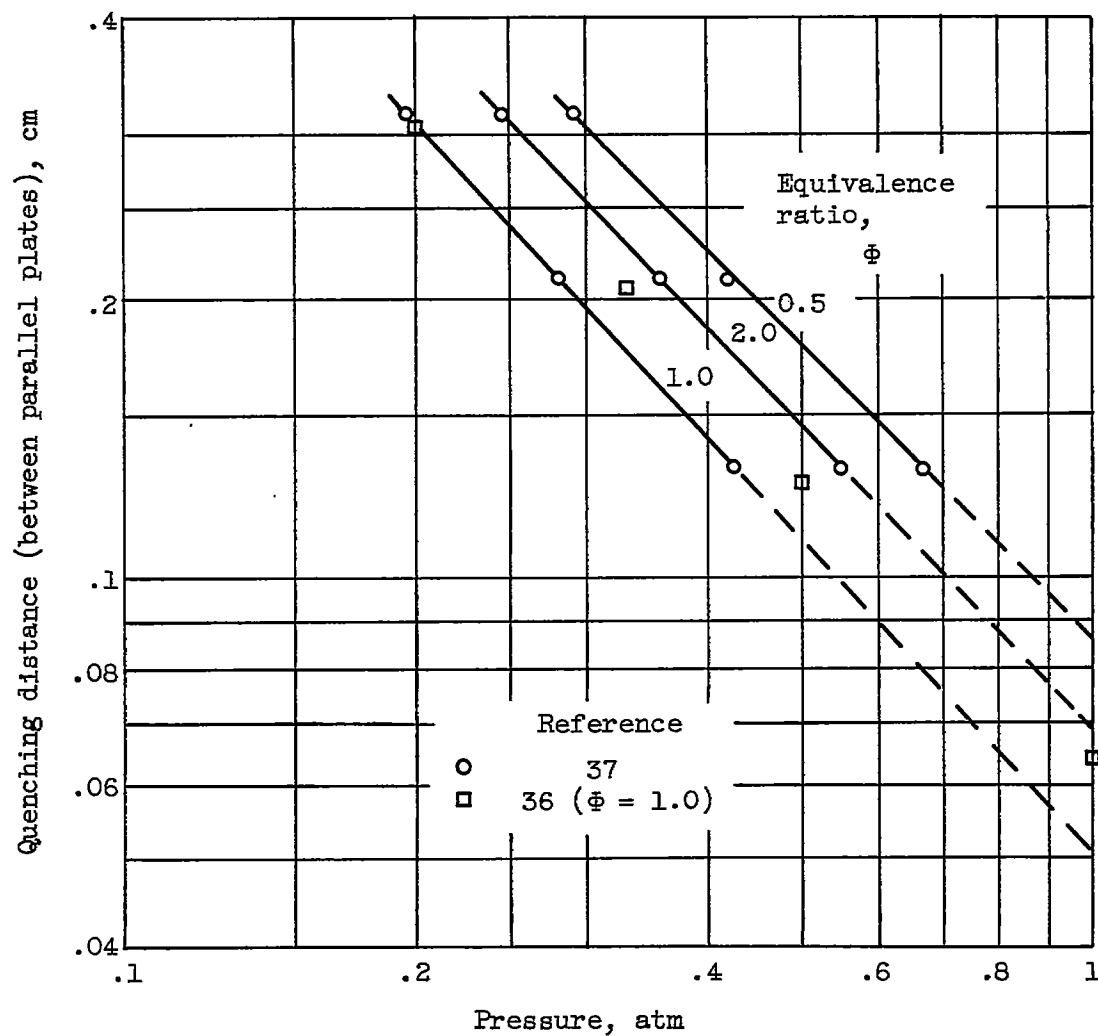


Figure 13. - Effect of pressure on quenching distance of hydrogen-air mixtures.

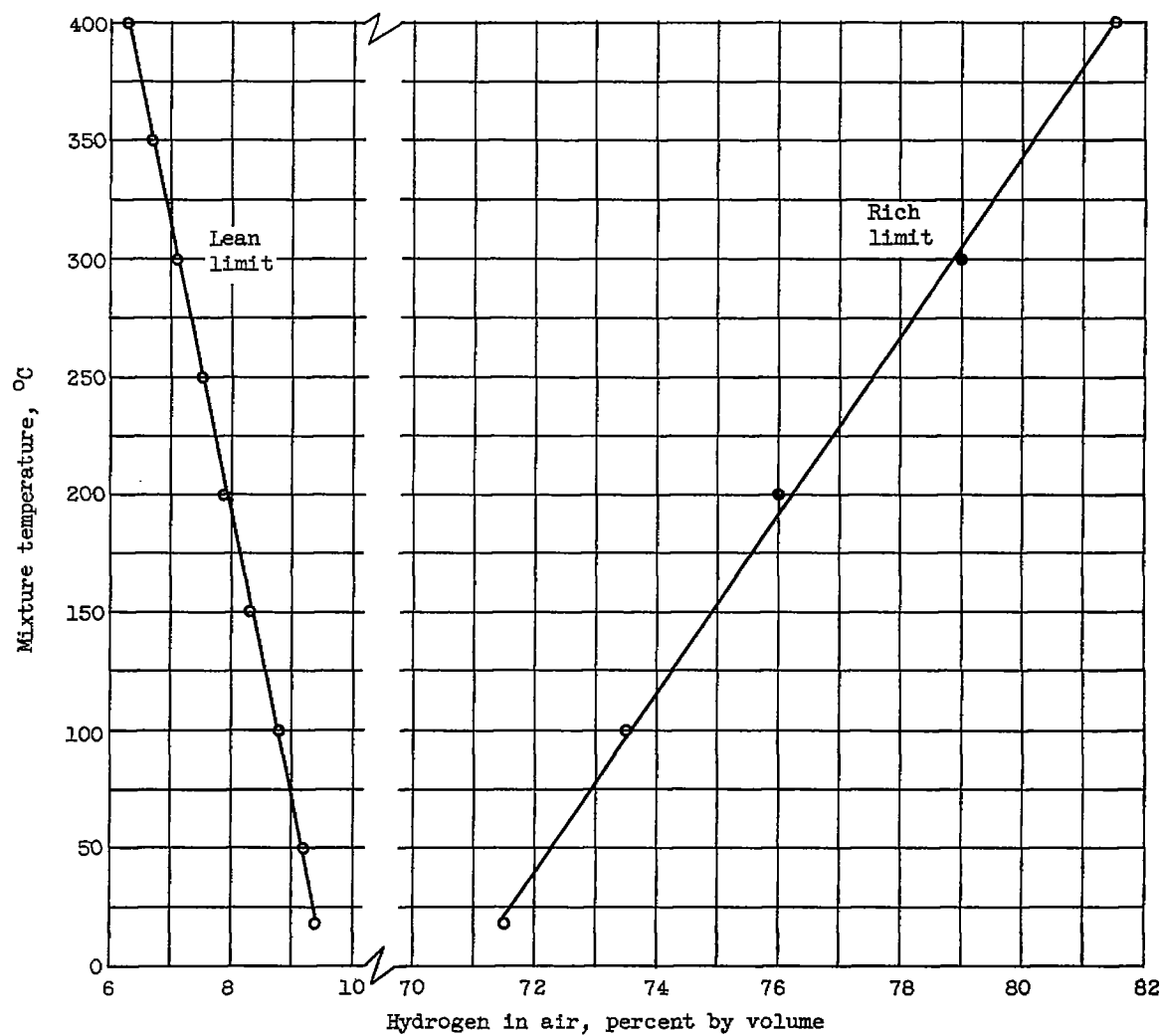


Figure 14. - Effect of temperature on flammability limits of hydrogen in air for downward propagation (ref. 44).

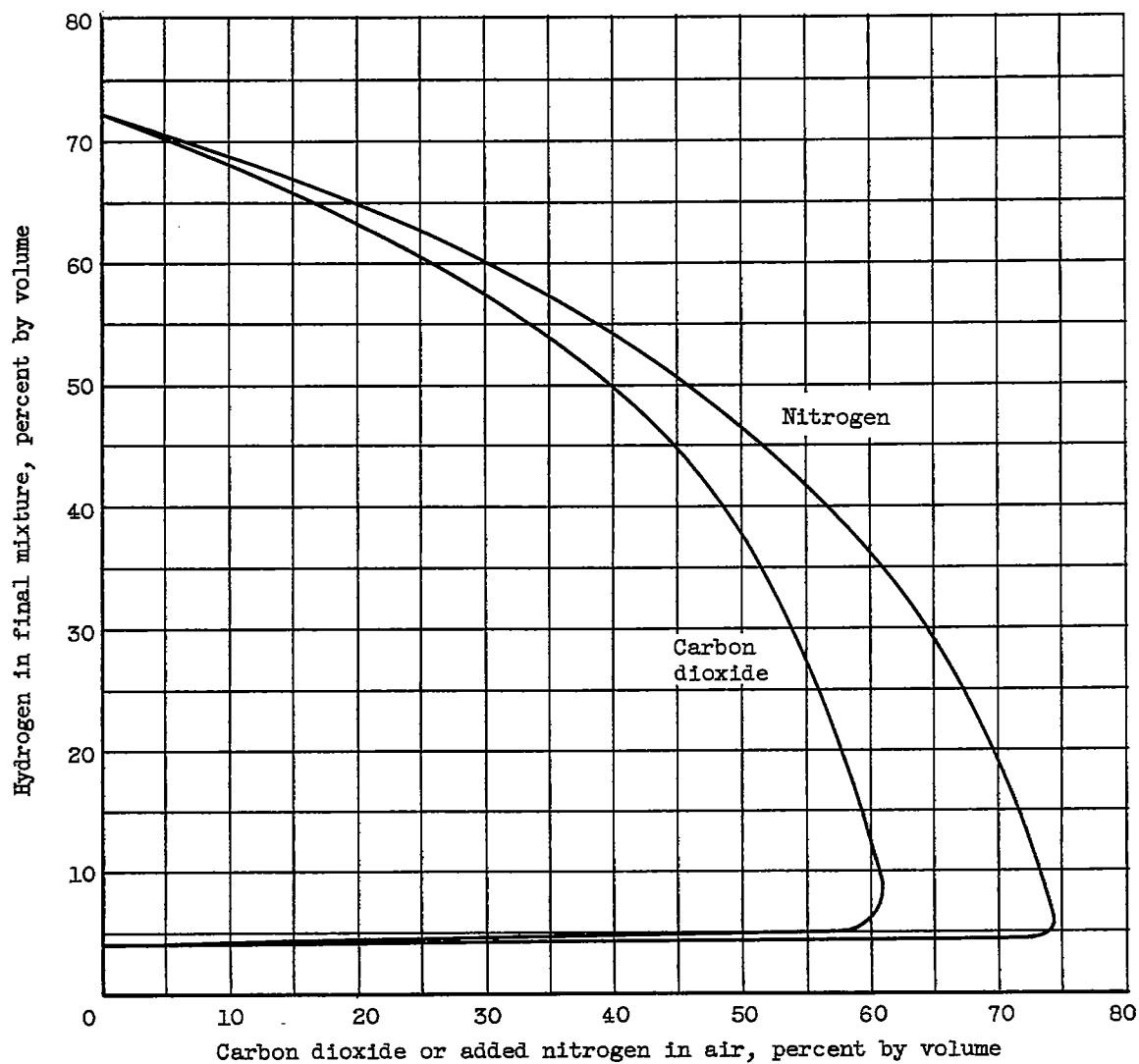


Figure 15. - Flammability limits of hydrogen in air diluted with nitrogen or carbon dioxide (ref. 42).



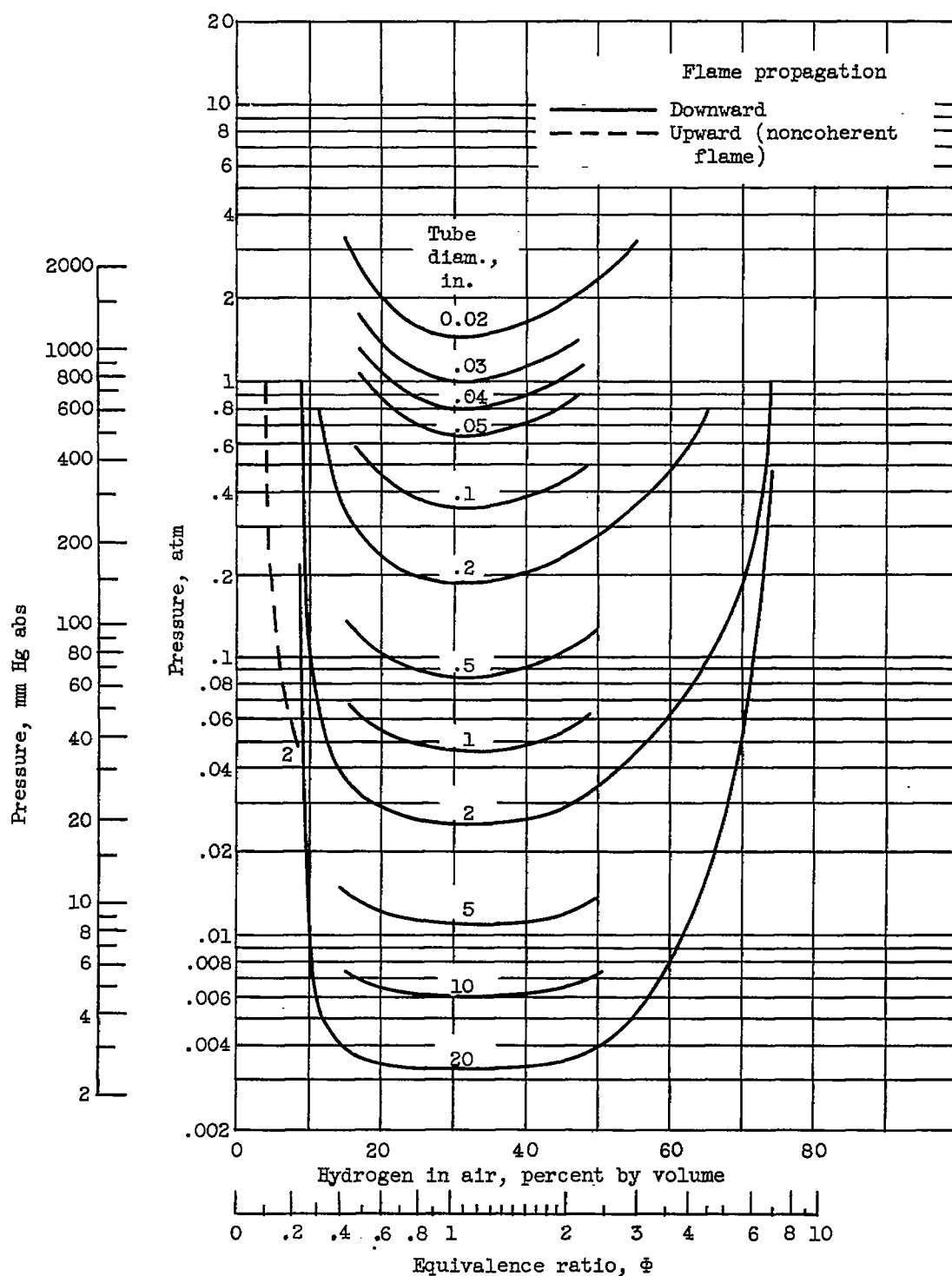


Figure 16. - Estimated pressure limits of flame propagation for hydrogen-air mixtures with various tube diameters. Based on extrapolations of quenching data of reference 37.

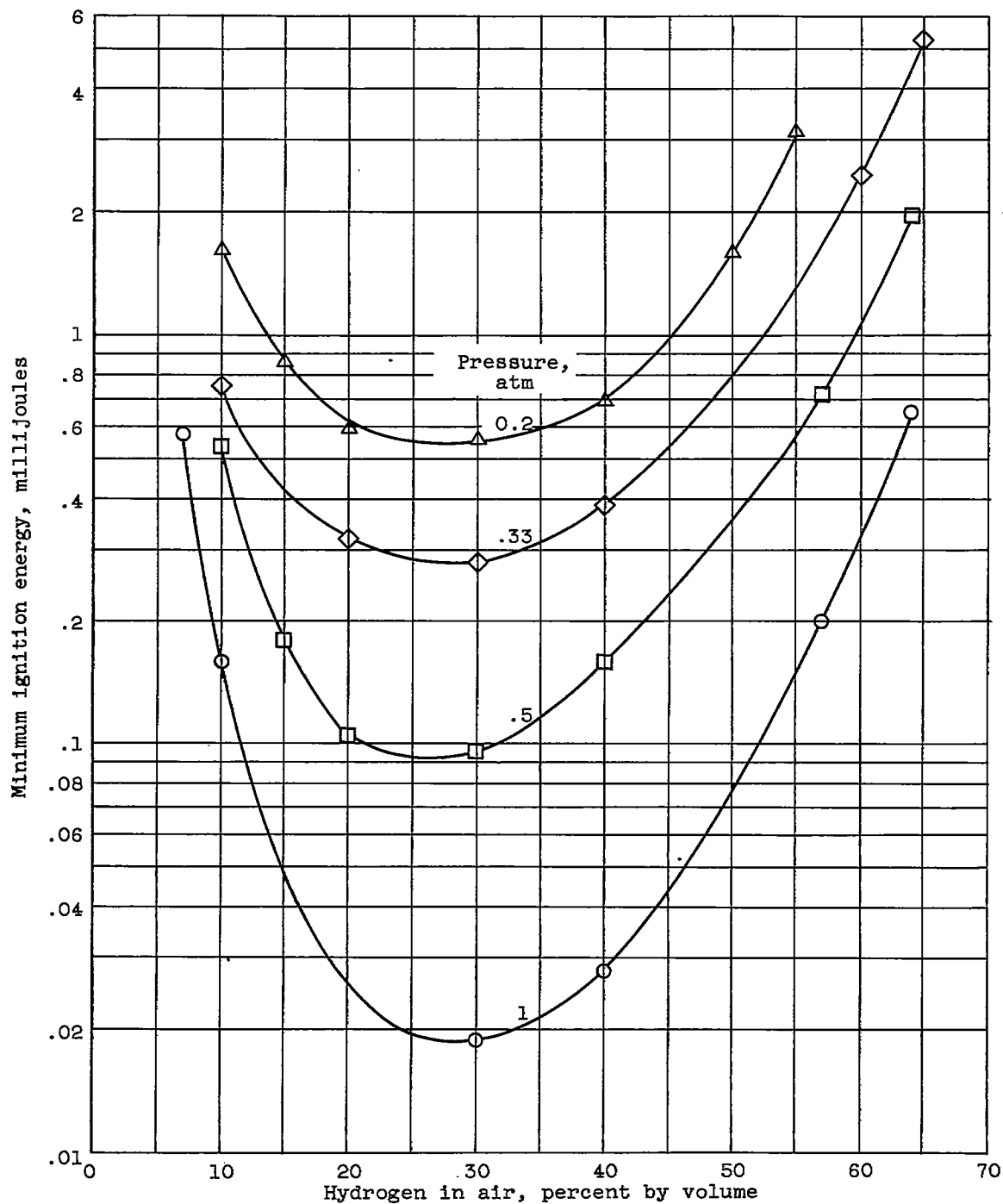


Figure 17. - Spark ignition energies for hydrogen-air mixtures at various pressures (ref. 36).

~~CONFIDENTIAL~~

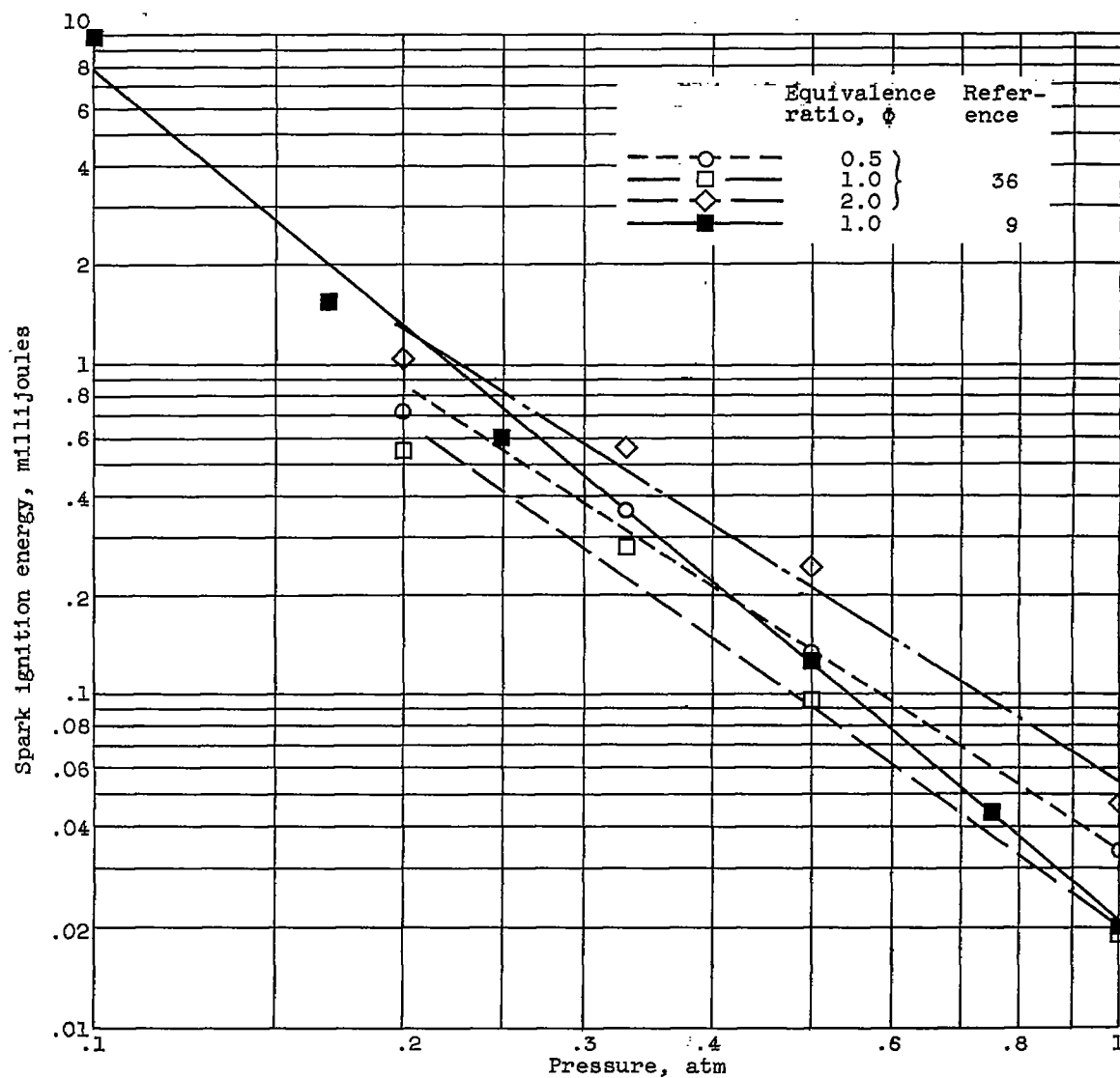


Figure 18. - Effect of pressure on spark ignition energy.

~~CONFIDENTIAL~~

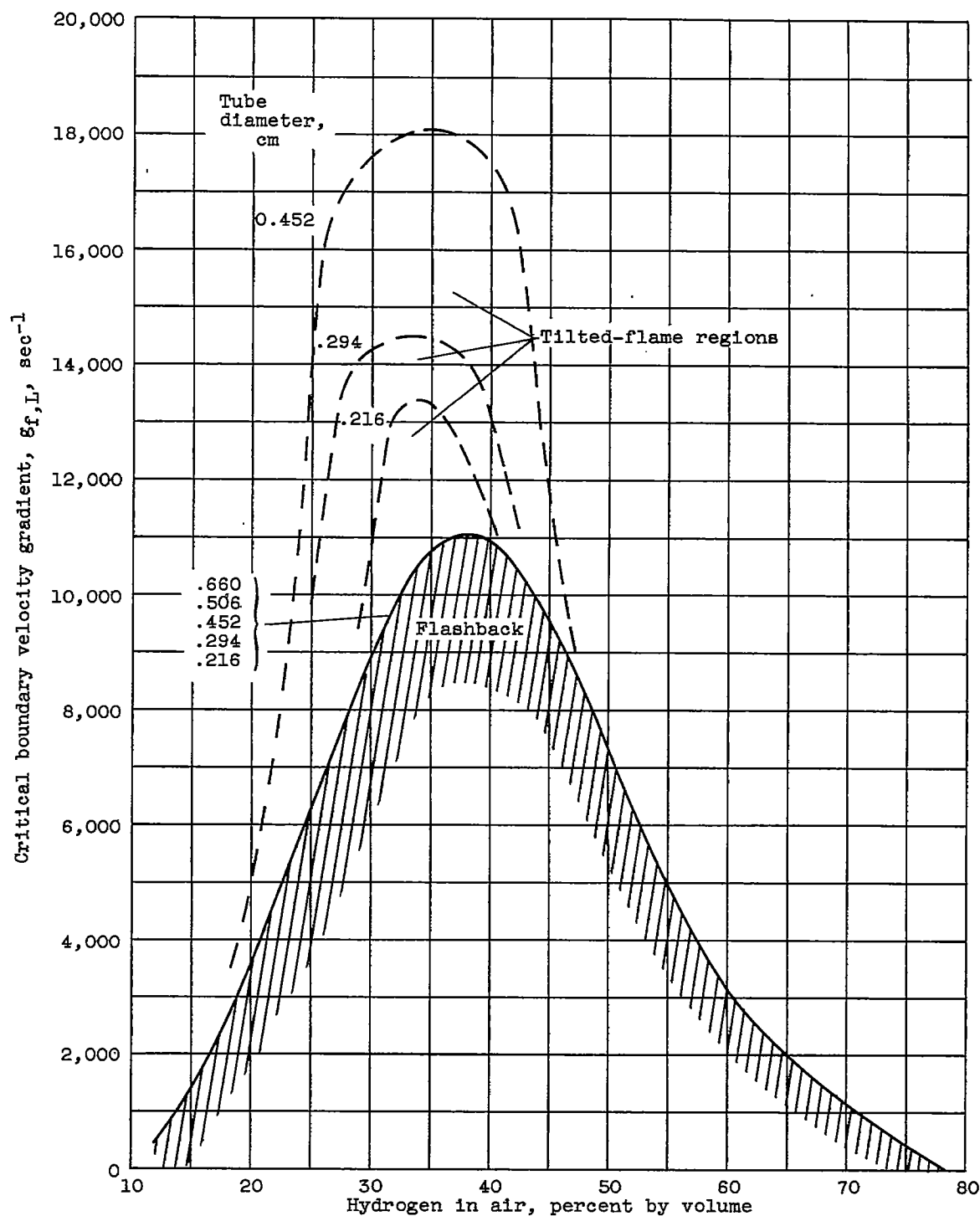


Figure 19. - Flashback of laminar hydrogen-air flames at atmospheric pressure (ref. 53).

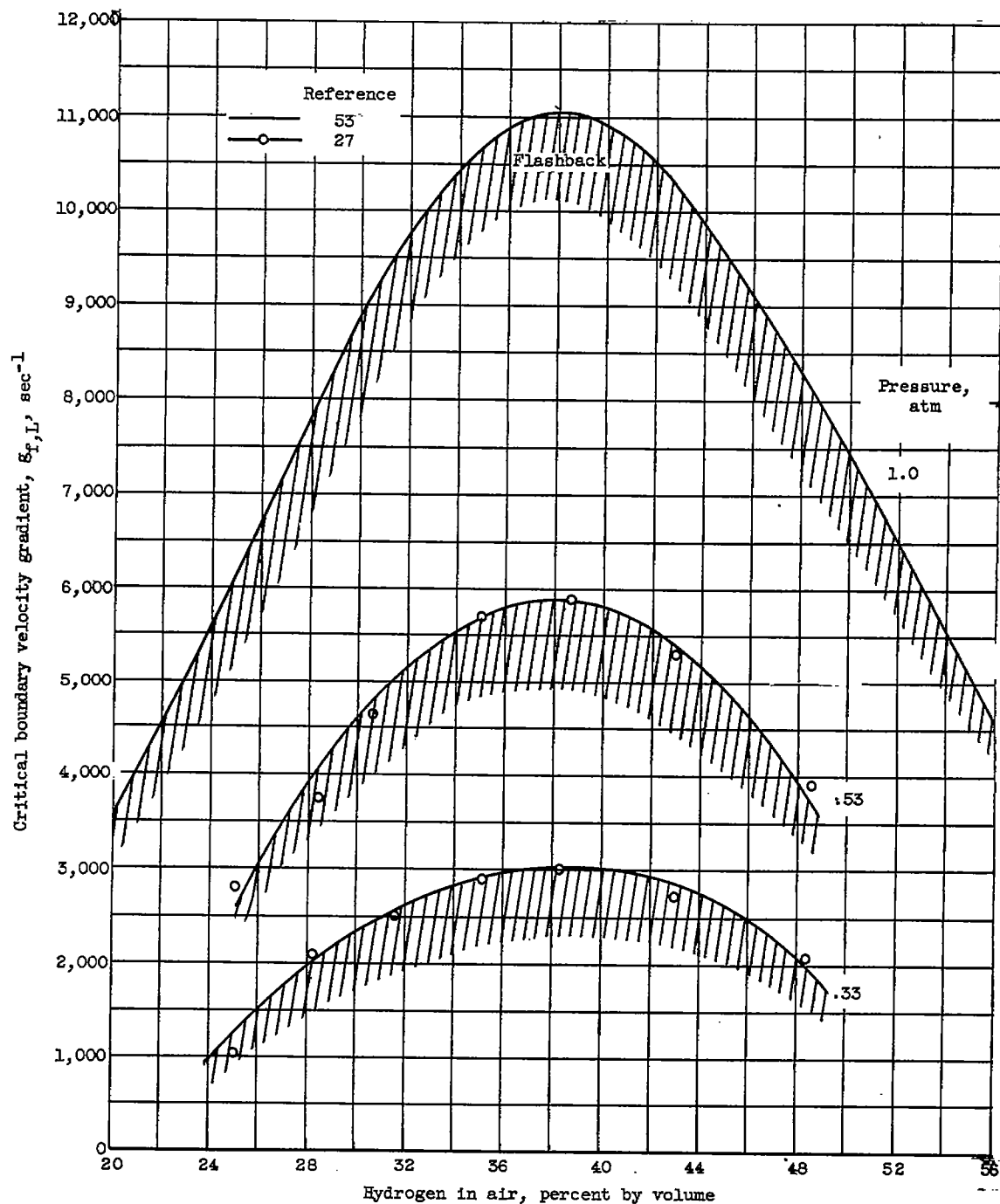


Figure 20. - Effect of pressure on critical boundary velocity gradient for flashback of laminar hydrogen-air flames.

4362

CN-10 back

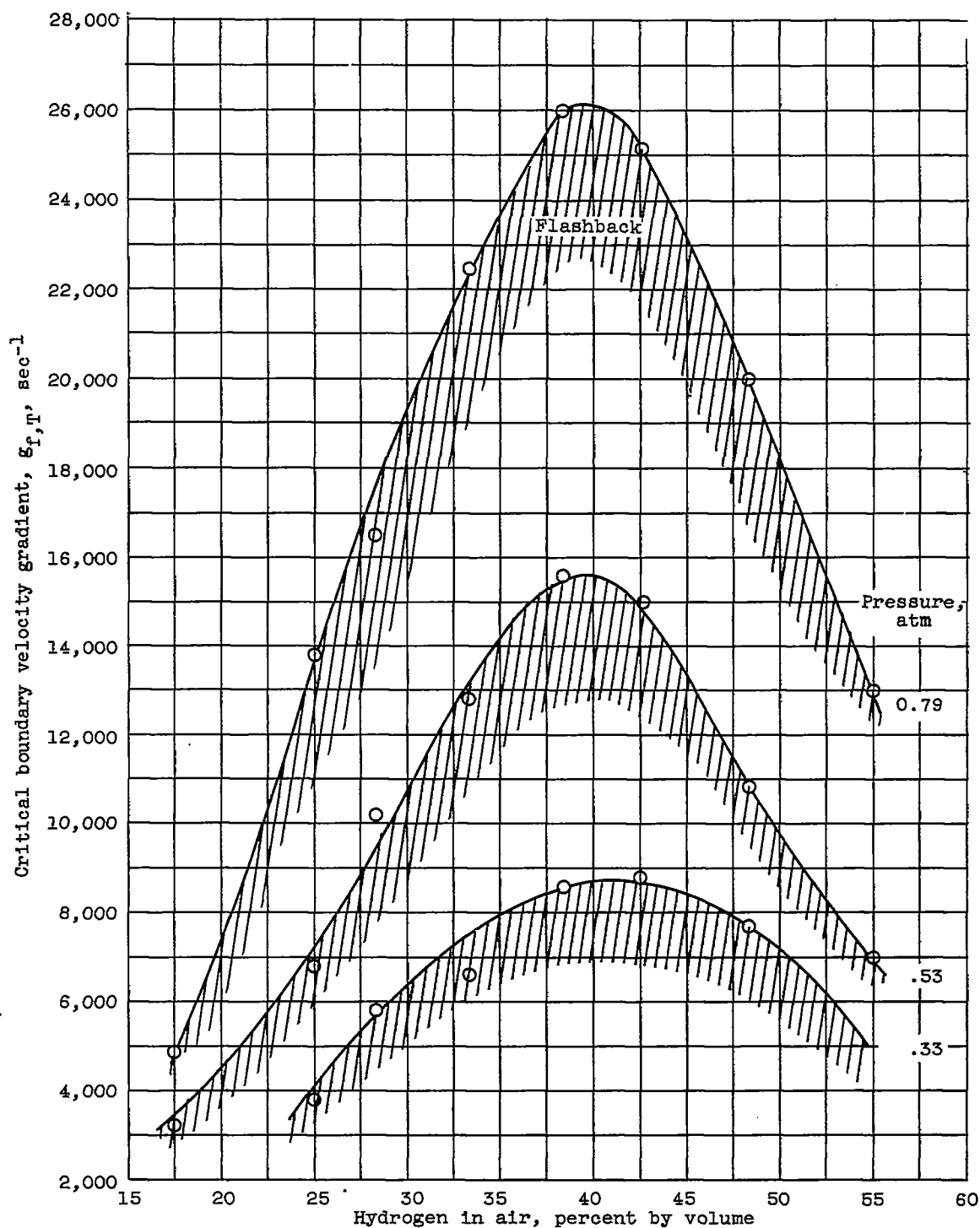


Figure 21. - Effect of pressure on critical boundary velocity gradient for flashback of turbulent hydrogen-air flames (ref. 33).

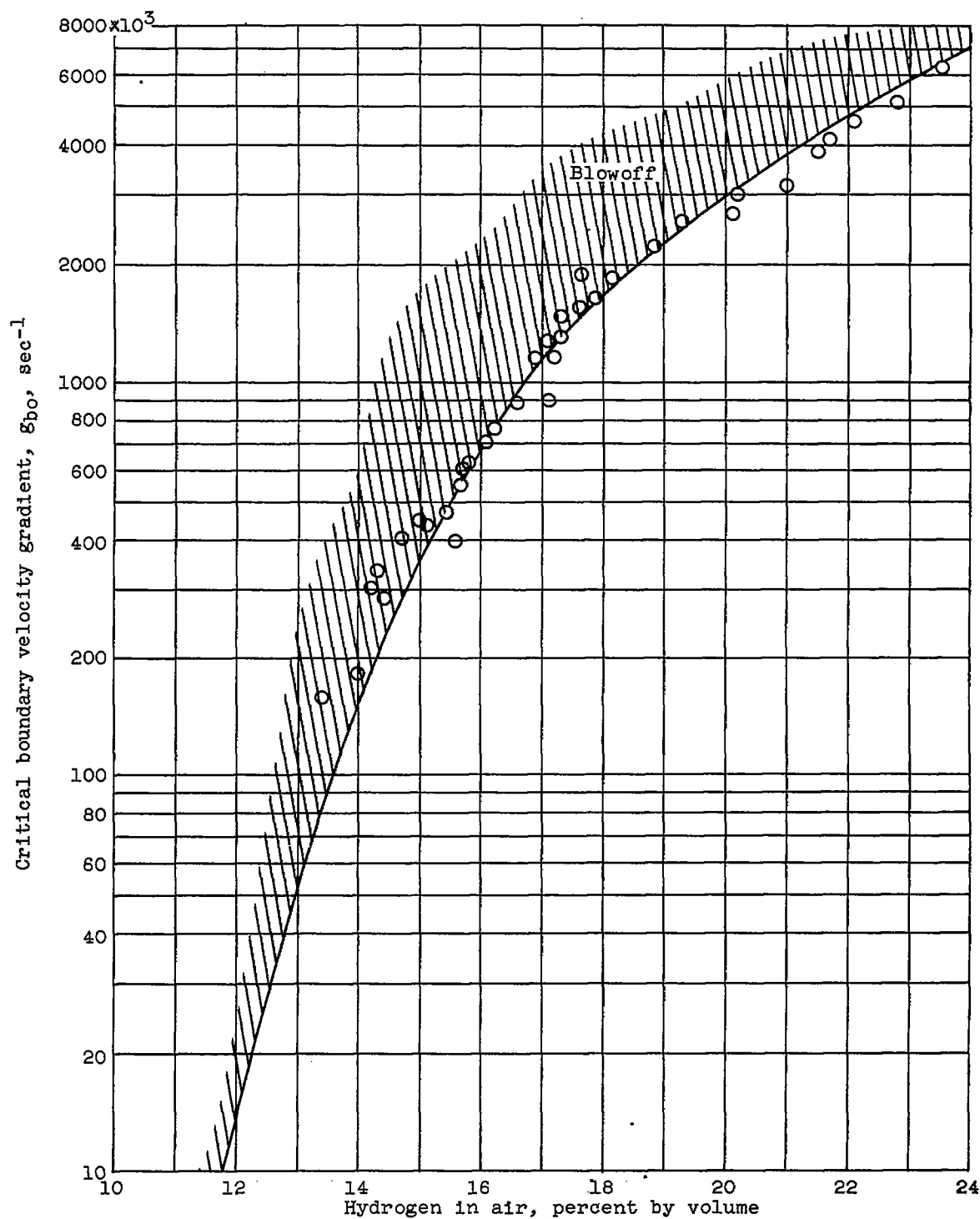


Figure 22. - Blowoff of hydrogen-air bunsen burner flames at atmospheric pressure (refs. 53 and 55).

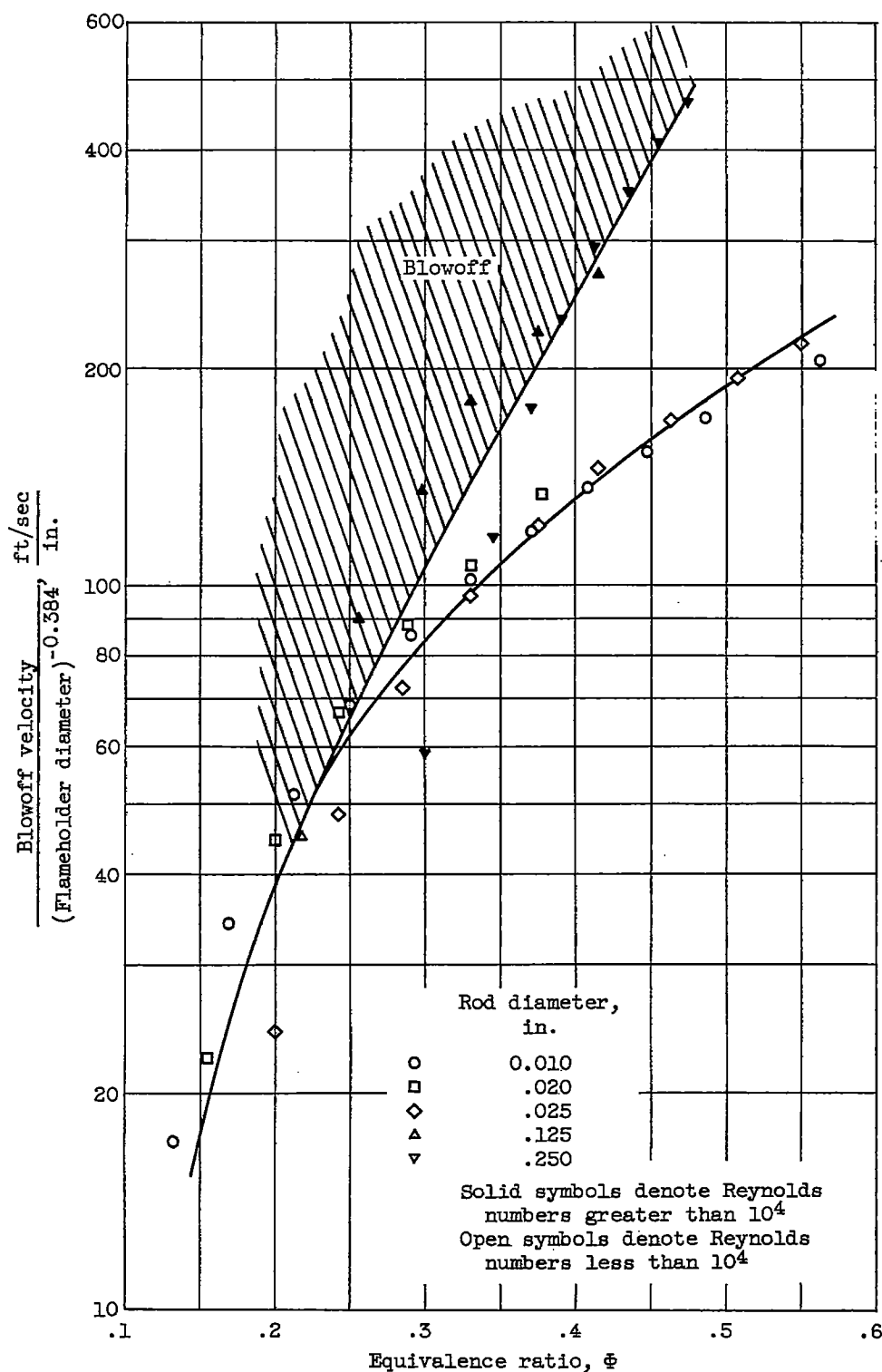


Figure 23. - Blowoff of lean hydrogen-air flames at atmospheric pressure from water-cooled cylindrical rods (ref. 57).



~~CONFIDENTIAL~~

NACA RM E57D24

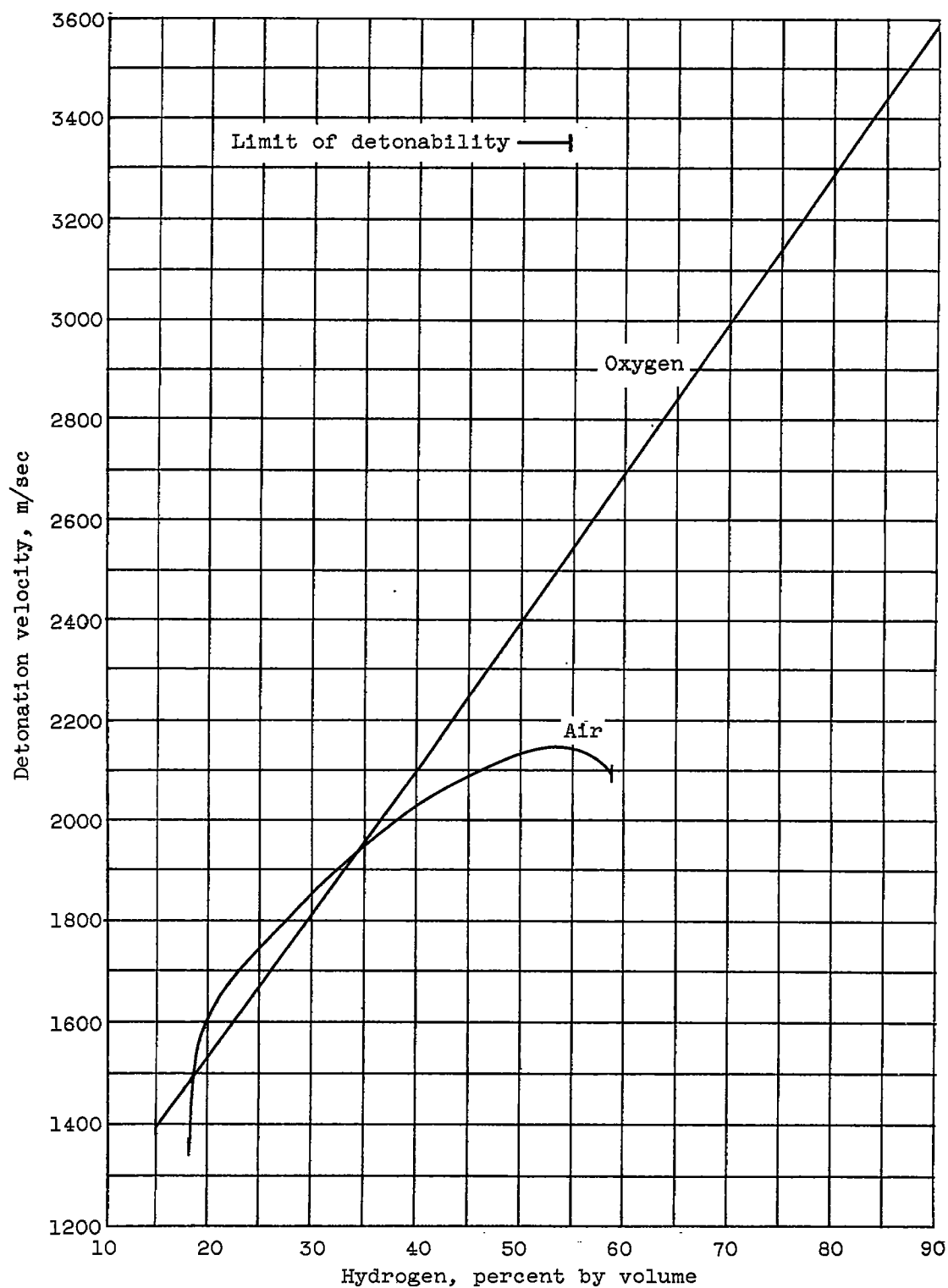
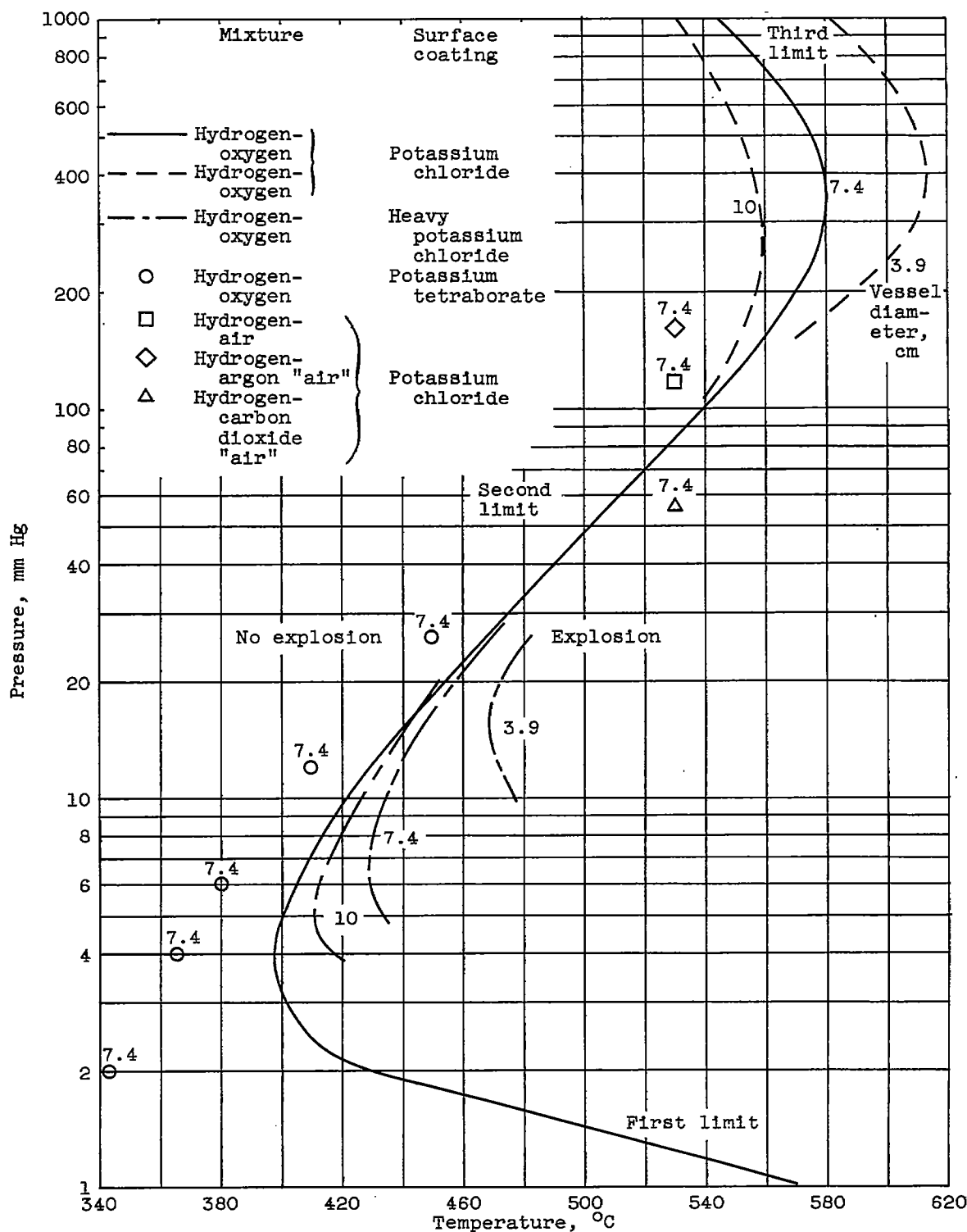


Figure 24. - Detonation velocities of hydrogen-air and hydrogen-oxygen mixtures (ref. 36).

~~CONFIDENTIAL~~



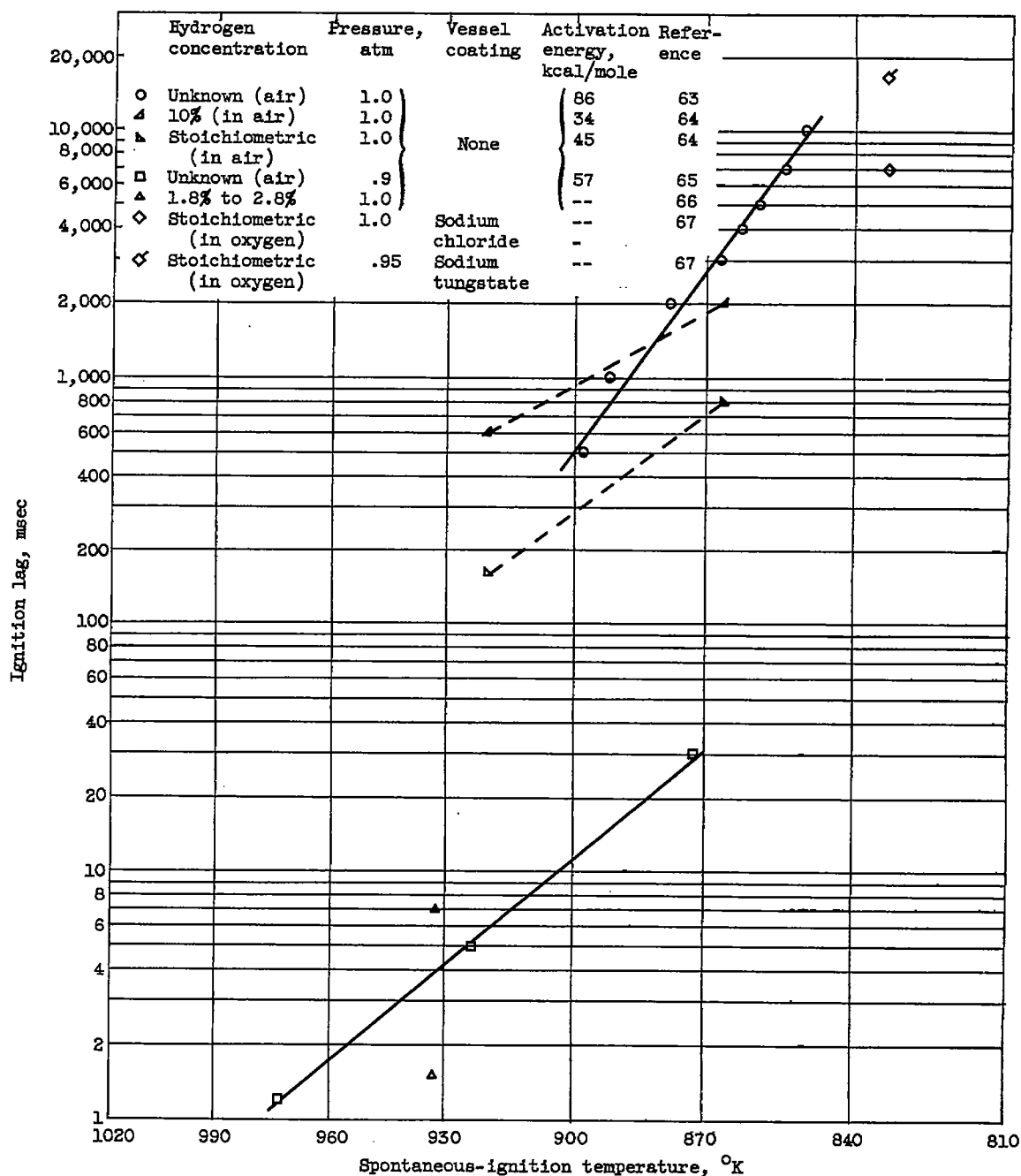


Figure 26. - Effect of spontaneous-ignition temperature on ignition lag.

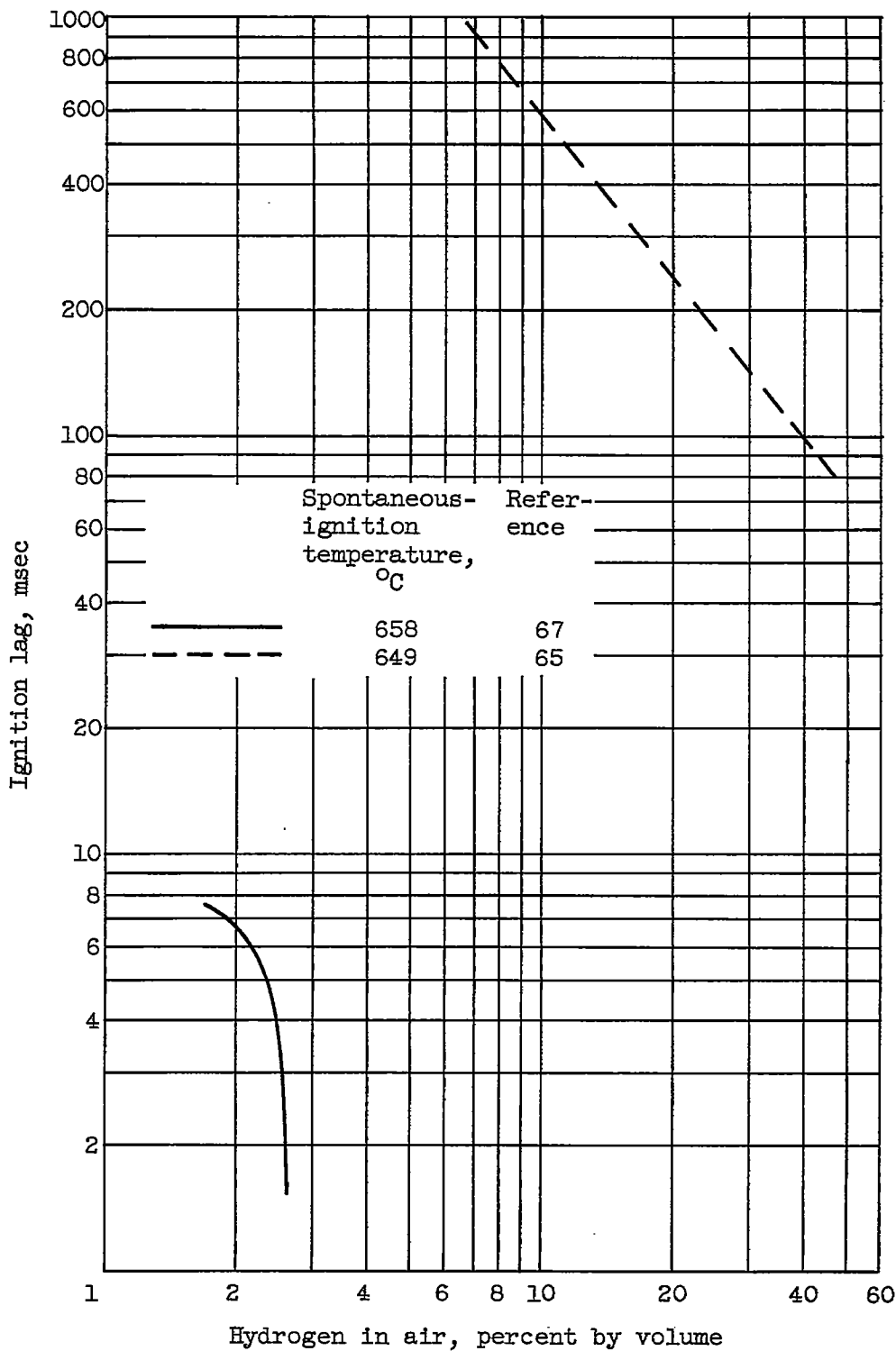


Figure 27. - Effect of hydrogen concentration on ignition lag at atmospheric pressure.

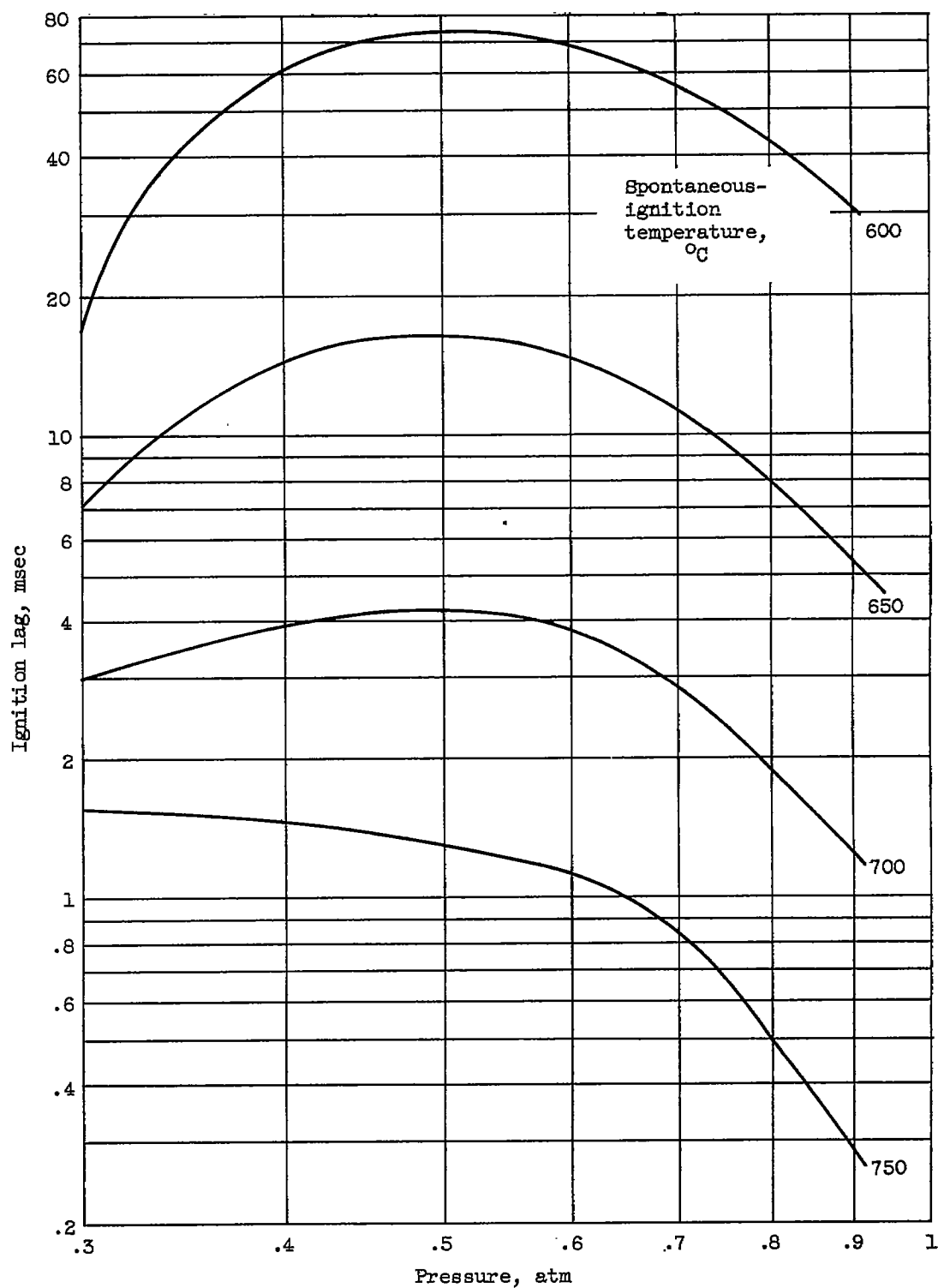
~~CONFIDENTIAL~~

Figure 28. - Effect of pressure on ignition lag of hydrogen-air mixtures (ref. 67).

~~CONFIDENTIAL~~

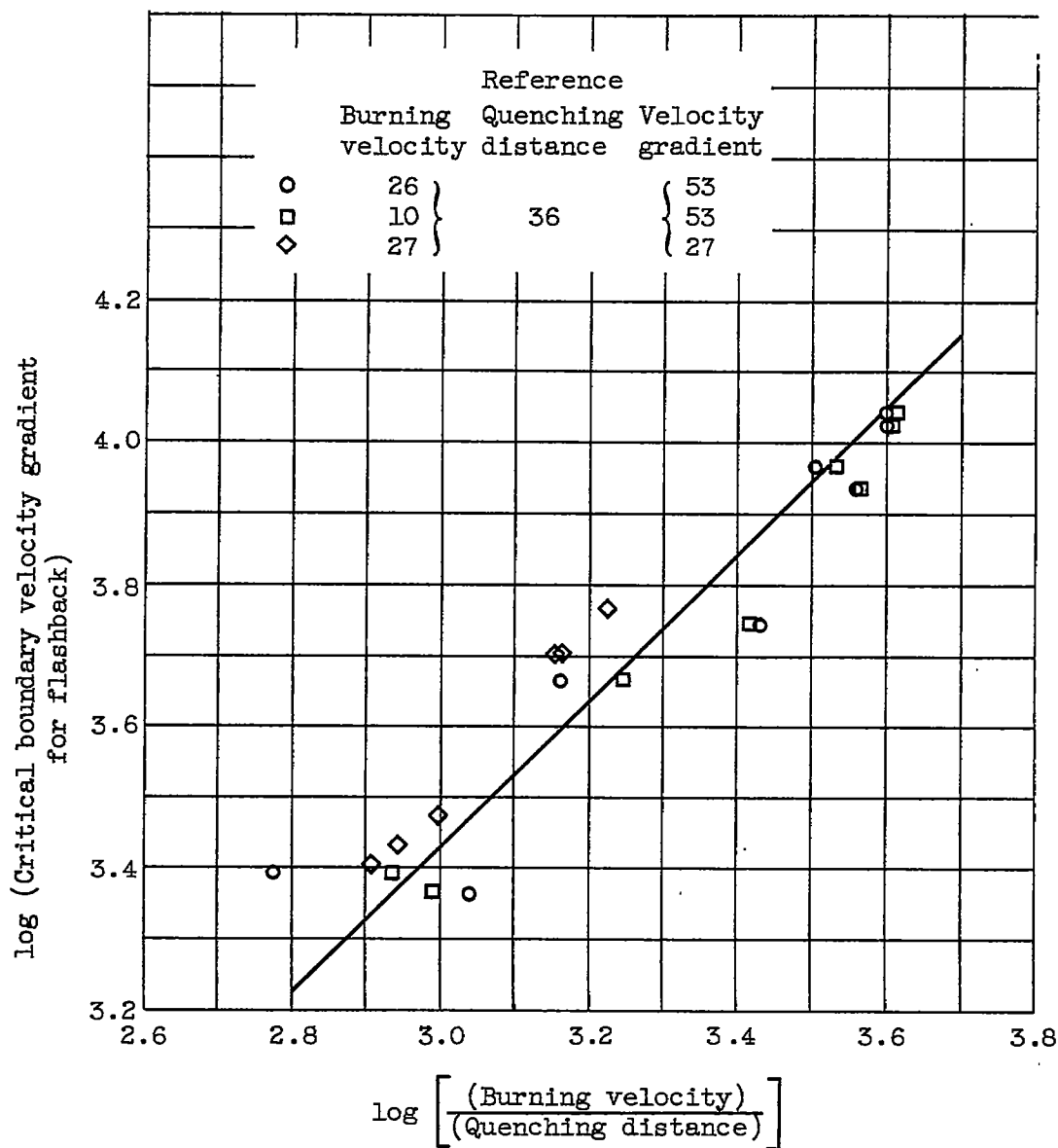


Figure 29. - Relation between reaction-rate parameters for hydrogen-air mixtures.

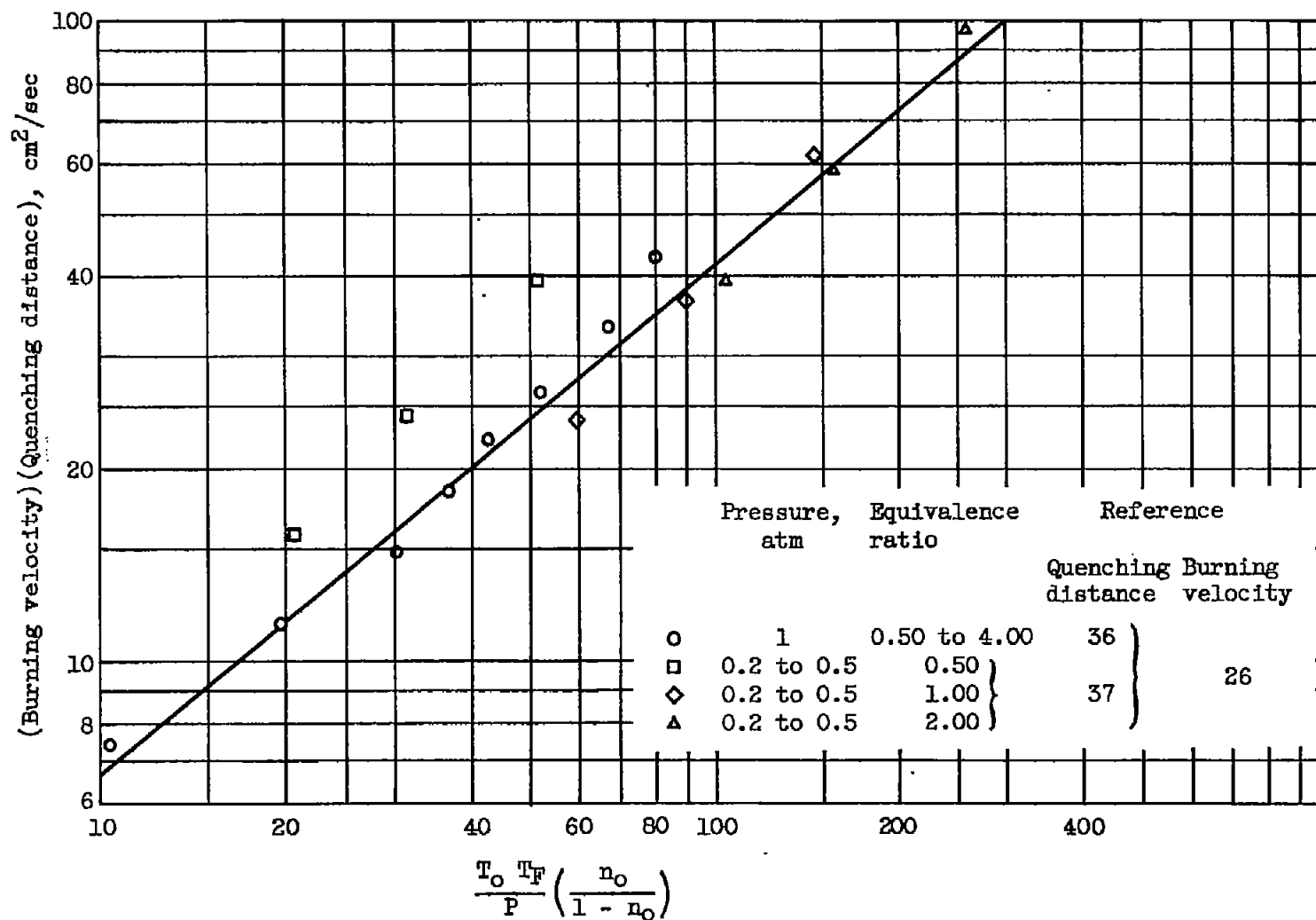


Figure 30. - Relation between product of quenching distance and burning velocity and transport parameters of hydrogen-air mixtures.

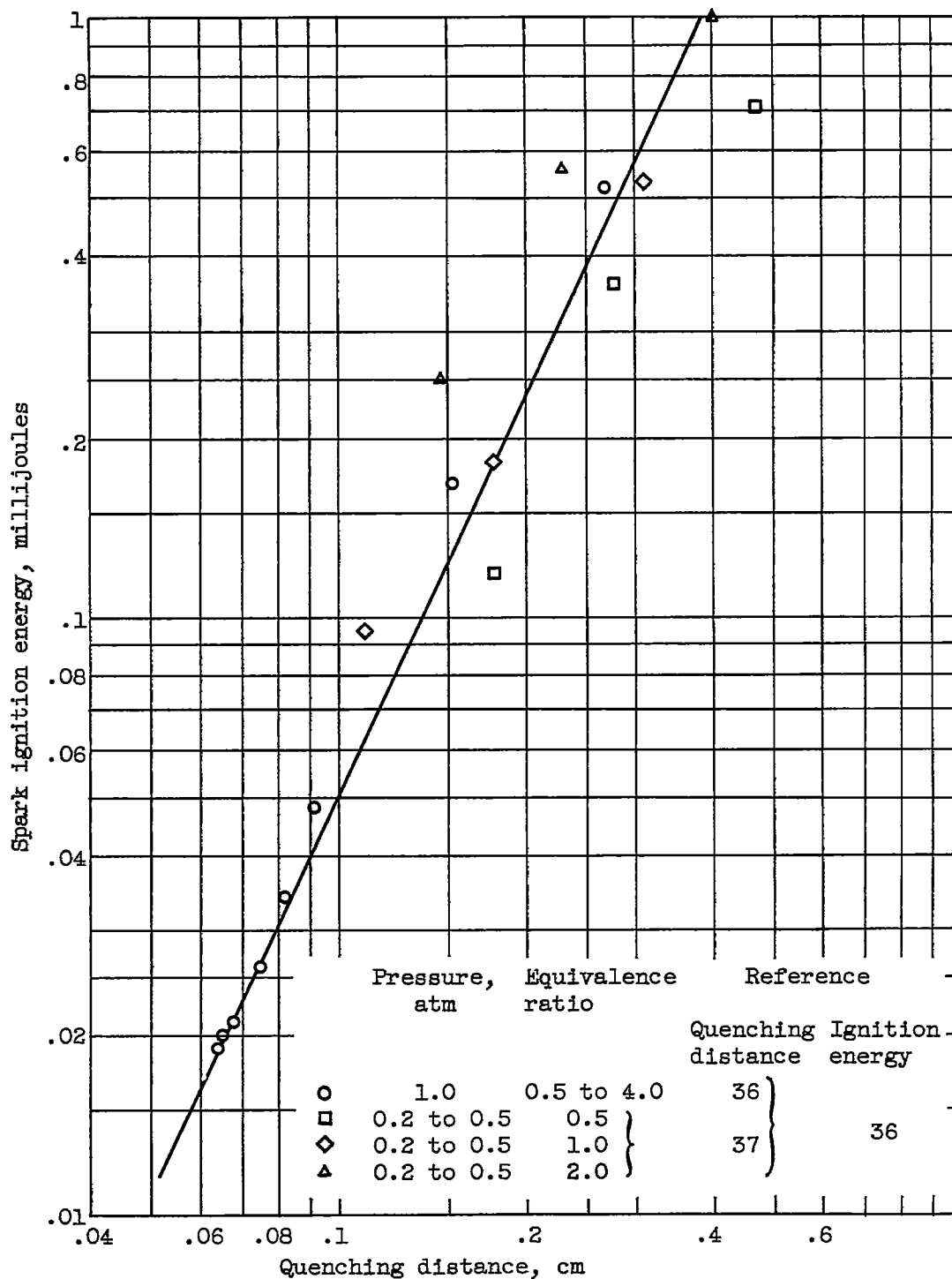


Figure 31. - Relation between spark ignition energy and quenching distance (between parallel plates) for hydrogen-air mixtures.



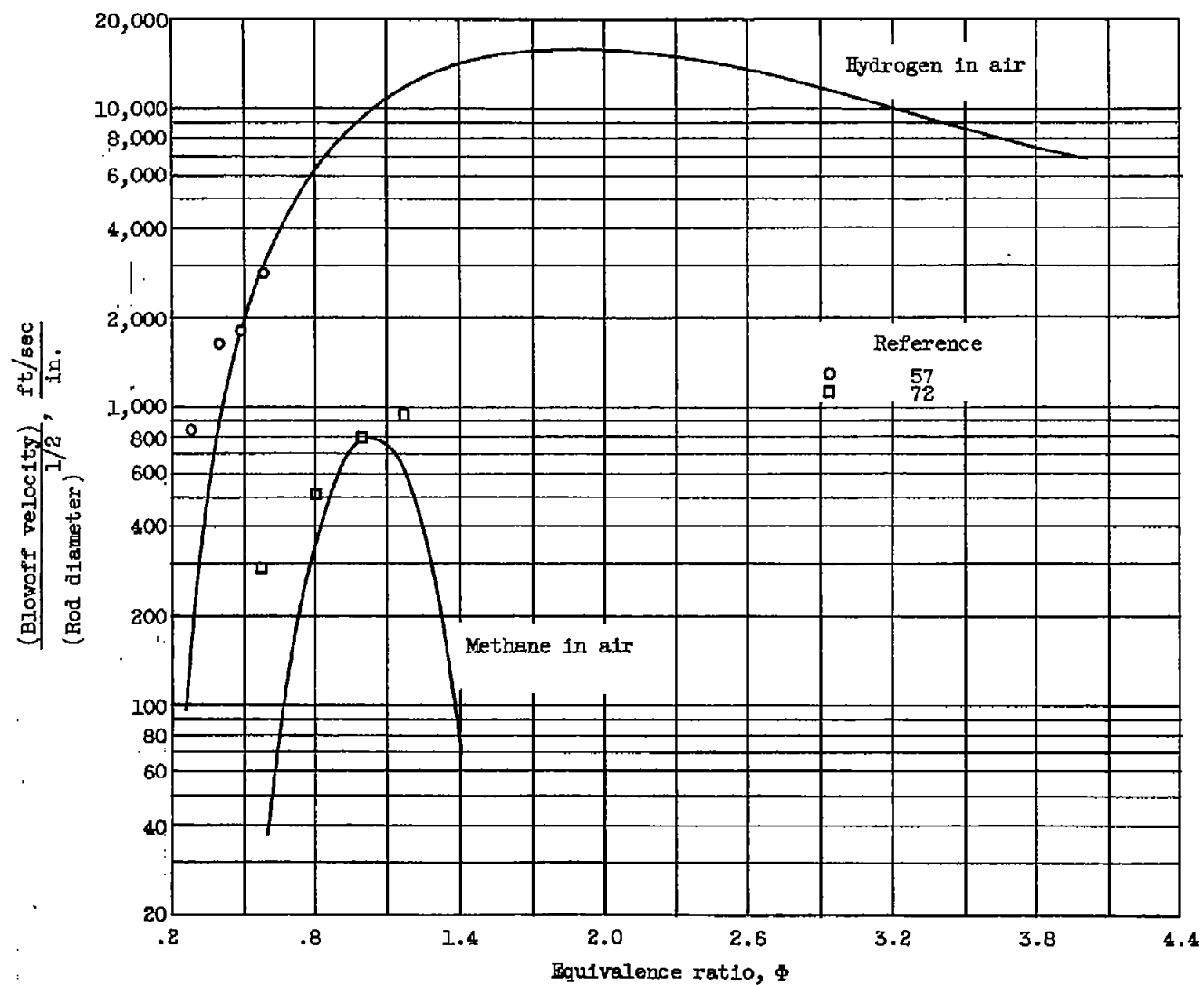


Figure 32. - Comparison of experimental data with blowoff curves calculated from flashback data of references 53 and 74. Cylindrical flameholders.